Universidade Federal de São Carlos – UFSCar

Centro de Ciências Exatas e de Tecnologia
Departamento de Física

Nicolás Armando Cabrera Carpio

Spin Glasses and Neural Networks: Phase Diagrams of the Classical and Semi-Classical Boltzmann Machines

São Carlos

2024

Nicolás Armando Cabrera Carpio

Spin Glasses and Neural Networks: Phase Diagrams of the Classical and Semi-Classical Boltzmann Machines

Master's thesis submitted to the Graduate Program of Physics at the Federal University of São Carlos, in partial fulfillment of the requirements for obtaining the degree of Master of Science in Physics.

Supervisor: Prof. Dr. Celso Jorge Villas-Bôas

São Carlos

2024

Nicolás Armando Cabrera Carpio

Spin Glasses and Neural Networks: Phase Diagrams of the Classical and Semi-Classical Boltzmann Machines / Nicolás Armando Cabrera Carpio. – São Carlos, 2024–

Supervisor: Prof. Dr. Celso Jorge Villas-Bôas

Tese Final de Mestrado – Universidade Federal de São Carlos – UFSCar
Centro de Ciências Exatas e de Tecnologia
Departamento de Física, 2024.

1. Classical and Semi Classical Boltzmann Machines. 2. Statistical Mechanics. I. Celso Jorge Villas-Bôas. II. Universidade Federal de São Carlos. III. Departamento de Física. IV. Spin Glasses and Neural Networks: Phase Diagrams of the Classical and Semi-Classical Boltzmann Machines .

Nicolás Armando Cabrera Carpio

Spin Glasses and Neural Networks: Phase Diagrams of the Classical and Semi-Classical Boltzmann Machines

Master's thesis submitted to the Graduate Program of Physics at the Federal University of São Carlos, in partial fulfillment of the requirements for obtaining the degree of Master of Science in Physics.

Approved. São Carlos, 2024.

Prof. Dr. Celso Jorge Villas-Bôas
Supervisor

Dr. Lucas Madeira
IFSC-USP

Prof. Dr. Raphael Fortes Infante Gomes
UNILA

São Carlos
2024

Este trabajo es dedicado a las personas que lo hicieron posible: Mis Padres.

Acknowledgements

In this journey of learning and growth, I find myself deeply grateful for the presence and support of those who have been guiding lights along my path.

To my parents, Armando and Leticia, whose unconditional love and unwavering sacrifices have been the bedrock upon which I have built my dreams. Their faith in me has been a constant beacon, guiding me through moments of doubt and sustaining me in times of storm. Thank you for teaching me the value of effort, the importance of integrity, and above all, for believing in my potential even when I did not.

To my mentor Celso, whose knowledge and wisdom have illuminated every step of this journey. His patience and guidance have been essential in the crafting of this work. Thank you for your dedication, for sharing your experience, and for instilling in me a passion for learning that transcends the pages of books, giving me the opportunity to embark on the path of research.

To my beloved Gabi, whose presence has been a constant source of joy and strength. Your love, patience, and understanding have been my refuge in difficult days and my inspiration in moments of triumph. Thank you for walking by my side, for your unwavering support, and for being my companion on this journey. Your faith in me has given me wings to soar higher than I ever imagined.

To my siblings, Mateo and Belén, whose bonds of blood and heart have been pillars of my life. Thank you for the shared moments that have shaped me, for your steadfast support. In every step of this journey, I have felt your presence and your love, and that has given me the strength to keep moving forward. You are and always will be my life companions, and I thank you for always being there, in good times and bad.

To my colleagues and friends, with whom I have shared not only hours of study but also moments and victories. Thank you for welcoming me as one of you. I want to thank Tiago and Matheus for the enriching discussions, again Matheus and Tiago, along with Gabriel, Amanda, Gubio, Sinara, Alexandre and Natan, thank you for making this journey a memorable and rewarding experience.

To Brazil, the land that embraced me and made me feel at home. Thank you for your warmth, your diversity, and your vibrant culture. In its landscapes and among its people, I found a second home, a place where I could grow and thrive with freedom and support. I am grateful for every experience lived and every friend made in this wonderful land. I would like to give special thanks to my professors, whose teachings have been the foundation of my knowledge. Special thanks to *Conselho Nacional de Desenvolvimento*

Científico e Tecnológico (CNPq) for financially supporting this project with the process 131088/2022-0.

Each of you has left an indelible mark on my life, and it is with a heart full of gratitude that I dedicate this achievement to you. Your teachings and your companionship have been the cornerstone of this success, and for that, I will be eternally grateful.

"I like to understand simple things very well, because my brain is very slow. So I think about them for a very, very long time."

Michel Talagrand.

Resumo

As máquinas de Boltzmann clássicas e quânticas tornaram-se modelos úteis para sistemas complexos em física estatística, mas também como algoritmos de aprendizado em redes neurais e problemas de otimização fora da física estatística. Essas redes neurais estocásticas que incorporam a distribuição de Boltzmann são capazes de aprender e representar distribuições de probabilidade sobre os dados de entrada, o que lhes permite capturar as correlações e dependências relacionadas inerentes aos sistemas que representam. Neste projeto, por meio de uma análise teórica baseada nos métodos *Réplica* e *Suzuki Trotter*, estudamos e comparamos os diagramas de fase da máquina de Boltzmann clássica (em ambas arquiteturas) e quântica, destacando as semelhanças e diferenças fundamentais entre elas. Os dois métodos mencionados acima nos permitem fazer a aproximação *semi clássica* na qual são ignoradas as correlações entre os neurônios, tanto clássicos quanto quânticos. Os diagramas de fase dessas máquinas são estudados para fornecer percepções profundas sobre seu comportamento no equilíbrio, mostrando como as transições entre diferentes estados da rede dependem das variações de alguns parâmetros de controle, como temperatura, campo transversal (apenas para o caso quântico), energia de interação (sinapses) ou intensidade do campo externo ("bias"). No caso de uma *máquina clássica de Boltzmann*, essas transições são descritas por alterações em termos de temperatura, que está diretamente relacionada às probabilidades de transição entre estados microscópicos; já no caso de uma *máquina quântica de Boltzmann*, é necessário considerar adicionalmente os efeitos do campo transversal que permite o tunelamento quântico, a coerência e a superposição.

Palavras-chaves: Aprendizado de máquina quântico, mecânica estatística, máquina de Boltzmann, aproximação semiclássica, aproximação de Suzuki-Trotter.

Abstract

Classical and quantum Boltzmann machines have become useful models for complex systems in statistical physics, but also learning algorithms on neural networks and optimization problems outside of statistical physics. These stochastic neural networks embodying the Boltzmann distribution, are capable of learning and representing probability distributions over input data that enables them to capture the related correlations and dependencies inherent in the systems they represent. In this project, through a theoretical analysis based on the *Replica* and *Suzuki Trotter* methods, we study and compare the phase diagrams of the classical (in both architectures) and quantum Boltzmann machine, highlighting the fundamental similarities and differences between them. The two methods mentioned above allow us to make the *semi classical* approximation in which the correlations between the neurons are ignored, both classical and quantum. The phase diagrams of these machines are studied in order to provide deep insights into its equilibrium behaviour, showing how transitions between different network states depend on variations of some control parameters like temperature, transverse field (just for the quantum case), interaction energy (Synapses) or external field strength (bias), we focus in the effects of the bias which is important in the context of neural networks. In the case of a *classical Boltzmann machine*, these transitions are described by changes in terms of the temperature that is directly related with the transition probabilities between microscopic states; while for a *quantum Boltzmann Machine*, it is necessary consider additionally effects from the transverse field that allows quantum tunneling, coherence and superposition.

Keywords: Quantum Machine Learning, Statistical Mechanics, Boltzmann Machine, Semi Classical Approximation, Suzuki-Trotter Approximation.

List of Figures

Contents

1 Introduction

Classical artificial neural networks (ANNs) have revolutionised the field of artificial intelligence and machine learning. Inspired by the structure and functioning of the human brain, ANNs are composed of layered artificial neurons that learn to perform tasks by modifying synaptic weights through training processes [1]. These networks have demonstrated a remarkable ability to solve complex problems in diverse areas, from image recognition [2] and natural language processing [3] to the simulation of physical phenomena [4, 5].

Although in physics some ANNs have been used to model complex systems [6], these networks themselves constitute complex systems. With large numbers of neurons interacting with each other through complex connections called synapses, ANNs have established themselves as interesting models for physics to its study. There are phenomena that emerge when many individuals interact, and these are a fundamental part of the study of statistical mechanics.

In this context, we identify a model for associative memory: the *Hopfield Networks* [7]. These networks present an emergent phenomenon related to the memorisation of patterns. This phenomenon arises by selecting the synapses between neurons in such a way that they depend directly on the patterns to be memorised, following Hebb's rule [8]. The relationship of these phenomena to statistical mechanics and physics lies on the study of how local interactions can give rise to complex global behaviours, a key area in the analysis of emergent phenomena.

Spin glasses, and in particular the Sherrington-Kirkpatrick (SK) model [9], provide a useful theoretical framework for understanding the properties of Hopfield lattices. The SK model describes a spin system with random interactions and has been fundamental in the study of disordered and complex systems. The relationship between Hopfield Networks and spin glasses lies on the structure of the interactions between neurons (or spins), which can be similar to that of spin glass models. This parallelism allows the application of techniques and concepts from spin-glass statistical mechanics to analyse the emergent behaviour of Hopfield Networks, such as the storage capacity and stability of memorised patterns [10, 11].

While *Hopfield networks* are a paradigmatic model for associative memory, there is another type of system key for learning: *the Boltzmann machines (BM)*. Although in practice they are the same systems (both related to the *SK* model), in essence they possess a remarkable difference: while in *Hopfield networks* the synaptic weights are chosen in a certain way, these must be adjusted in a learning process in *BM* [12]. Among the many architectures and uses for neural networks, *BM* have become one of the paradigmatic

models for generative modelling, where the networks learn the probability distribution of the data and thereby generate data that follow these probability distributions [13].

Besides, quantum machine learning is an emerging branch that combines principles of quantum computing and machine learning, with the aim of developing algorithms that take advantage of the unique properties of quantum systems. These properties include entanglement, superposition, interference, vacuum fluctuations, and tunneling, which can potentially speed up certain computations and allow data to be handled at scales that would be unattainable for classical algorithms [14]. This broad field of research can be divided into 3 categories: Classical Machine Learning(ML) with quantum data [15, 6], speed-up for classical ML [16, 17], and quantum machine learning used on quantum data [18, 19].

Among the many quantum machine learning algorithms, Quantum Neural Networks (QNN) have positioned themselves as one of the most important and enigmatic. As in the classical universe, QNNs have a vast number of architectures ranging from variations circuits [20] to quantum perceptron-based architectures [21], not forgetting to mention continuous variable neural networks [22]. One of the most promising quantum machine learning architectures is the Quantum Boltzmann Machine (QBM) [23]. The QBM is an extension of the Classical Boltzmann Machine (CBM) which, as we already said, is a stochastic neural network model used to model complex probability distributions. While the CBM uses thermal fluctuations to explore state configurations, the QBM uses thermal and quantum fluctuations, which opens up new possibilities for state exploration and optimization of objective functions in high-dimensional spaces.

Despite having many approaches to QNN, many of these fail to bridge the nonlinear and dissipative dynamics characteristic of neural networks with the unitary and linear dynamics of quantum mechanics. This problem is relevant to obtain a complete and mature quantum neural network model [24]. This is why we believe that the *QBM* is an interesting model to study.

The study of the phase diagram of a neural network, whether classical or quantum, is crucial to understand the dynamics of the system under different conditions, optimize the network parameters to improve its performance and stability, predict how the network will respond to changes in external or internal conditions, and compare classical and quantum approaches. The learning phase is typically found at the transition between ordered and disordered phases [13], where the network can better explore and generalize real world data configurations. In this transition region, the system is flexible enough to adjust to new data configurations (disordered phase) while maintaining sufficient structure not to over fit (ordered phase).

In this sense, statistical mechanics provides us with a powerful framework for studying disordered systems: *The Replica Method*. This method, introduced by David Sher-

rington and Scott Kirkpatrick [9], allows us to analyse and understand the thermodynamic properties and phase transitions of these complex systems, enabling the *semi-classical* approximation. In particular, it has been successfully applied to the Sherrington-Kirkpatrick model [25, 26] and to Hopfield lattices [27, 28, 29].

As it is well known, the phase diagrams for the SK model (without an external field) and Hopfield networks are widely studied. Although these models are interesting in the realm of spin glasses, they do not reflect the effects of having a different external field for each spin. Now, as far as we know, the effects of random biases have been little studied, highlighting studies such as that of Nogueia et al. [30], where they study the effects of bimodal random external fields. That is, the value of the bias can be h_0 with a probability of P and $-h_0$ with a probability of $1-P$. In other words, the probability distribution for these external fields is two Dirac deltas $P(h_i) = P\delta(h_i - h_0) + (1-P)\delta(h_i + h_0)$. Another similar study can be found in [31], which differs in that zero external fields are considered for some sites. That is, they consider that the external fields follow the following probability distribution: $P(h_i) = P_+\delta(h_i - h_0) + P_0\delta(h_i) + P_-\delta(h_i + h_0)$, where $P_+ + P_0 + P_- = 1$. Despite considering different external fields for each site in the network, these studies only consider at most three different fields. This can be a drawback for studying neural networks, as there can be as many biases as there are neurons in the network.

In this regard, we will follow the direction of Hadjiagapiou [32] and Soares et al. [33], where random external fields following a Gaussian distribution are considered. With this, we can account for a variety of external fields acting on each neuron. Following this logic, our intention with this dissertation is not to "reinvent the wheel", but rather to introduce the study of neural networks as complex systems through physics. Motivated by this, we will consider three architectures: the BM, the Restricted Boltzmann Machine (RBM), which are classical formulations, and the QBM. In principle, these are different, but as we will see throughout this text, they have several common points concerning their macroscopic behavior. The differentiating factor of this text from those previously cited is that here we will consider the effects of both the mean of the biases h_0 and their standard deviation h, which we will call mean bias and variance bias, respectively.

Concerning the QBM, spin glasses in the presence of transverse fields, which introduce quantum effects into the system, have also been consistently studied [34]. The singularity in quantum spin glass models lies on the possibility of tunneling through barriers (which become infinitely high in the thermodynamic limit) of the free energy landscape in classical spin glass models due to quantum fluctuations induced by the transverse field. In a classical system, overcoming an infinitely high barrier is quite challenging for thermal fluctuations at any finite temperature; it is like walking up Everest if it had a height reaching Mars—it could take us a lifetime, and we still wouldn't make it! However, quantum fluctuations can allow a system to cross such a barrier if its width is small enough

that the area remains finite. Indeed, it is observed that the widths of the barriers decrease with the system size, suggesting a symmetric image in the replica space of the free energy landscape [35]. Nevertheless, the study of the effects of biases on the phase diagrams for these quantum systems is still under investigation.

Therefore, the main goal of this dissertation is to study the phase diagrams. Especially, we focus in the effects of biases on the macroscopic behavior of these complex systems, both for classical and quantum systems. Finally, to offer a concise and comprehensive guide to this thesis and facilitate reading through its logical structure and main ideas, we have organized it into seven chapters, with the current Chapter being the Introduction, as it follows:

- In Chapter 2, we will present the objectives of this dissertation.
- In Chapter 3, we will present some basic concepts fundamental to understanding the following chapters. In this chapter we will also briefly introduce the neural network models that we will study throughout this text.
- In Chapter 4, we will introduce the replica formalism, used to find the order parameters necessary to study and draw the phase diagrams of our systems. For this, we will use this formalism in the simplest model of this dissertation: the *BM*. Then, having studied this formalism, we will present the analytically found boundaries for the system without biases, in order to compare the numerical calculations with these analytical boundaries. Next, through numerical calculations, we will draw the phase diagrams for the system with different biases. Finally, we will analyze one of the recurrent problems when using the replica formalism: Negative Entropy! And we will analyze the stability of the solutions found and how it is affected by the biases.
- Having introduced the replica formalism, in Chapter 5, we will use this formalism to analyze the macroscopic properties of the *RBM*. First, through numerical calculations, we will compute the phase diagram for the system without biases, then by calculating the phase diagrams for different biases, we will analyse the effects of these on the macroscopic behavior of the neural network.
- In Chapter 6, we will begin by introducing the Suzuki-Trotter formalism to transform the quantum Hamiltonian into an effective classical Hamiltonian. Then, with the classical Hamiltonian, we will use the replica formalism to find the order parameters for the *QBM* in the semi-classical approximation, and finally, with them, compute the phase diagram at zero temperature. Finally, we will analyse the stability of the solutions found.
- Finally, in Chapter 7, we will present our conclusions and the next steps to follow in the research.

2 Objectives

The main objective of this project is to conduct a theoretical comparative analysis between the phase diagrams of classical and quantum Boltzmann machines in the semi classical approximation, using the Replica and Suzuki-Trotter methods, to understand the fundamental similarities and differences in the behavior of these stochastic neural networks at equilibrium. To achieve this, we divide the project into several stages related to the following specific objectives:

1. Employ the Replica and Suzuki-Trotter methods to perform semi classical approximations for both classical and quantum Boltzmann machines.

2. Compute and compare the phase diagrams of classical (in both architectures) and quantum Boltzmann machine in the semi classical approximation, highlighting the transitions between different phases of the network.

3. Analyse how variations in control parameters, such as temperature, transverse field (for quantum machines), interaction energy (synapses), and the intensity of the external field ("bias"), affect the transitions between network states.

3 Classical and Quantum Boltzmann Machine

In this section, we introduce some basic concepts of Statistical Mechanics and Monte Carlo methods that we will use in this document. We also want to introduce the models of NN which we will study through this text.

3.1 Statistical Mechanics Concepts

Statistical Mechanics provides a powerful framework for understanding the behavior of systems at thermal equilibrium. At its core lies the application of statistical methods to predict the collective behavior of a large number of individual particles, atoms, molecules or in the case at hand, neurons!!

In order to study the emergent properties of a microscopic many body system we need the functional of the probability distribution at equilibrium. A strategy to derive this distribution is using the maximum entropy principle [36]. For this end, let us consider the expression for the entropy:

$$S = -\sum_{\sigma} P(\sigma) ln P(\sigma), \tag{3.1}$$

being $P(\sigma)$ the probability of finding the system in a given state σ.

Our objective is to find the normalized distribution that maximizes the entropy (3.1), with the restriction of being normalized and with a constant average energy:

$$\sum_{\sigma} P(\sigma) = 1, \tag{3.2}$$

$$\sum_{\sigma} P(\sigma) E(\sigma) = \langle E \rangle. \tag{3.3}$$

By using the Lagrange multipliers we are able to find the probability $P(\sigma)$. Thus, we can write the Lagrangian introducing the multipliers α and β:

$$L = -\sum_{\sigma} P(\sigma) ln P(\sigma) - \beta \left(\sum_{\sigma} P(\sigma) E(\sigma) - \langle E \rangle \right) - \alpha \left(\sum_{\sigma} P(\sigma) - 1 \right). \tag{3.4}$$

Variation with respect to $P(\sigma)$ gives the desired probability distribution:

$$P(\sigma) = \frac{e^{-\beta E(\sigma)}}{Z}, \tag{3.5}$$

where:

$$Z = \sum_{\sigma} e^{-\beta E(\sigma)}, \tag{3.6}$$

is the Partition Function, and the parameter β is the inverse of the temperature: $\beta = \frac{1}{K_B T}$ (from here we will set $K_\beta = 1$). It seems a little strange to define a temperature for a NN (in particular if it is an ANN). Actually, it comes more naturally than we imagine if we think temperature as a level of noise or agitation in the system without considering the microscopic mechanisms causing that noise or agitation.

Other crucial quantity in Statistical Mechanics is the free energy, defined as follows:

$$F = \langle E(\sigma) \rangle - \frac{S}{\beta}. \tag{3.7}$$

Using Equations (3.1) and (3.5), we can write the following relationship between the free energy F and the partition function Z:

$$F = -\frac{1}{\beta} \ln(Z). \tag{3.8}$$

Note that according to Eq. (3.7), the principle of maximum entropy is equivalent to minimizing the free energy. It's also worth emphasizing that, in the Boltzmann-Gibbs distribution (Eq. 3.5), states with low energy have a higher probability of appearing at equilibrium. Conversely, as indicated in Eq. (3.7), the entropic term, weighted by temperature, competes with the tendency for states with low energy, allowing for other energy configurations. As temperature (T) approaches zero ($\beta \to \infty$), we meet a deterministic dynamics and the system's energy is minimized, whereas as T approaches infinity ($\beta \to 0$), the entropic term dominates, allowing for all energy states.

3.2 Markov Chain Monte Carlo

Markov Chain Monte Carlo (MCMC) methods are a class of algorithms widely used in statistics and computational science for sampling from probability distributions. These techniques use the principles of Markovian dynamics, where the evolution of a system over time is governed by the Markov property, which states that the future state of the system depends only on its current state and not by its past states.

Formally, given a sequential set of random variables

$$\{X_i : i = 1, 2, 3, ..., t\}, \tag{3.9}$$

where X_i is the configuration of the system at the time i. The evolution of this system is stochastic, thus governed by the transition probabilities:

$$P(X_{g+1} | X_0, X_1, ..., X_g : g \in i). \tag{3.10}$$

If this process is Markovian, *i.e.*, if it satisfies the Markov property, the transition probabilities become:

$$P(X_{g+1} | X_g : g \in i). \tag{3.11}$$

The transition to the new state $g+1$ just depends on the current state g. By renaming the variables $u = X_{g-1}$ and $v = X_g$, we can write:

$$P(u \to v) = P(X_g|X_{g-1}). \tag{3.12}$$

$P(u \to v)$ is the transition probability from the configuration u to configuration v. Since P is a probability, it must satisfy the Kolmogorov axioms [37]. In particular,

- Each transition probability is a positive, real number.
- The sum of all transition probabilities is unitary:

$$\sum_v P(u \to v) = 1. \tag{3.13}$$

This way, the time evolution of such systems may be described by the probability function P_u of finding the system in the configuration u at a time t and the transition probability $P(u \to v)$. We can write $P_v(t + \Delta t)$ of finding the system in the configuration v at a time $t + \Delta t$:

$$P_v(t + \Delta t) = \sum_u P_u P(u \to v). \tag{3.14}$$

Using Eq. (3.13), we can get:

$$\sum_v P_{eq}(v)P(v \to u) = \sum_u P_{eq}(u)P(u \to v), \tag{3.15}$$

the above equation is the *global balance condition*, from this condition we can construct the *detailed balance condition* [38]:

$$P_{eq}(v)P(v \to u) = P_{eq}(u)P(u \to v), \tag{3.16}$$

where $P_{eq}(u)$ is the equilibrium distribution of the system in the state u which, in our case, represents the *Boltzmann distribution*. The above condition means that the process has to be microscopically reversible [39].

3.3 Boltzmann Machine

This section explores an archetype of generative models known as energy-based models. An energy-based model utilizes principles from physics, such as energy functions, to represent and generate data. These models conceptualize data as configurations within an energy landscape, where each configuration is associated with an energy value. Lower energy configurations correspond to more probable data samples. The model's objective is to learn this energy function from the training data, enabling it to generate new samples consistent with the observed data distribution. In other words, these models have the

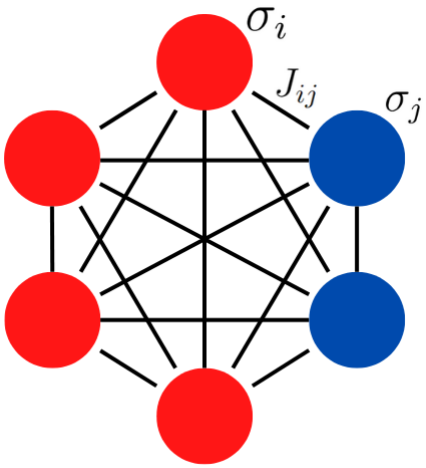

Figure 1 – Architecture of a Boltzmann Machine, the red circles represent visible neurons, the blue circles represent hidden neurons, and the lines represent the connections characterised by the weights J_{ij}. Both classes of neurons can be in a excited ($\sigma_i = 1$) or a rest state ($\sigma_i = -1$)

ability to comprehend any data distribution and subsequently produce new samples that mirror the original distribution. The discussion particularly centers around two types: the BM and the RBM. Furthermore, the chapter explores the learning approach involving the minimization of Kullback-Leibler(KL) divergence.

3.3.1 Boltzmann Machines

As we said above, a BM is a generative energy-based model with energy function:

$$H(\sigma) = -\sum_{i<j} J_{ij}\sigma_i\sigma_j - \sum_i \sigma_i h_i. \tag{3.17}$$

In the context of magnetic systems, the Ising spin variable $\sigma_i = \pm 1$ represents if the state of the microscopic magnetic moment is pointing up (1) or down (-1). Within the context of the Boltzmann Machine, the Ising spin σ_i is the state of the neuron i, thus we define $\sigma_i = 1$ if the neuron is excited and $\sigma_i = -1$ is the neuron is at rest. The variables J_{ij} and h_i represent the connection weights (or synapses) between neuron i and neuron j and the bias (or in the context of physics an external field) applied the neuron i, respectively.

As we can see in Fig.(1), the architecture of the BM is the one where every neuron in the network is connected with all the other neurons by the synapse J_{ij}. We also can distinguish between visible neurons and hidden neurons. The visible units are termed as such because they are used to represent data, and the hidden units introduce higher-order dependencies among the original nodes.

At equilibrium the system is described by the Boltzmann distribution:

$$P(\sigma) = \frac{e^{-\beta H(\sigma)}}{Z}, \tag{3.18}$$

Once again, Z is the partition function of the network. At this point we should note that knowing this partition function we can know the free energy, Eq.(3.8), of the system and thus characterise its properties at equilibrium.

Following the Detailed-balance condition Eq.(3.16), we can construct the probability transition that governs the dynamics towards equilibrium of the neural network as:

$$P\left(\sigma_i(t+1)\right) = \frac{e^{\beta\left(\sigma_i(t+1)\sum_{j\neq i} J_{ij}\sigma_j(t)+h_i\right)}}{2\cosh\beta\left(\sum_{j\neq i} J_{ij}\sigma_j(t)+h_i\right)}. \tag{3.19}$$

The equation (3.19) is interpreted as the probability of the neuron i be in the state $\sigma_i(t+1)$ at a time $t+1$, here we should point out that the state of the neuron at the next step of time depends on the local field $b_i(t) = \sum_{j\neq i} J_{ij}\sigma_j(t) + h_i$, that it is simply the input signal to neuron i at a time $t+1$. The aforementioned Eq.(3.19) establishes a probability distribution over the dataset, which is parameterized by $\mathbf{J}$ and $\mathbf{b}$. Given that the dataset conforms to a true data distribution, our objective is to identify the parameters that most accurately represent this distribution. Additionally, we introduce the criterion that the learned distribution should allow for efficient sampling. Thus, we arrive at a generative model of the data.

3.3.2 Restricted Boltzmann Machines

In the previous section, we have introduced a BM, but, despite the theoretical milestone, the practical utility of BM's are limited due to their computationally expensive training process, particularly for high-dimensional data. To address this challenge, RBM's introduce constraints that disallow connections among visible nodes and among hidden nodes, thereby enabling more efficient model training.

The architecture of the RBM is a bipartite graph, where we have two different layers: visible layer σ_i and hidden layer s_a. The neurons in one layer are not connected among them but they are connected with all the neurons in the other layer. The state of the neurons in each layer are Ising type, i.e., $\sigma_i = s_a = \pm 1$. Thus, the energy function of the RBM is:

$$H(\sigma, s) = -\sum_{i,a} J_{ia}\sigma_i s_a - \sum_i \sigma_i h_i - \sum_a s_a c_a, \tag{3.20}$$

where J_{ia} is the connection between visible neuron i and hidden neuron a, σ_i is the state of visible neuron i with bias h_i and s_a is the state of hidden neuron a with bias c_a.

The network state at equilibrium obey the Boltzmann distribution:

$$P(\sigma, s) = \frac{e^{-\beta H(\sigma,s)}}{Z}, \tag{3.21}$$

where $Z = \sum_\sigma \sum_s e^{-\beta H(\sigma,s)}$.

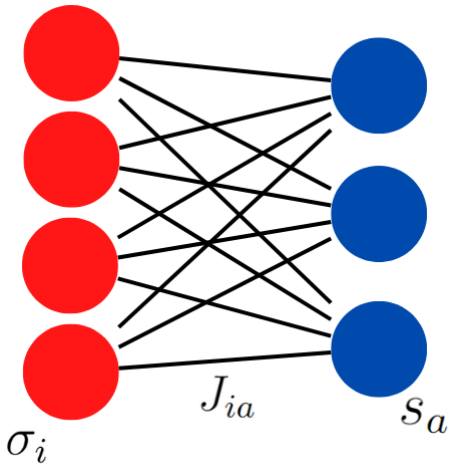

Figure 2 – Architecture of a restricted Boltzmann Machine, the red circles represent visible neurons, the blue circles represent hidden neurons and the lines represent the connections characterized by the weights J_{ia}. Both classes of neurons can be in a excited ($\sigma_i = 1$) or a rest state ($\sigma_i = -1$)

Now, we aim to go into the dynamics of the RBM. The crucial simplification in the RBM, compared with the BM, lies in the fact that units in the same layers are not connected: they are thus conditionally independent given the nodes in the other layer, and exploiting this fact we can compute the individual probabilities. And, according to Bayes' rule, we can write:

$$P(s|\sigma) = \frac{P(\sigma, s)}{\sum_s P(\sigma, s)}. \tag{3.22}$$

By using Eq.(3.20) into Eq.(3.21) and summing over the hidden units s, it is straightforward to get:

$$P(s|\sigma) = \prod_a P(s_a|\sigma), \tag{3.23}$$

where:

$$P(s_a|\sigma) = \frac{e^{\beta s_a (c_a + \sum_i \sigma_i J_{ia})}}{2\cosh\left[\beta\left(c_a + \sum_i \sigma_i J_{ia}\right)\right]}. \tag{3.24}$$

Process (3.22) is called *recognition*, where given the states of visible neurons we can easily sample the states of hidden neurons. Equation (3.24) is the probability that given the states of the neurons in the visible layer, the state of neuron a in the hidden layer will be s_a.

Then, the network can reconstruct the states of the visible neurons with the states of the hidden neurons by carrying out the converse process given by:

$$P(\sigma|s) = \prod_i P(\sigma_i|s), \tag{3.25}$$

where:

$$P(\sigma_i|s) = \frac{e^{\beta\sigma_i (h_i + \sum_a s_a J_{ia})}}{2\cosh\left[\beta(h_i + \sum_a s_a J_{ia})\right]}. \tag{3.26}$$

This process is usually called *reconstruction*. Note that in both processes (3.24) and (3.26) the transition probability depends on the input signal and it is controlled by the temperature. Finally, as we only have access (to input the data for the training or when the machine generate new samples) to visible units in the RBM we need the marginal distribution of these variables. We can get this marginal distribution summing over the hidden units (marginalizing):

$$P(\sigma) = \sum_{s} P(\sigma, s). \tag{3.27}$$

With a little bit of algebra (and absolutely no sarcasm intended, it requires less than a page of calculation!) we get:

$$P(\sigma) = \frac{1}{Z} e^{-F_c}, \tag{3.28}$$

with:

$$F_c = -\beta \sum_i \sigma_i h_i - \sum_a \ln \left(2 \cosh \beta \left(\sum_i J_{ia} \sigma_i + c_a \right) \right), \tag{3.29}$$

F_c is often called *clamped free energy*[40].

3.4 Training Process

The aim of the RBM as a generative model is to learn the marginal distribution $P_d(\sigma)$ belonging to the training data, *i.e.*, in the learning process the parameters $\theta \in \{J_{ia}, b_i, c_a\}$ must be determinated such that the distribution $P(\sigma)$ generated by the network be as close as possible to $P_d(\sigma)$. The parameters θ can be learned by maximizing the data log-likelihood or, equivalently, minimizing the so called Kullback-Leibler (KL) divergence[41], that quantifies the loss of information if the distribution generated by the network $P(\sigma)$ replaces the data distribution $P_d(\sigma)$, and it is given by:

$$D_{KL}(P_d(\sigma)||P(\sigma)) = \sum_{t=1}^{T} P_d(\sigma^t) \ln \frac{P_d(\sigma^t)}{P(\sigma)}. \tag{3.30}$$

The sum is over a dataset $\{\sigma^1, \sigma^2, \sigma^3, ..., \sigma^T\}$, where $\sigma^i = (\sigma_1^i, \sigma_2^i, \sigma_3^i, ..., \sigma_N^i)$ is an example of the dataset (which contains T examples) if N is the number of neurons in the visible layer. We can observe that the term $P_d(\sigma^t) \ln P_d(\sigma^t)$ does not depend on the parameters and its gradient with respect to them is *zero*, thus minimizing (3.30) is equivalent to minimizing:

$$L(\theta) = -\sum_t P_d(\sigma^t) \ln P(\sigma) = -\langle \ln P(\sigma) \rangle_{data}. \tag{3.31}$$

Using Eq.(3.27) and Eq.(3.29), we get:

$$L(\theta) = \langle F_c \rangle_{data} + \ln Z. \tag{3.32}$$

We can use the gradient descent algorithm to update the parameters θ. At each iteration θ is updated by:

$$\Delta\theta = \theta^{new} - \theta^{old} = -\alpha\nabla_\theta L(\theta), \tag{3.33}$$

where α is the learning step that controls the size of each step in the descent. The gradient $\nabla_\theta L(\theta)$ also controls the size of the step since, as the gradient approaches the minimum, it becomes smaller and smaller. The choice of α is fundamental because if α is too large, the algorithm may oscillate around the minimum of the cost function (3.32) or even diverge. Conversely, if the learning step is too small, the algorithm may converge slowly towards the minimum.

Using Eq.(3.32) and Eq.(3.20) is easy to obtain:

$$\nabla_{J_{ij}} L(J_{ij}, h_i, c_a) = -\beta(\langle\sigma_i s_a\rangle_{data} - \langle\sigma_i s_a\rangle_{model}), \tag{3.34}$$

$$\nabla_{h_i} L(J_{ij}, h_i, c_a) = -\beta(\langle\sigma_i\rangle_{data} - \langle\sigma_i\rangle_{model}), \tag{3.35}$$

$$\nabla_{c_j} L(J_{ij}, h_i, c_a) = -\beta(\langle s_a\rangle_{data} - \langle s_a\rangle_{model}). \tag{3.36}$$

Finally, Eq.(3.33) becomes:

$$\Delta J_{ij} = -\alpha\beta(\langle\sigma_i s_a\rangle_{data} - \langle\sigma_i s_a\rangle_{model}), \tag{3.37}$$

$$\Delta h_i = -\alpha\beta(\langle\sigma_i\rangle_{data} - \langle\sigma_i\rangle_{model}), \tag{3.38}$$

$$\Delta c_j = -\alpha\beta(\langle s_a\rangle_{data} - \langle s_a\rangle_{model}). \tag{3.39}$$

3.5 Quantum Boltzmann Machine

Having briefly explored the principles of the classical Boltzmann machine, our attention now shifts towards its quantum analogue, the QBM. QBMs uses the intrinsic properties of quantum mechanics, such as superposition and entanglement, to efficiently explore and represent high-dimensional states.

In a QBM, qubits replace classical spins[23, 42]:

$$H(\sigma) = -\sum_{i<j} J_{ij}\sigma_i^z\sigma_j^z - \sum_i \sigma_i^z h_i. \tag{3.40}$$

The Hamiltonian (3.40) is a diagonal matrix with dimension $2^N \times 2^N$ where its diagonal elements are the possible states of the network, and the operators σ_i^z are the Pauli matrix z acting on the ith qubit and in the qubit $j \neq i$ is acting the identity operator:

$$\sigma_i^z = \underbrace{I \otimes \cdots I}_{i-1} \otimes \overbrace{\sigma^z}^{i} \otimes \underbrace{I \cdots \otimes I}_{N-i}, \tag{3.41}$$

where:

$$\sigma^z = \begin{pmatrix} 1 & 0 \\ 0 & -1 \end{pmatrix}, \tag{3.42}$$

and

$$I = \begin{pmatrix} 1 & 0 \\ 0 & 1 \end{pmatrix}. \tag{3.43}$$

We know that the the eigenvalues of Eq.(3.42) are $(-1, 1)$ with eigenvectors $|0\rangle = \begin{pmatrix} 0 \\ 1 \end{pmatrix}$ and $|1\rangle = \begin{pmatrix} 1 \\ 0 \end{pmatrix}$, respectively.

The thermal state of this network is described by the density matrix[23]:

$$\rho = \frac{e^{-\beta H(\sigma)}}{Z}, \tag{3.44}$$

where $Z = Tre^{-\beta H(\sigma)}$.

As the Hamiltonian (3.40) is a diagonal matrix, by the matrix exponentiation through Taylor expansion $e^{-\beta H} = \sum_{k=0}^{\infty} \frac{1}{K!}(H(\sigma))^K$ we can see that the density matrix (3.44) is also a diagonal matrix and thus, a classical one, where the entries of the diagonal are simply the Boltzmann probabilities of the 2^N states.

To introduce quantum effects, we simply add off-diagonal terms to the density matrix, for instance by introducing a transversal field:

$$H_T = -\Omega \sum_i \sigma_i^x, \tag{3.45}$$

where,

$$\sigma_i^x = \underbrace{I \otimes \cdots I}_{i-1} \otimes \overbrace{\sigma^x}^{i} \otimes \underbrace{I \cdots \otimes I}_{N-i}, \tag{3.46}$$

with:

$$\sigma^x = \begin{pmatrix} 0 & 1 \\ 1 & 0 \end{pmatrix}. \tag{3.47}$$

With this extra term in the Hamiltonian, the density matrix (3.44) has off-diagonal terms related with quantum effects, such as superposition, entanglement between qubits and tunnelling[43].

3.5.1 Training a Quantum Boltzmann Machine

We have defined the QBM Hamiltonian (3.40) plus the non-commuting term (3.45):

$$H(\sigma) = -\sum_{i<j} J_{ij}\sigma_i^z\sigma_j^z - \sum_i h_i\sigma_i^z - \Omega\sum_i \sigma_i^x. \tag{3.48}$$

In this section our aim is to define the training process for this QNN . In this QNN, both data and models are represented by a density matrix ρ (or density operators). Essentially, a density matrix serves as a more general form of a probability distribution, reverting to a conventional probability distribution when it becomes diagonal. The density matrix ρ has trace one ($Tr(\rho) = 1$) and is a positive semi-definite Hermitian operator[44].

We follow the method proposed in [45]. The function we want to minimize is the quantum relative entropy, that is a generalization of the KL divergence:

$$S(\rho||\Pi) = Tr(\rho \ln \rho - \rho \ln \Pi), \tag{3.49}$$

where ρ is the data density matrix and $\Pi = \frac{e^{-\beta H}}{Z}$ is the thermal state generated by the QBM, with $Z = Tr(e^{-\beta H})$. As in the classical case, the first therm of the relative entropy does not depend on the parameters, thus the function that we will minimize for the training is:

$$L_\rho = -Tr(\rho \ln \Pi). \tag{3.50}$$

We can write the above equation as:

$$L_\rho = -Tr(\rho(-\beta H)) + Tr(\rho \ln Z) = \beta \langle H \rangle_\rho + \langle \ln Z \rangle_\rho, \tag{3.51}$$

where $\langle O \rangle_\rho \equiv Tr(\rho O)$ is the expectation value of the operator O taken with respect the density matrix ρ, and $Tr(\rho \ln Z) = \ln Z Tr(\rho) = \ln Z$.

The learning process is given by gradient descent with the cost function Eq.(3.51). Now, we need to calculate the gradient:

$$\partial_\theta L_\rho = \beta \partial_\theta \langle H \rangle_\rho + \partial_\theta \ln Z, \tag{3.52}$$

here, $\partial_\theta = \frac{\partial}{\partial \theta}$ and $\theta \in \{J_{ia}, h_i, \Omega\}$.

The first term is obtained using Eq.(3.48) and

$$\langle H(\sigma) \rangle_\rho = -\sum_{ij} J_{ij} \langle \sigma_i^z \sigma_j^z \rangle_\rho - \sum_i h_i \langle \sigma_i^z \rangle_\rho - \Omega \sum_i \langle \sigma_i^x \rangle_\rho, \tag{3.53}$$

thus, we can obtain:

$$\partial_{J_{ij}} \langle H \rangle_\rho = -\langle \sigma_i^z \sigma_j^z \rangle_\rho, \tag{3.54}$$

$$\partial_{h_i} \langle H \rangle_\rho = -\langle \sigma_i^z \rangle_\rho, \tag{3.55}$$

$$\partial_\Omega \langle H \rangle_\rho = -\sum_i \langle \sigma_i^x \rangle_\rho. \tag{3.56}$$

For the second term of Eq.(3.51) we need use the Duhamel's formula to obtain[46]:

$$\partial_\theta \ln Z = -\beta \frac{Tr(e^{-\beta H} \partial_\theta H)}{Tr(e^{-\beta H})}, \tag{3.57}$$

using Eq.(3.48) we can obtain:

$$\partial_{J_{ij}} \ln Z = \beta \langle \sigma_i^z \sigma_j^z \rangle_\Pi, \tag{3.58}$$

$$\partial_{h_i} \ln Z = \beta \langle \sigma_i^z \rangle_\Pi, \tag{3.59}$$

$$\partial_\Omega \ln Z = \beta \sum_i \langle \sigma_i^x \rangle_\Pi. \tag{3.60}$$

With the gradients in hand, we can write the gradient descent equations:

$$\Delta J_{ij} = -\alpha\beta(\langle \sigma_i^z \sigma_j^z \rangle_\rho - \langle \sigma_i^z \sigma_j^z \rangle_\Pi), \tag{3.61}$$

$$\Delta h_i = -\alpha\beta \left(\langle \sigma_i^z \rangle_\rho - \langle \sigma_i^z \rangle_\Pi \right), \tag{3.62}$$

$$\Delta \Omega = -\alpha\beta \left(\sum_i \langle \sigma_i^x \rangle_\rho - \sum_i \langle \sigma_i^x \rangle_\Pi \right), \tag{3.63}$$

where α is the learning step and, as in the classical case, it controls the size of the steps in the gradient descent algorithm.

4 Phase Diagram of the Boltzmann Machine

Having briefly explained the systems to be analyzed, this chapter focuses on the detailed exploration of the phase diagram of the Boltzmann Machine using the replica formalism. The replica method is a powerful technique used to solve problems in disordered systems, allows us to unravel phase transitions and the nature of equilibrium states in systems with multiple solutions or configurations. Throughout this chapter, by the application to the Boltzmann machine, the theoretical development of the replica method will be discussed, its relationship with the mean field approximation, and the results obtained from the characterization of the phase diagram.

4.1 Replica Method

We start considering the BM with the energy function Eq.(3.17):

$$H(\sigma) = -\sum_{i<j} J_{ij}\sigma_i\sigma_j - \sum_i h_i\sigma_i. \tag{4.1}$$

The sum of the first term on the right side of the above equation runs over all pairs of neurons, then we have $N(N-1)/2$ connection terms. From the second term we should remark that every neuron has a different external field. In neural networks this is the rule because each neuron requires a different bias to finely adjust the activation of each one and provide flexibility in representing specific features. This prevents undesirable symmetries and allows neurons to diverge in their learned patterns, enhancing the network's ability to represent and distinguish complex patterns. Additionally, individual biases facilitate better convergence during training and help compensate for different scales in the input data, optimizing the network's learning and generalization capabilities [47, 48, 49].

We assume that the synapses (J_{ij}) and the biases (h_i) are independent and identically distributed (i.i.d.) random variables following Gaussian distribution functions:

$$P(J_{ij}) = \sqrt{\frac{N}{2\pi J^2}}\exp\left[-\frac{N}{2J^2}\left(J_{ij}-\frac{J_0}{N}\right)^2\right]; \quad P(h_i) = \sqrt{\frac{1}{2\pi h^2}}\exp\left[-\frac{1}{2h^2}(h_i-h_0)^2\right], \tag{4.2}$$

with mean and variance

$$[J_{ij}]_a = \frac{J_0}{N}, \qquad [(\Delta J_{ij})^2]_a = \frac{J^2}{N}, \tag{4.3}$$

$$[h_i]_a = h_0, \qquad [(\Delta h_i)^2]_a = h^2, \tag{4.4}$$

where

$$[\cdot]_a = \int \prod_{i<j} P(J_{ij})dJ_{ij} \int \prod_i P(h_i)dh_i, \tag{4.5}$$

is called *configurational average*.

Now, we want to study the properties of the network at equilibrium. In order to do this we need to calculate the free energy given by Eq.(3.8). The problem here lies on the fact that Eq.(3.8) depends on the realisation of J_{ij} and h_i:

$$F(J,h) = -\frac{1}{\beta} ln(Z(J,h)), \tag{4.6}$$

this is very inconvenient, as it appears to imply that the physical properties of this class of systems are different for each specific configuration of the disorder in the synapses and the external fields. Fortunately, we know that the free energy per neuron $f = F/N$ in the thermodynamic limit has the self-averaging property [50]:

$$f \underset{N\to\infty}{=} [f]_a. \tag{4.7}$$

The free energy $[f]_a$ is easier to handle because it does not explicitly depend on the realisation of synapses ($\mathbf{J}$) and biases ($\mathbf{h}$). Thus, in the thermodynamic limit:

$$f = -\lim_{N\to\infty} \frac{1}{\beta N} [\ln(Z)]_a. \tag{4.8}$$

4.1.1 Replica Trick

We saw that the free energy has a dependence on the disorder in the synapses and biases and the configurational average of $\ln(Z)$ must be taken, which is difficult to calculate due to the complicated dependence on $\{\mathbf{J}\}$ and $\{\mathbf{h}\}$ and the non-linearity of the logarithm. We can handle this issue by using the relation:

$$[\ln(Z)]_a = \lim_{n\to 0} \frac{[Z^n]_a - 1}{n}. \tag{4.9}$$

Thus, in the replica method, supported by the above relationship, one basically takes the product of n replicas of the system, evaluate the configurational average and finally calculate the limit $n \to 0$.

We give a simple derivation of Eq.(4.9) in the Appendix A. The replica method actually has a "caveat": You will note that we will evaluate Z^n with n integer in mind, thus the relation (4.9) is meaningless since integers cannot continuously approach 0. On the other hand there exists a method more rigorous than the replica trick: *the cavity approximation*. However, in most cases, both methods produce the same result [51, 52].

Now, using Eq.(4.9) into Eq.(4.8) we get:

$$f = -\frac{1}{\beta} \lim_{N\to\infty} \lim_{n\to 0} \frac{[Z^n]_a - 1}{Nn}. \tag{4.10}$$

With the recipe at hand, we first write the replicated partition function

$$[Z^n]_a = \int \prod_{i<j} P(J_{ij}) dJ_{ij} \int \prod_i P(h_i) dh_i \, \mathrm{Tr} \exp\left[\beta \sum_{\alpha=1}^{n} \sum_{i<j} J_{ij} \sigma_i^\alpha \sigma_j^\alpha + \beta \sum_{\alpha=1}^{n} \sum_i h_i \sigma_i^\alpha\right], \quad (4.11)$$

Here, σ_i^α is the state of the neuron i in the replica α. We should note that the first term in the exponential only depends on J_{ij} and the second term does on h_i, thus the terms can be divided and integrated separately to obtain:

$$[Z^n]_a = \mathrm{Tr} \prod_{i<j} \exp\left[\frac{J^2\beta^2}{2N}(\sum_\alpha \sigma_i^\alpha \sigma_j^\alpha)^2\right] \exp\left[\frac{J_0\beta}{N} \sum_\alpha \sigma_i^\alpha \sigma_j^\alpha\right] \prod_i \exp\left[\frac{h^2\beta^2}{2}(\sum_\alpha \sigma_i^\alpha)^2\right] \exp\left[\beta h_0 \sum_\alpha \sigma_i^\alpha\right]. \quad (4.12)$$

To evaluate the trace, we linearize the quadratic terms in the exponential by using the Hubbard-Stratonovich (HS) transformation, we get (the details of the calculations are in Appendix B):

$$[Z^n]_a = f(N,n) \int \prod_{\alpha<\gamma} dq_{\alpha\gamma} \int \prod_\alpha dm_\alpha \exp\left[-\frac{\beta^2 J^2}{2} N \sum_{\alpha<\gamma} q_{\alpha\gamma}^2 - \frac{\beta J_0}{2} N \sum_\alpha m_\alpha^2\right] \mathrm{Tr} \exp\left[\beta^2 \sum_{\alpha<\gamma} (J^2 q_{\alpha\gamma} + h^2) \sum_i \sigma_i^\alpha \sigma_i^\gamma + \beta \sum_\alpha (J_0 m_\alpha + h_0) \sum_i \sigma_i^\alpha\right], \quad (4.13)$$

where

$$f(N,n) = \exp\left[\frac{\beta^2}{s} N n (J^2 + n h^2)\right]. \quad (4.14)$$

We have obtained a partition function without correlations between neurons, *i.e.* using the replica method, we made the mean field approximation. The cost of this approximation is the emergence of correlations between neurons in different replicas and the integrals over the variables $q_{\alpha\gamma}$ and m_α. The parameters $q_{\alpha\gamma}$ and m_α were introduced in the mathematical manipulations in the integrals (see Appendix B) are the order parameters of the system [27]. We are not considering the constants that emerge from Gaussian integrals because they become 1 in the limit $n \to 0$.

Manipulating the trace term in the Eq.(4.13) we obtain:

$$[Z^n]_a = f(N,n) \int dq_{\alpha\gamma} \int dm_\alpha \exp\left[-\frac{\beta^2 J^2}{2} N \sum_{\alpha<\gamma} q_{\alpha\gamma}^2 - \frac{\beta J_0}{2} N \sum_\alpha m_\alpha^2\right] \exp\left[N \ln\left(Tr_\alpha e^L\right)\right], \quad (4.15)$$

where $Tr_\alpha = \prod_\alpha \sum_{\sigma^\alpha}$, $\sigma^\alpha = \pm 1$ and

$$L = \beta^2 \sum_{\alpha<\gamma} (J^2 q_{\alpha\gamma} + h^2) \sigma^\alpha \sigma^\gamma + \beta \sum_\alpha (J_0 m_\alpha + h_0) \sigma^\alpha. \quad (4.16)$$

We have an integral of the form $\int dx \int dy \exp[-NG(x,y)]$, the exponent in the integral [1] is proportional to N, thus in the thermodynamic limit ($N \to \infty$), the value of the integral is determined by the minimum point (steepest descent method) of $G(x,y)$ with:

$$G(q_{\alpha\gamma}, m_\alpha) = \frac{\beta^2 J^2}{2} \sum_{\alpha<\gamma} q_{\alpha\gamma}^2 + \frac{\beta J_0}{2} \sum_\alpha m_\alpha^2 - \ln\Big(Tr_\alpha e^L\Big). \tag{4.17}$$

Then, the partition function simply reads:

$$[Z^n]_a = f(N,n) \exp\left[-\frac{\beta^2 J^2}{2} N \sum_{\alpha<\gamma} q_{\alpha\gamma}^2 - \frac{\beta J_0}{2} N \sum_\alpha m_\alpha^2\right] \exp\Big[N \ln\Big(Tr_\alpha e^L\Big)\Big]. \tag{4.18}$$

The parameters $q_{\alpha\gamma}$ and m_α can be determined by the condition that G must have an extreme point, i.e., $\frac{\partial G}{\partial q_{\alpha\gamma}} = \frac{\partial G}{\partial m_\alpha} = 0$, thus obtaining:

$$q_{\alpha\gamma} = \frac{Tr_\alpha e^L \sigma^\alpha \sigma^\gamma}{Tr_\alpha e^L} = \langle \sigma^\alpha \sigma^\gamma \rangle_L \,, \tag{4.19}$$

$$m_\alpha = \frac{Tr_\alpha e^L \sigma^\alpha}{Tr_\alpha e^L} = \langle \sigma^\alpha \rangle_L \,. \tag{4.20}$$

The subscripts L mean that the expected value is taken with respect to e^L, the variables above represent the order parameters of the network. The physical significance of them is as follows: m_α is the magnetization similar to the Ising model, which indicates the degree of alignment of the spins in one replica (α) and provides insight into the macroscopic magnetic properties of the network. On the other hand, $q_{\alpha\gamma}$ is the overlap parameter, and measures the similarity between the spin configurations of different replicas and in the replica symmetric solution this parameter is just the square of the magnetization [9].

Now, using Eq.(4.18) into Eq.(4.10) we are able to write the free energy as:

$$-\beta f = \lim_{n\to 0} \left(\frac{\beta^2}{2}(J^2/2 + nh^2) - \frac{\beta^2 J^2}{2n} \sum_{\alpha<\gamma} q_{\alpha\gamma}^2 - \frac{\beta J_0}{2n} \sum_\alpha m_\alpha^2 + \frac{1}{n} \operatorname{Tr}_\alpha e^L \right). \tag{4.21}$$

4.1.2 Replica Symmetric Solution

In order to evaluate the limit in the above equation, we need an explicit dependence of $q_{\alpha\gamma}$ and m_α on the replicas, the simplest assumption is that the order parameters does not depend on the replica indices (replica symmetry), *i.e.*,

$$q_{\alpha\gamma} = q \qquad \forall\ \alpha \neq \gamma, \qquad\qquad q_{\alpha\gamma} = 0 \qquad \forall\ \alpha = \gamma, \tag{4.22}$$

$$m_\alpha = m \qquad \forall\ \alpha. \tag{4.23}$$

[1] To calculate such integral we need another "trick": invert the order of the limits in Eq.(4.10). Such inversion does not seem rigorous, mathematically speaking, however, the results are consistent [51, 52].)

Thus, we have $n(n-1)/2$ identical order parameters in the case of $q_{\alpha\gamma}$ and n in the case of m_α. Then, the replica symmetric free energy is:

$$-\beta f = \frac{\beta^2 J^2}{4} - \lim_{n\to 0}\left(\frac{\beta^2 J^2}{2n}\frac{n(n-1)}{2}q^2 + \frac{\beta J_0}{2n}nm^2 - \frac{1}{n}\operatorname{Tr}_\alpha e^L\right). \tag{4.24}$$

Evaluating the limit, we obtain:

$$-\beta f = \frac{\beta^2 J^2}{4} + \frac{\beta^2 J^2}{4}q^2 - \frac{\beta J_0}{2}m^2 + \lim_{n\to 0}\frac{1}{n}\operatorname{Tr}_\alpha e^L. \tag{4.25}$$

We know that (see Appendix B.1 for a detailed derivation):

$$\lim_{n\to 0}\frac{1}{n}\operatorname{Tr}_\alpha e^L = \int Dz \ln[2\cosh\left(\beta\tilde{H}(z)\right)] - \frac{\beta^2}{2}(J^2 q + h^2), \tag{4.26}$$

with $Dz = \frac{1}{\sqrt{2\pi}}e^{-z^2/2}dz$ and $\tilde{H}(z) = \sqrt{J^2 q + h^2}z + J_0 m + h_0$. Thus, the Eq.(4.25) can be written as:

$$-\beta f = \frac{\beta^2 J^2}{4}(1-q)^2 - \frac{\beta J_0}{2}m^2 + \int Dz \ln[2\cosh\left(\beta\tilde{H}(z)\right)] - \frac{\beta^2}{2}h^2. \tag{4.27}$$

Finally, the order parameters are obtained by the extremization condition of the free energy:

$$m = \int Dz \tanh\left(\beta\tilde{H}(z)\right), \tag{4.28}$$

$$q = \int Dz \tanh^2(\beta\tilde{H}(z)). \tag{4.29}$$

4.2 Phase Diagram

Having encountered the equations of state (4.28 and 4.29) we are able to draw the phase diagram. We identify three different phases:

- Paramagnetic (P) phase, characterized by $m = q = 0$.
- Ferromagnetic (F) phase with $m \neq 0$ and $q \neq 0$.
- Spin Glass (SG) phase with $m = 0$ and $q \neq 0$.

4.2.1 Phase Diagram for no biases network

First we will describe the boundaries between the above phases for no biases ($h_0 = h = 0$). The boundaries between Paramagnetic with the Ferromagnetic and Spin Glass phases were solved analytically, but the boundary between Spin Glass with Ferromagnetic phases is a little more complicated, needed to be solved numerically.

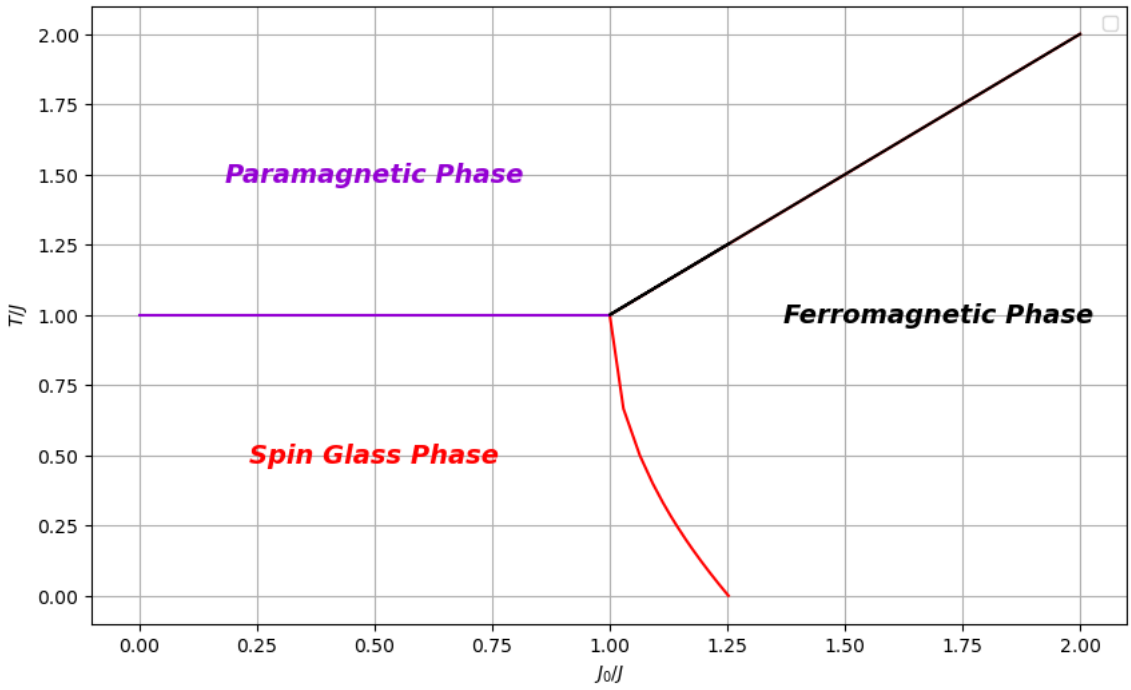

Figure 3 – Phase diagram (temperature versus mean coupling between the spins) of the Boltzmann Machine with no biases.

Figure 3 shows the phase diagram obtained. The P-SG boundary, depicted by the violet line, is a horizontal line at $T/J = 1$. While both phases exhibit zero magnetization ($m = 0$), they are qualitatively different. In the P phase, the zero magnetization results from thermal fluctuations, allowing states ± 1 with equal probability, resulting in zero magnetization at each site in the network. In contrast, the SG phase presents a different scenario: although the net magnetization is zero, each site can have a non-zero magnetization (m_i), with some sites having $m_i > 0$ and others $m_i < 0$, due to disorder in the synapses. The two phases can be quantitatively distinguished by the value of q, In the P phase, this order parameter is zero, whereas in the SG phase, q is non-zero.

The black line in Figure 3 represents the P-F boundary. This phase transition is characterized by spontaneous symmetry breaking, where the phase space that the system can explore is limited. Spontaneous symmetry breaking occurs when a system that is symmetric under some symmetry group goes into a state that is not symmetric. In the context of the P-F boundary, this means that while the paramagnetic (P) phase allows for equal probabilities of states $+1$ and -1, resulting in zero net magnetization, the ferromagnetic (F) phase favors one state over the other. This results in a non-zero magnetization, breaking the symmetry as the system chooses one direction (either positive or negative magnetization) spontaneously [53, 54, 55]

The red line represents the SG-F boundary; however, this is not the correct boundary due to the effects of Replica Symmetry Breaking (RSB). When these effects are considered, the red line disappears and it is replaced by a vertical line at $J_0/J = 1$, which serves as the

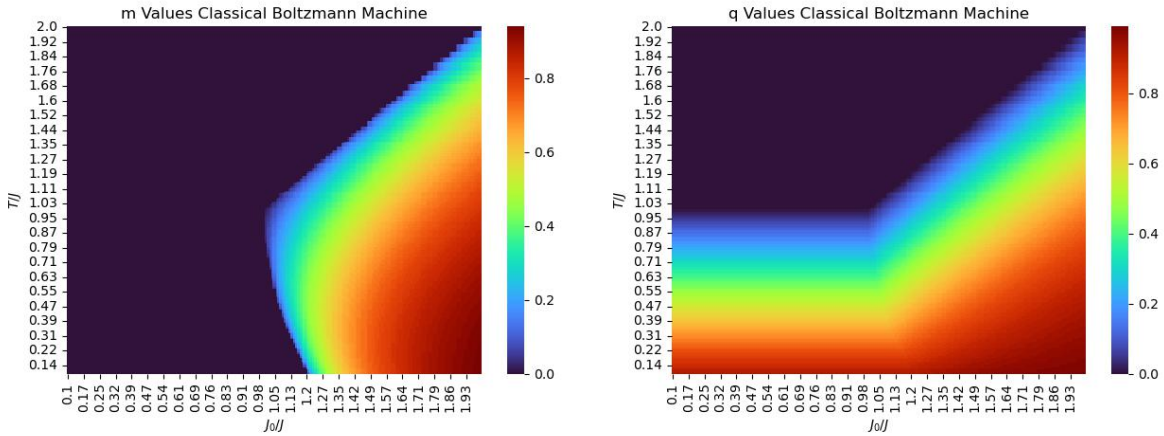

(a) m Phase diagram of the BM.

(b) q Phase diagram of the BM.

Figure 4 – Phase diagram of the Boltzmann Machine with no biases. (a): m heat map for the system without biases. (B): q heat map for the system without biases.

boundary between the Spin Glass (SG) phase and a Mixed (M) phase. The Mixed phase is essentially a ferromagnetic phase with RSB [27]. The boundary between the Mixed and Ferromagnetic (F) phases is defined by the AT line [56], as discussed in the final section of this chapter.

4.2.2 Effects of the Biases in the Boltzmann Machine

Furthermore, we solve numerically the equations of state (4.28 and 4.29) to see the effects of the biases in the behavior of the network. In order to facilitate the numerical calculations hereafter, we used $J = 1$ and every other magnitude is measured as a function of this coupling, for example the mean bias we will write simply as h_0, but actually the magnitude is h_0/J.

At first, in order to compare the results from the previous section, we solved the system without biases. Figure 4 illustrates the resulting phase diagram. In Figure 4a, we present the phase diagram for the m order parameter. Here, we can only distinguish two regions: one in the purple region with $m = 0$, and another with $m \neq 0$. Two phases are characterized by having zero magnetization, SG and P phases, so we can only differentiate the Ferromagnetic phase from the other two phases using the m order parameter. To distinguish all the phases, we need to examine the q phase diagram (Figure 4b), where we can recognize the Paramagnetic phase in the purple region, with $q = 0$ and $m = 0$. In addition, the q together with the m diagram permit us to note the Spin Glass phase in the region below $T/J = 1$ with $m = 0$ and $q \neq 0$. In this context, this two phase diagrams allows us to clearly identify the three phases; the boundaries are the same as those found in the previous section in Fig. 3.

Now, we want to examine the effect of the biases on the behavior of the network.

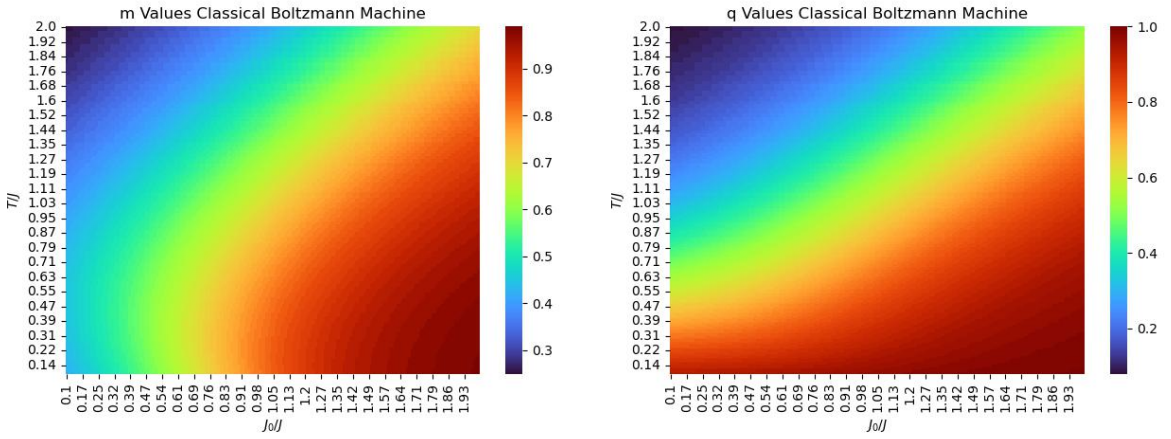

(a) m Phase diagram of the BM. (b) q Phase diagram of the BM.

Figure 5 – Phase diagram of the Boltzmann Machine with mean bias $h_0 = 0.5$. (a): m heat map for the system with mean bias $h_0 = 0.5$. (B): q heat map for the system with mean bias $h_0 = 0.5$

.

Given that the biases follow a Gaussian distribution function, we solve the problem for different mean bias values $h_0 = 0.5$ and $h_0 = 1.5$, keeping the variance $h = 0$. Additionally, we solve the problem for different variance values $h = 0.5$ and $h = 1.5$, keeping the mean bias $h_0 = 0$.

Our objective is to analyze separately how the mean bias h_0 and the variance h affect the phase diagram. By addressing the mean bias and the variance independently, we can obtain a clearer understanding of the specific influence of each of these parameters on the overall behavior of the network.

If we add a low mean bias to the system ($h_0 = 0.5$), the sizes of the Paramagnetic and Spin Glass phases decrease considerably. In both Figures 5a and 5b, we observe that the regions with zero magnetization (m) and overlap (q) values, indicative of the Paramagnetic Phase, almost disappear, leaving only a small Paramagnetic Phase.

In Figure 5a, we can distinguish a large area divided into three regions: one with low magnetization (blue area), one with medium magnetization (yellow area), and one with high magnetization (red area). This differentiation in magnetization levels is a clear signal of the Ferromagnetic phase. The existence of non-zero q values in the region above $T/J = 1$ in Figure 5b, coupled with the low m values in Figure 5a, indicates the presence of a small Spin Glass phase.

These observations highlight how introducing a mean bias affects the phase diagram of the system, specifically shrinking the Paramagnetic and Spin Glass phases and stimulating the growth of the Ferromagnetic phase.

When we increase the mean bias to $h_0 = 1.5$, we observe in Figure 6 that the Paramagnetic and Spin Glass phases have practically disappeared, leaving only the

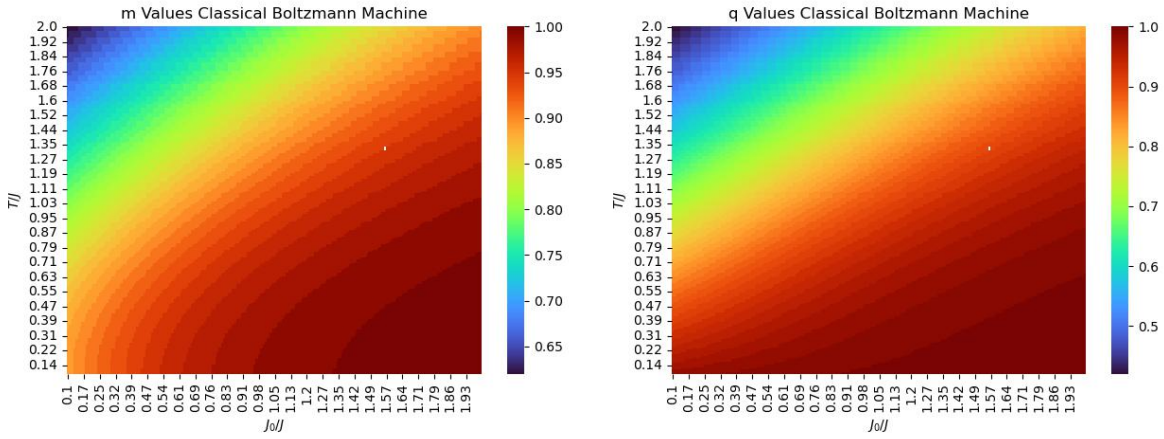

(a) m Phase diagram of the BM. (b) q Phase diagram of the BM.

Figure 6 – Phase diagram of the Boltzmann Machine with mean bias $h_0 = 1.5$. (a): m heat map for the system with mean bias $h_0 = 1.5$. (B): q heat map for the system with mean bias $h_0 = 1.5$

.

Ferromagnetic phase. This phase is characterized by non-zero values of m and q, and a larger region of high magnetization (red area). This is indicative of a Ferromagnetic phase without spontaneous symmetry breaking because a symmetry breaking already exists, known as *Explicit Symmetry Breaking (ESB)*, generated by the non-zero bias.

Although I call this phase Ferromagnetic due to the non-zero magnetization ($m \neq 0$), it is generally referred to as Paramagnetic because the ground state is unique. This is in contrast to the two-fold degenerate ground state of the Ferromagnetic phase without bias, and because there is no symmetry breaking [57].

We also highlight the emergence or increase in size of magnetization and overlap "equipotential" bands. The boundaries of these bands represent transitions from high to low magnetization as the control parameter J_0 decreases or the temperature T increases.

The mean bias h_0 acts similarly to applying an equal bias to each neuron; it magnetizes the network. A high mean bias could potentially trap the learning process because the highest possible magnetization ($m = 1$) represents a highly ordered state, which is not useful for representing real-world data.

The effects of the variance bias h are represented in figures 7 and 8. In the m phase diagram with $h = 0.5$, Fig. 7a, we can see that the region with $m = 0$ increases resulting in a reduced in size Ferromagnetic phase, if we see q phase diagram Fig. 7b we note that not only the Ferromagnetic phase is reduced, but also the paramagnetic phase has almost completely disappeared, *i.e.*, most part of the q phase diagram has q different from zero, this two events result in a Spin Glass phase occupying most part of the phase diagram.

If we increment the value of the variance bias to $h = 1.5$, the Ferromagnetic Phases completely vanish, as we show in Fig. 8a, the Paramagnetic phase only occupies a tiny

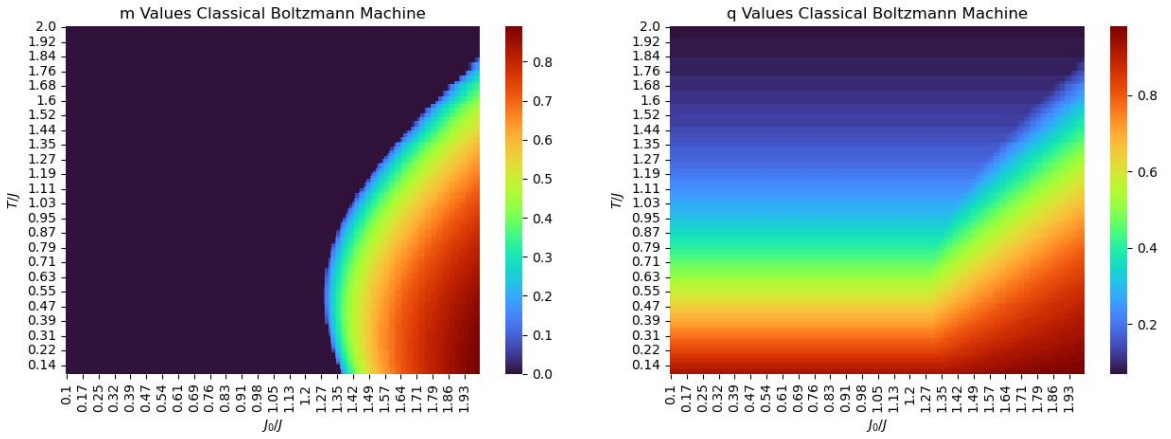

(a) m Phase diagram of the BM. (b) q Phase diagram of the BM.

Figure 7 – Phase diagram of the Boltzmann Machine with variance bias $h = 0.5$. (a): m heat map for the system with variance bias $h = 0.5$. (B): q heat map for the system with variance bias $h = 0.5$

.

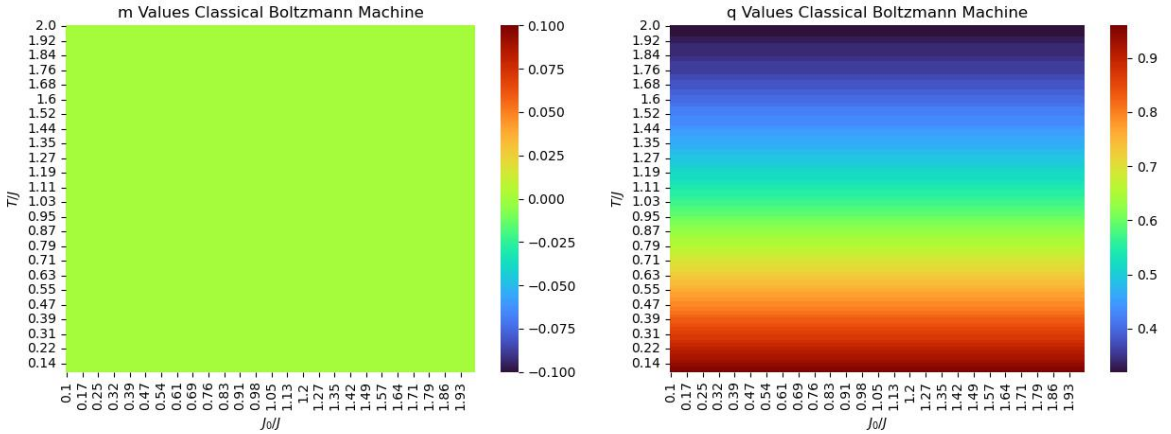

(a) m Phase diagram of the BM. (b) q Phase diagram of the BM.

Figure 8 – Phase Diagram of the Boltzmann Machine with variance bias $h = 1.5$. (a): m heat map for the system with variance bias $h = 1.5$. (B): q heat map for the system with variance bias $h = 1.5$

.

region above the line $T = 1.92$. with this configuration the systems just features Spin Glass phase.

The variance bias increase the disorder in the system, because it measures the difference in the biases at each site in the network, in other words, a high value of the variance bias is a high difference between the external fields for the different sites and as the mean bias is zero, we could have high(both positive and negative) bias, making difficult ordering the system and each neuron is magnetized separately, as in the spin glass phase.

4.3 Almeida-Thouless line

The free energy Eq.(B.50) has the problem of negative entropy at very low temperature (see Appendix B.4):

$$f = -\sqrt{\frac{2}{\pi}}J + \frac{T}{2\pi}, \tag{4.30}$$

for $T \to 0$.

If we compare the above equation with Eq.(3.7), we get the entropy:

$$S = -\frac{1}{2\pi}. \tag{4.31}$$

This issue arises from the assumption of RS solutions. Therefore, it is necessary to test the validity of the RS assumption. To analyze the stability of the solution, we examine the Hessian matrix of Eq. (4.17), which contains the second derivatives of the function. For Eq. (4.17) to represent a minimum, the Hessian matrix must have non-negative eigenvalues.

Almeida and Thouless demonstrated that only one eigenvalue is crucial (they showed that the other eigenvalues are positive and thus not problematic) [56]. This crucial eigenvalue is known as the *Replicon Eigenvalue*. For our system, the replicon is given by:

$$\lambda_r = \beta^2 J^2[1 - \beta^2 J^2(1-q^2) + 2\beta^4 J^4 q(1-q^2) - \beta^4 J^4(r-q^2)], \tag{4.32}$$

where:

$$r = \int Dz \tanh^4(\beta\tilde{H}(z)), \tag{4.33}$$

again, with $Dz = \frac{1}{\sqrt{2\pi}}e^{-z^2/2}dz$ and $\tilde{H}(z) = \sqrt{J^2q + h^2}z + J_0 m + h_0$. Using the form of r and Eq.(4.29) we, from the condition of $\lambda_r > 0$, get:

$$\left(\frac{T}{J}\right)^2 > \int Dz \operatorname{sech}^4(\beta\tilde{H}(z)), \tag{4.34}$$

The AT line is the line represented by the equation:

$$\left(\frac{T}{J}\right)^2 = \int Dz \operatorname{sech}^4(\beta\tilde{H}(z)), \tag{4.35}$$

The condition (4.34) says us that the RS solutions are reliable above the AT line, then the RS assumption is correct here, and then, there exists a RSB below the AT line.

We solved numerically the right side of the Eq.(4.35) in the whole phase diagram ($0 \leq T/J \leq 2$ and $0 \leq J_0/J \leq 2$). First, we solved for a system without bias ($h_0 = 0$ and $h = 0$), the results, presented in Fig. 9, show that in the paramagnetic phase and most part of the ferromagnetic phase the replicas are symmetric. The whole Spin Glass phase, and a small part of the Ferromagnetic phase present *RSB*. The AT line separates

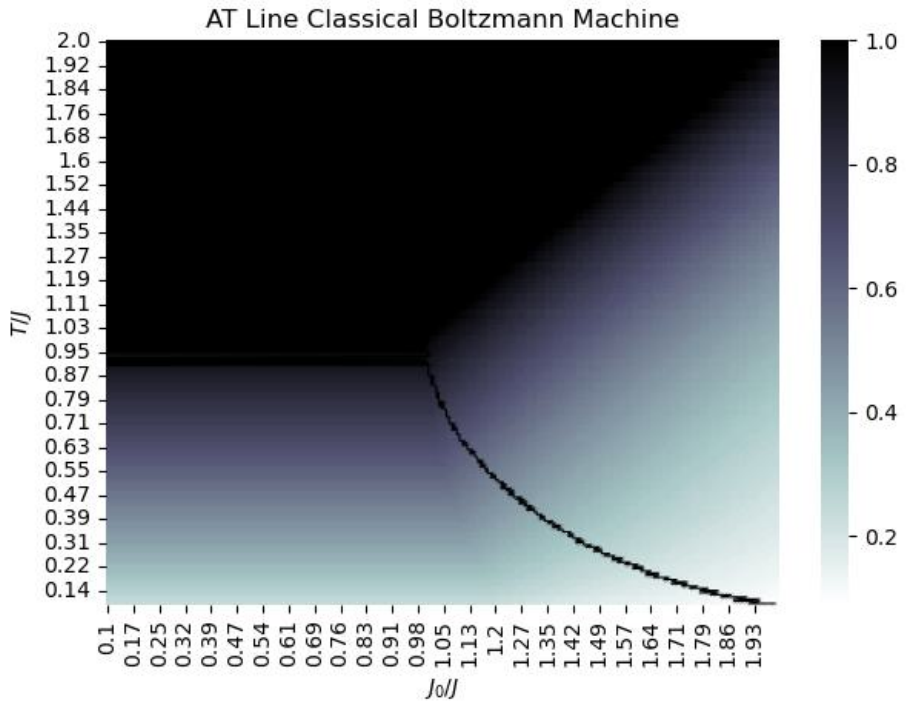

Figure 9 – Heat map of the values of the right side of Eq.(4.34), the curve is the AT line represented by the Eq.(4.35)

the Replica Symmetric Ferromagnetic (RS-F) phase with the RSB Ferromagnetic phase (also known as Mixed phase).

Furthermore, we solved for different mean and variance biases. With a mean bias of $h_0 = 0.5$ and a variance bias of $h = 0$, the region of RSB is smaller compared to the system without bias. This reduction is due to the diminished Spin Glass and *RSB-F* phases under these parameters, as evidenced in Fig. 10a.

Increasing the mean bias results in a further decrease in the RSB region. This observation is made by comparing Figures 10a and 10b. The reduction in the RSB region follows the reduction of the *SG* and *RSB F* phases.

In contrast, the reduction of the RSB region for different variance biases follows a different mechanism, known as *ESB*. This mechanism is well understood in the *Ising* model. In Figures 11a and 11b, we observe a reduction in the RSB region despite the fact that, for these parameters, the Spin Glass phase increases in size, similar to the Ferromagnetic phase in the Ising model. This behavior can be attributed to an *ESB*, where the introduction of variance bias breaks the symmetry of the system, thereby affecting the stability and extent of the RSB region.

In the Ising model, a similar phenomenon occurs where an external magnetic field breaks the symmetry and resulting in a explicit symmetry breaking [58]. This analogy helps to clarify the observed reduction in the RSB region despite the expansion of the

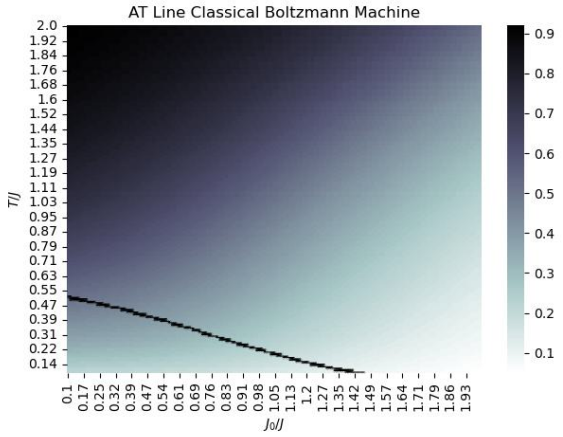

(a) AT line with mean bias $h_0 = 0.5$.

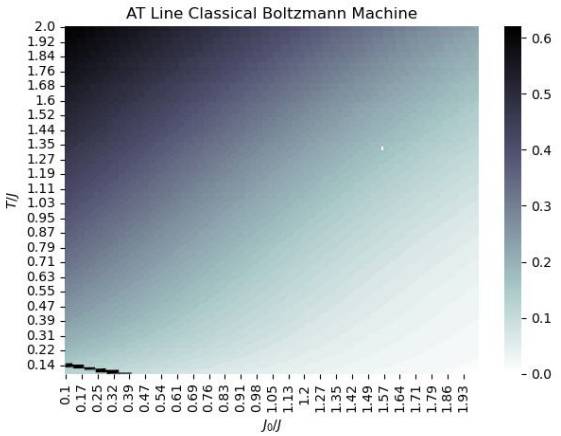

(b) AT line with mean bias $h_0 = 1.5$.

.

Figure 10 – AT line for different mean biases and variance bias $h = 0$

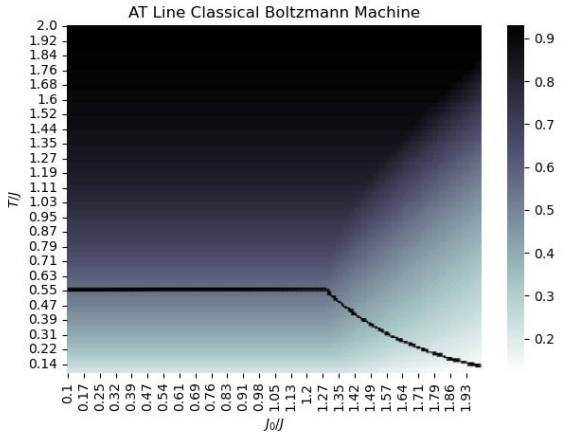

(a) AT line with variance bias $h = 0.5$.

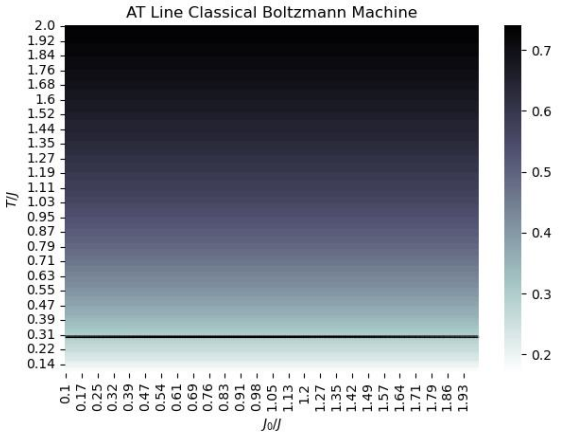

(b) AT line with variance bias $h = 1.5$.

Figure 11 – AT line for different variance biases and mean bias $h_0 = 0$

.

Spin Glass phase under the influence of variance bias.

5 Phase Diagram of the Restricted Boltzmann Machine

In this chapter we apply the replica method to study the phase diagram of the RBM paying attention to how biases in visible and hidden neurons impact on equilibrium properties of the network. As we explained earlier the RBMs are a type of two layer neural network which makes it easier to learn by making connections only within layers and not between. We will investigate how the two classes of neurons (visible and hidden) biases effect the phase diagram of RBM in our discussion. Biases have important influence upon determining the first time activation probability of neurons [59], thus impact the overall dynamics in network.

5.1 Replica Symmetric Restricted Boltzmann Machine

In the previous chapter, we presented the idea behind the Replica formalism, here we will expose the principal results obtained without going into the replica method in depth. The Detailed calculations can be found in the Appendix C.

First, we will start with the energy function of the RBM (Eq.(3.20)):

$$H(\sigma, s) = -\sum_{i=1}^{N_v}\sum_{a=1}^{N_h} J_{ia}\sigma_i s_a - \sum_{i=1}^{N_v}\sigma_i h_i - \sum_{a=1}^{N_h} s_a c_a. \tag{5.1}$$

In the above equation, σ_i and s_a are Ising neurons taking values from $\{-1, 1\}$ for the visible and hidden neurons, respectively (as described in the previous section). The neural network includes N neurons, with N_v neurons in the visible layer and N_h neurons in the hidden layer. The parameter J_{ia} is the synaptic connection between the i-th neuron in the visible layer and the a-th neuron in the hidden layer. Finally, h_i and c_a are the biases applied to the visible and hidden layers, respectively.

The parameters are independently drawn from normal distributions:

$$P(J_{ia}) = \sqrt{\frac{L}{2\pi J^2}}\exp\left[-\frac{L}{2J^2}\left(J_{ia} - \frac{J_0}{L}\right)^2\right]; \tag{5.2}$$

$$P(h_i) = \sqrt{\frac{1}{2\pi h^2}}\exp\left[-\frac{1}{2h^2}(h_i - h_0)^2\right]; \tag{5.3}$$

$$P(c_a) = \sqrt{\frac{1}{2\pi c^2}}\exp\left[-\frac{1}{2c^2}(c_a - c_0)^2\right], \tag{5.4}$$

with mean and variance

$$[J_{ia}]_a = \frac{J_0}{L}, \qquad [(\Delta J_{ia})^2]_a = \frac{J^2}{L}, \tag{5.5}$$

$$[h_i]_a = h_0, \qquad [(\Delta h_i)^2]_a = h^2, \tag{5.6}$$

$$[c_a]_a = c_0, \qquad [(\Delta c_a)^2]_a = c^2, \tag{5.7}$$

where $L = \sqrt{N_v N_h}$ and $[.]_a$ is defined in a similar way as Eq.(4.5) but adding the integral over the hidden bias $\mathbf{c}$.

After defining the energy model and the distribution functions, we are able to write the replicated partition function:

$$[Z^n]_a = \int \prod_{i,a} P(J_{ia}) dJ_{ia} \int \prod_i P(h_i) dh_i \int \prod_a P(c_a) dc_a \\ \mathrm{Tr} \exp\left[\beta \sum_\alpha \sum_{i,a} J_{ia} \sigma_i^\alpha s_a^\alpha + \beta \sum_\alpha \sum_i h_i \sigma_i^\alpha + \beta \sum_\alpha \sum_a c_a s_a^\alpha\right]. \tag{5.8}$$

Solving the Gaussian integrals and then applying the HS transformation, we obtain:

$$[Z^n]_a = \int\int \prod_{(\alpha,\gamma)} dq_{\alpha\gamma} d\bar{q}_{\alpha\gamma} \int\int \prod_\alpha dm_\alpha d\bar{m}_\alpha \exp\left[-\frac{\beta^2 J^2}{2} L \sum_{(\alpha,\gamma)} q_{\alpha\gamma}\bar{q}_{\alpha\gamma} - \frac{\beta J_0 L}{4} \sum_\alpha m_\alpha \bar{m}_\alpha\right] \\ \mathrm{Tr}_v \exp\left[\sum_{(\alpha,\gamma)} G_{\alpha\gamma} \sum_i \sigma_i^\alpha \sigma_i^\gamma + \sum_\alpha P_\alpha \sum_i \sigma_i^\alpha\right] \mathrm{Tr}_h \exp\left[\sum_{(\alpha,\gamma)} \bar{G}_{\alpha\gamma} \sum_a s_a^\alpha s_a^\gamma + \sum_\alpha \bar{P}_\alpha \sum_a s_a^\alpha\right]. \tag{5.9}$$

The notation $\sum_{(\alpha,\gamma)}$ means that we have two summations one for α and one for γ but with $\gamma \neq \alpha$, the summation without parenthesis means that we are considering also the equal terms. in the above equation, Tr_v and Tr_h are the traces over the visible and hidden neurons, respectively and with:

$$G_{\alpha\gamma} = \frac{\beta^2 J^2 q_{\alpha\gamma}}{2} \frac{L}{N_v} + \frac{\beta^2 h^2}{2}, \qquad P_\alpha = \beta J_0 m_\alpha \frac{L}{4N_v} + \beta h_0, \tag{5.10}$$

$$\bar{G}_{\alpha\gamma} = \frac{\beta^2 J^2 \bar{q}_{\alpha\gamma}}{2} \frac{L}{N_h} + \frac{\beta^2 c^2}{2}, \qquad \bar{P}_\alpha = \beta J_0 \bar{m}_\alpha \frac{L}{4N_h} + \beta c_0. \tag{5.11}$$

Note, that we obtained in Eq.(5.9) a partition function without correlations between visible and hidden neurons (Mean Field Approximation), similar as in the BM. The new price are correlations between replicas and 4 integrals to be solved, the new four parameters (as in the previous chapter) are the order parameters, we have two for the visible neurons: $q_{\alpha\gamma}$, m_α and two for the hidden neurons: $\bar{q}_{\alpha\gamma}$, $\bar{m}_\alpha$.

By rewriting the traces we can obtain:

$$[Z^n]_a = \int\int \prod_{(\alpha,\gamma)} dq_{\alpha\gamma} d\bar{q}_{\alpha\gamma} \int\int \prod_{\alpha} dm_\alpha d\bar{m}_\alpha \exp\left[-L\left(\frac{\beta^2 J^2}{2}\sum_{(\alpha,\gamma)} q_{\alpha\gamma}\bar{q}_{\alpha\gamma} + \beta J_0 \sum_\alpha m_\alpha \bar{m}_\alpha \right.\right.$$
$$\left.\left. -k \ln \mathrm{Tr}_v \exp\left(\sum_{(\alpha,\gamma)} G_{\alpha\gamma}\sigma^\alpha\sigma^\gamma + \sum_\alpha P_\alpha \sigma^\alpha\right) - \frac{1}{k}\ln \mathrm{Tr}_h \exp\left(\sum_{(\alpha,\gamma)} \bar{G}_{\alpha\gamma} s^\alpha s^\gamma + \sum_\alpha \bar{P}_\alpha s^\alpha\right)\right)\right], \tag{5.12}$$

with $k = \sqrt{\frac{N_v}{N_h}}$.

The integrals can be solved by the steepest descent method, obtaining:

$$[z^n]_a = e^{-L\tilde{f}(q_{\alpha\gamma}, m_\alpha, \bar{q}_{\alpha\gamma}, \bar{m}_\alpha)}, \tag{5.13}$$

where:

$$\tilde{f} = \frac{\beta^2 J^2}{2}\sum_{(\alpha,\gamma)} q_{\alpha\gamma}\bar{q}_{\alpha\gamma} + \beta J_0 \sum_\alpha m_\alpha \bar{m}_\alpha - k \ln \mathrm{Tr}_v \exp\left(\sum_{(\alpha,\gamma)} G_{\alpha\gamma}\sigma^\alpha\sigma^\gamma + \sum_\alpha P_\alpha\sigma^\alpha\right)$$
$$- \frac{1}{k}\ln \mathrm{Tr}_h \exp\left(\sum_{(\alpha,\gamma)} \bar{G}_{\alpha\gamma} s^\alpha s^\gamma + \sum_\alpha \bar{P}_\alpha s^\alpha\right). \tag{5.14}$$

By the condition of a minimum in $\bar{f}$, the order parameters yields:

$$q_{\alpha\gamma} = < \sigma^\alpha \sigma^\gamma >_h, \qquad m_\alpha = < \sigma^\alpha >_h, \tag{5.15}$$
$$\bar{q}_{\alpha\gamma} = < s^\alpha s^\gamma >_v, \qquad \bar{m}_\alpha = < s^\alpha >_v, \tag{5.16}$$

where the expected value for the visible neurons is taken over the hidden neurons distribution, *i.e.*,

$$< . >_v = \frac{\mathrm{Tr}_v \,.\exp\left(\sum_{(\alpha,\gamma)} G_{\alpha\gamma}\sigma^\alpha\sigma^\gamma + \sum_\alpha P_\alpha\sigma^\alpha\right)}{\mathrm{Tr}_v \exp\left(\sum_{(\alpha,\gamma)} G_{\alpha\gamma}\sigma^\alpha\sigma^\gamma + \sum_\alpha P_\alpha\sigma^\alpha\right)}, \qquad v \longleftrightarrow h. \tag{5.17}$$

The notation $v \longleftrightarrow h$ means that the same equation is obtained for the h by interchanging $G_{\alpha\gamma}$, P_α and σ^α by $\bar{G}_{\alpha\gamma}$, $\bar{P}_\alpha$ and s^α, respectively. We note that for the visible order parameters the average is taken with respect the hidden system, and vice versa.

Using this results, we can write the free energy as

$$-\beta f = -\lim_{n\to 0}\frac{1}{n}\left(\frac{\beta^2 J^2}{2}\sum_{(\alpha,\gamma)} q_{\alpha\gamma}\bar{q}_{\alpha\gamma} + \beta J_0\sum_\alpha m_\alpha\bar{m}_\alpha - k\Psi_v - \frac{1}{k}\Psi_h\right), \tag{5.18}$$

with:

$$\Psi_v = \ln \mathrm{Tr}_v \exp\left(\sum_{(\alpha,\gamma)} G_{\alpha\gamma}\sigma^\alpha\sigma^\gamma + \sum_\alpha P_\alpha\sigma^\alpha\right). \qquad v \longleftrightarrow h \tag{5.19}$$

Assuming Replica Symmetry in the four order parameters, we get the replica symmetric free energy:

$$-\beta f = \frac{\beta^2 J^2}{2} q\bar{q} - \beta J_0 m\bar{m} + \int Dz \ln 2\cosh[\sqrt{2G}z + p] - G + \frac{1}{k}\int Dz \ln 2\cosh[\sqrt{2\bar{G}}z + \bar{P}] - \bar{G}, \tag{5.20}$$

where

$$G = \frac{\beta^2 J^2 q}{2}\frac{L}{N_v} + \frac{\beta^2 h^2}{2}, \qquad P = \beta J_0 m \frac{L}{4N_v} + \beta h_0, \tag{5.21}$$

$$\bar{G} = \frac{\beta^2 J^2 \bar{q}}{2}\frac{L}{N_h} + \frac{\beta^2 c^2}{2}, \qquad \bar{P} = \beta J_0 \bar{m} \frac{L}{4N_h} + \beta c_0. \tag{5.22}$$

Finally, the self-consistent equations for the order parameters yields:

$$q = \int Dz \tanh^2(\sqrt{2\bar{G}}z + \bar{P}), \qquad m = \int Dz \tanh\left(\sqrt{2\bar{G}}z + \bar{P}\right), \tag{5.23}$$

$$\bar{q} = \int Dz \tanh^2(\sqrt{2G}z + P), \qquad \bar{m} = \int Dz \tanh\left(\sqrt{2G}z + P\right), \tag{5.24}$$

where, again, $Dz = \frac{1}{2\pi}e^{-z^2/2}dz$. Note that in the equations of state above, the order parameters for the visible subsystem depends on the order parameters and the bias of the hidden and vice versa.

5.2 Phase Diagram of the RBM

In order to calculate the phase diagram for the RBM, we solved numerically the equations of state Eq.(5.23) and Eq.(5.24). *Hartnett et al* showed [57] that only the *SG-F* boundary is affected by the relative fraction of hidden spins $y_h = N_h/N$. They worked out in a system with no external fields(in our case no bias: $h_0 = h = c_0 = c = 0$) and showed that the boundary does not depart to much from the boundary with $y_h = 0.5$ that is the same for a full connected system. For this reason, we(and expecting the same behavior for systems with bias) just solved for a relative fraction of hidden neurons $y_h = 1/2$ with $N_v = N_h = 10^9$.

For a system without bias we can see in Fig. 12 that the phase diagram is the same for the BM, we found the same phases (*SG*, *P* and *F*) and boundaries, we also note that the two subsystems are in the same phases simultaneously, i.e. if the hidden neurons subsystem is in the ferromagnetic phase the visible subsystem is also in the ferromagnetic phase, this result is expected if the take a look to the equations of state((5.23 and (5.24)), this is because it depends on the order parameters from the other subsystem and, for example, if one the visible subsystem is in a paramagnetic phase with $m = q = 0$ then the hidden subsystem will be in the paramagnetic phase due to the arguments of the equation (5.24) becomes zero.

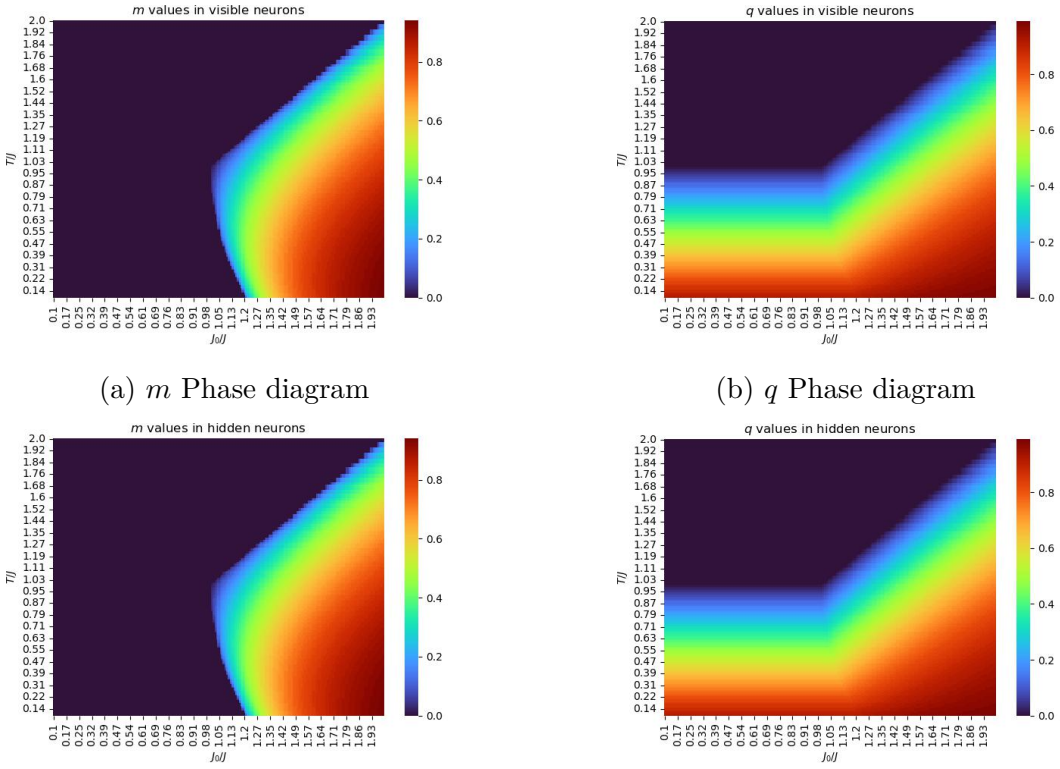

(a) m Phase diagram

(b) q Phase diagram

(c) $\bar{m}$ Phase diagram

(d) $\bar{q}$ Phase diagram

Figure 12 – Phase diagram for the Restricted Boltzmann Machine for no bias: $h_0 = 0$, $h = 0$, $c_0 = 0$ and $c = 0$. (a) Phase diagram for the order parameter m corresponding to the visible neurons. (b) Phase diagram for the order parameter q corresponding to the visible neurons. (c) Phase diagram for the order parameter $\bar{m}$ corresponding to the hidden neurons. (d) Phase diagram for the order parameter $\bar{q}$ corresponding to the hidden neurons.

5.2.1 Effect of the bias in the RBM

In view of the results from a RBM in absence of bias, we expect that the system with bias presents the same behaviour of the BM, to verify this we solve the equations (5.23) and (5.24) for different situations, we want to see independently the impact of the mean bias(h_0 and c_0) and the variance bias(h and c) in the phase diagram of the two type of neurons.

The RBM behaviour does not seem the same compared with the BM when the bias shows up. If we look into the Fig. 13, we can note small deviations in the phase diagrams. In the $\bar{m}$ phase diagram for the hidden neurons Fig. 13c the curve delimiting the yellow region to the blue region is more sharp compared with the m phase diagram for the visible neurons Fig. 13a, we also remark the blue region below $T/J = 1$ is greater than the visible subsystem. The q phase diagrams seems more similar than the m diagrams, they have minimal differences. The differences encountered in the phase diagrams could be related to the fact that the mean bias h_0 affects directly the hidden order parameters as we can see in equation (5.24) so it has less influence in the visible order parameters Eq.(5.23).

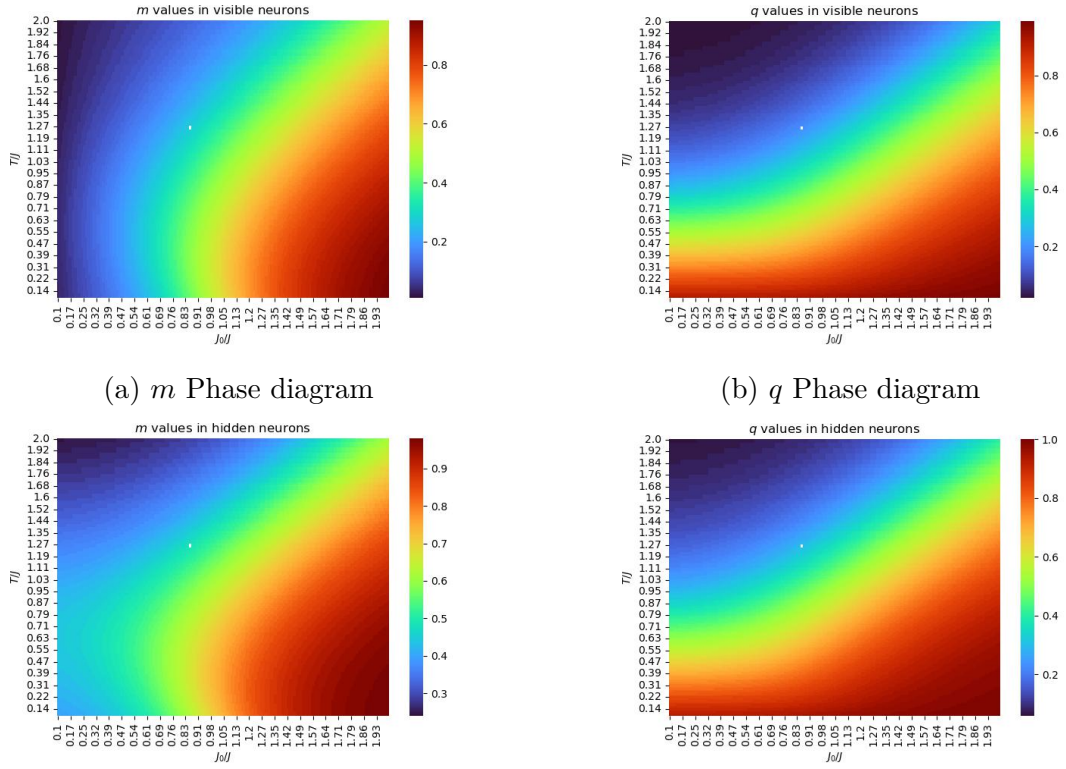

(a) m Phase diagram

(b) q Phase diagram

(c) $\bar{m}$ Phase diagram

(d) $\bar{q}$ Phase diagram

Figure 13 – Phase diagram for the Restricted Boltzmann Machine with mean and variance bias: $h_0 = 0.5$, $h = 0$, $c_0 = 0$ and $c = 0$. (a) Phase diagram for the order parameter m corresponding to the visible neurons. (b) Phase diagram for the order parameter q corresponding to the visible neurons. (c) Phase diagram for the order parameter $\bar{m}$ corresponding to the hidden neurons. (d) Phase diagram for the order parameter $\bar{q}$ corresponding to the hidden neurons.

The fact that it has more impact in the m phase diagram than the q diagram may be due to h_0 is directly related with m "field" (P) Eq.(5.21).

In Fig. 14 the effects of the mean bias $h_0(= 1.5)$ on the $\bar{m}$ diagram is more evident. Figs. 14c and 14d show that there is not spin glass phase in the hidden subsystem due to there is no region with $\bar{m} = 0$ and $\bar{q} \neq 0$. There exists only *Ferromagnetic* phase in the red, yellow and light blue regions and *Paramagnetic* in the little dark blue region at high temperatures. Conversely, Figs. 14a and 14b show that the visible neurons display a small *Spin Glass* phase when $m \approx 0$ and $q \neq 0$, the *Paramagnetic* phase is greater in this subsystem and the *Ferromagnetic* phase is smaller compared with the hidden neurons. Then, it seems that the fields impact in a similar way that the *BM* but affecting principally the other subsystem. For the sake of confirm the above claim, we made more experiments[1].

For a variance field $h = 0.5$ on the visible neurons, we observe no differences in

[1] We use the word "experiments" in the sense that we solve the equations of state for another situations for the purpose of see the behavior of the system in such situations and it seems very tiring for the reader and for me the phrase "We solved the equations" on each page.

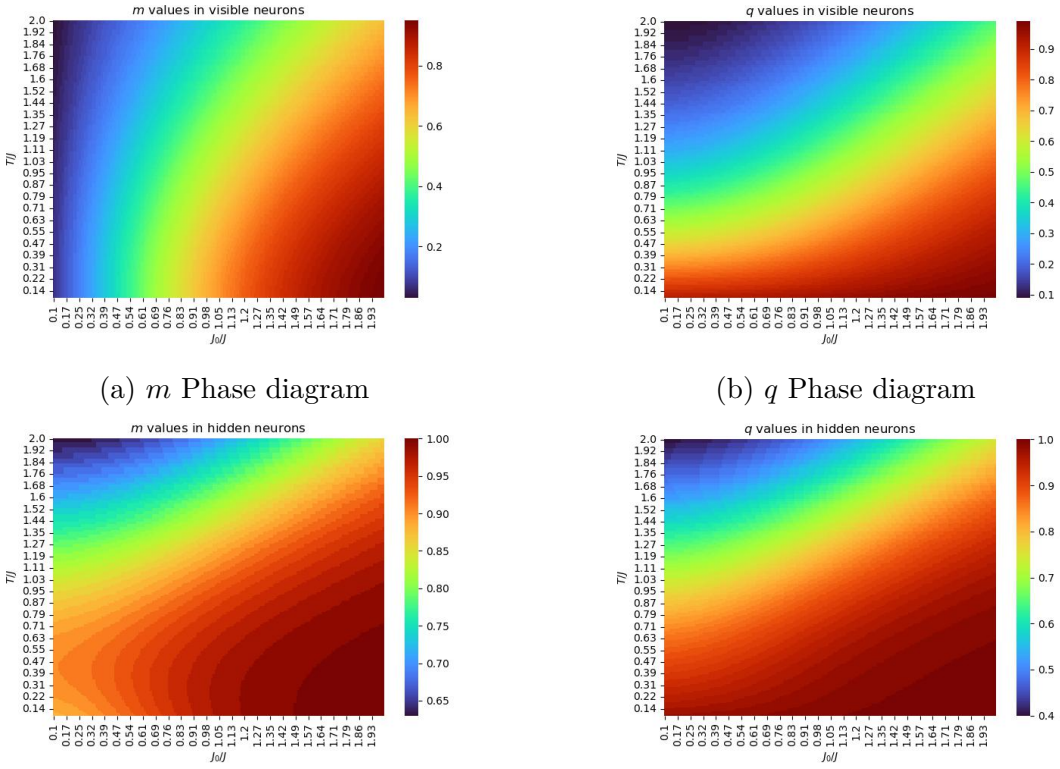

(a) m Phase diagram

(b) q Phase diagram

(c) $\bar{m}$ Phase diagram

(d) $\bar{q}$ Phase diagram

Figure 14 – Phase diagram for the Restricted Boltzmann Machine with mean and variance bias: $h_0 = 1.5$, $h = 0$, $c_0 = 0$ and $c = 0$. (a) Phase diagram for the order parameter m corresponding to the visible neurons. (b) Phase diagram for the order parameter q corresponding to the visible neurons. (c) Phase diagram for the order parameter $\bar{m}$ corresponding to the hidden neurons. (d) Phase diagram for the order parameter $\bar{q}$ corresponding to the hidden neurons.

the m Fig.15a with the $\bar{m}$ Fig.15c diagrams, the purple region (no magnetization) seems to be equal in the two subsystems and then, they have the same *Ferromagnetic* region area ($m \neq 0$ and $\bar{m} \neq 0$); meanwhile, the purple region (*Paramagnetic phase*) in the q and $\bar{q}$ diagrams (Figs. 15b and 15d, respectively) is too tiny, being even smaller in the hidden subsystem, thus, affecting more to the hidden neurons. As in the *BM* the *Spin Glass* phase growths, decreasing the *Paramagnetic* phase due to the variance bias . In addition, when the variance bias on visible neurons is increased to $h = 1.5$ is observed that while the magnetization phase diagrams, Figs. 16a and 16c does not show much difference leaving a system with a little magnetized region ($m = \bar{m} \neq 0$) in both type of neurons, the differences between the q Fig. 16b and the $\bar{q}$ Fig. 16d diagrams are a bit more dramatic, the observations agree with the *BM* in the sense that the variance field growths the *SG* phase destroying the *Paramagnetic* and *Ferromagnetic* regimes, in the context of the *RBM* this variance field on the visible neurons also growths the spin glass, but it increases more in the hidden system, as we can see in the Fig. 16d: the yellow and red regions are larger than the same regions in the visible subsystem (Fig.16b)

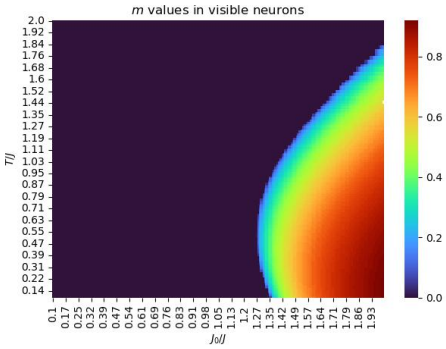

(a) m Phase diagram

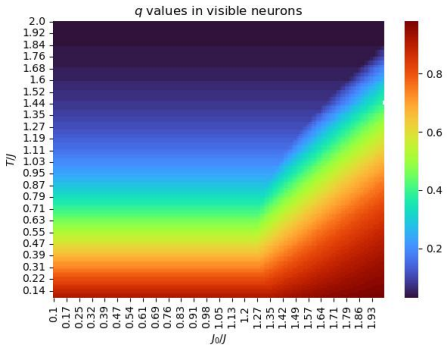

(b) q Phase diagram

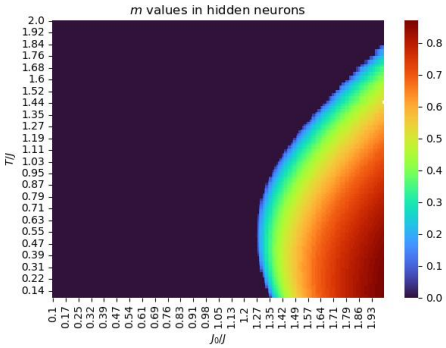

(c) $\bar{m}$ Phase diagram

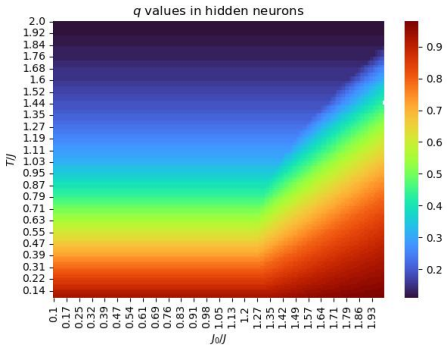

(d) $\bar{q}$ Phase diagram

Figure 15 – Phase diagram for the Restricted Boltzmann Machine with mean and variance bias: $h_0 = 0$, $h = 0.5$, $c_0 = 0$ and $c = 0$. (a) Phase diagram for the order parameter m corresponding to the visible neurons. (b) Phase diagram for the order parameter q corresponding to the visible neurons. (c) Phase diagram for the order parameter $\bar{m}$ corresponding to the hidden neurons. (d) Phase diagram for the order parameter $\bar{q}$ corresponding to the hidden neurons.

Finally, we did the experiments with the bias on the hidden neurons. The results confirm our claim: in the case with a mean bias on hidden neurons($c_0 = 0.5, 1.5$) is observed the same behavior that the case with a mean bias on visible neurons(h_0) just that c_0 affects directly on the visible subsystem (see Figs. 20 and 21 in Appendix C.3) and, as expected, it further affects the magnetization diagrams, as we can see in Figs. 20a, 20c for $c_0 = 0.5$ and Figs. 21a, 21c for $c_0 = 1.5$. Furthermore, the experiments with a variance bias c on hidden neurons show that, similar as the case of visible variance bias h, it impacts on the behavior of the *overlap* diagrams (see Figs. 22 and 23), affecting more the visible subsystem, as shown in the Figs. 20b and 20d for $c = 0.5$ and Figs. 21b and 21d for $c = 1.5$.

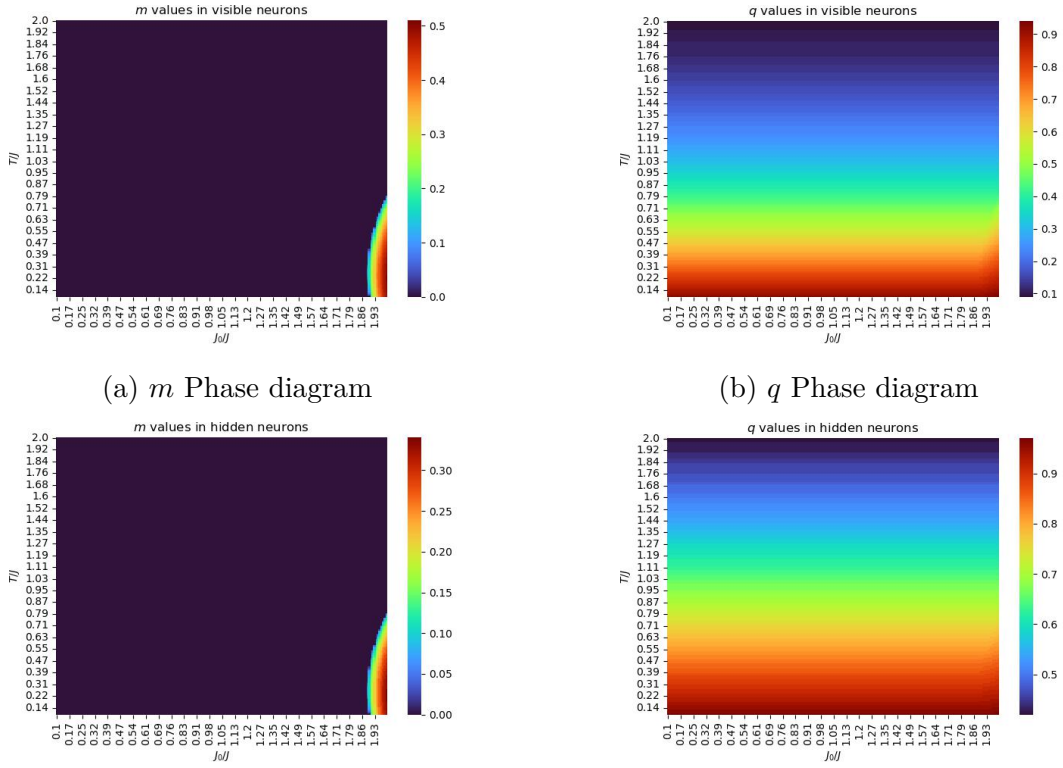

(a) m Phase diagram

(b) q Phase diagram

(c) $\bar{m}$ Phase diagram

(d) $\bar{q}$ Phase diagram

Figure 16 – Phase diagram for the Restricted Boltzmann Machine with mean and variance bias: $h_0 = 0$, $h = 1.5$, $c_0 = 0$ and $c = 0$. (a) Phase diagram for the order parameter m corresponding to the visible neurons. (b) Phase diagram for the order parameter q corresponding to the visible neurons. (c) Phase diagram for the order parameter $\bar{m}$ corresponding to the hidden neurons. (d) Phase diagram for the order parameter $\bar{q}$ corresponding to the hidden neurons.

6 Phase Diagram of the Semi classical Boltzmann Machine

In this chapter, our aim is to illustrate the phase diagrams to the *SCBM* with and without bias. We call it *Semi Classical* due to we will use the *Mean Field(often called Semi classical) Approximation* in the *Quantum Boltzmann Machine (QBM)*. In this approximation Quantum Correlations are not taken into account between Qubits in the network, however, another quantum effects(as superposition, tunneling and interference) are present. In the next sections we will, first, apply the Suzuki-Trotter decomposition [60, 61] in order to find an *effective Classical Hamiltonian*, then with this effective Hamiltonian at hand we will apply the replica formalism in order to find the *Semi Classical Equations of state* and finally calculate the phase diagrams at $T = 0$

6.1 Suzuki-Trotter Formalism

The basic idea behind the Suzuki-Trotter formalism is to transform a quantum Hamiltonian with a dimension d into an effective classical Hamiltonian with a price to be paid ("A soul for a soul"): an extra dimension. For example, if we had an 2d-lattice the resulting effective Hamiltonian would represent a 3d system. Let us start with the Hamiltonian of the *QBM* (Eq. 3.48):

$$H(\sigma) = -\sum_{i<j} J_{ij}\sigma_i^z\sigma_j^z - \sum_i h_i\sigma_i^z - \Omega\sum_i \sigma_i^x. \tag{6.1}$$

We separate the above Hamiltonian into two parts: Diagonal and non Diagonal Hamiltonian:

$$H(\sigma) = H_0 + H_q, \tag{6.2}$$

with:

$$H_0 = -\sum_{i<j} J_{ij}\sigma_i^z\sigma_j^z - \sum_i h_i\sigma_i^z, \qquad H_q = -\Omega\sum_i \sigma_i^x. \tag{6.3}$$

Then, the partition function reads:

$$Z = \mathrm{Tr}\, e^{-\beta(H_0+H_q)}. \tag{6.4}$$

By applying the Trotter formula, we can write:

$$Z = \mathrm{Tr}\Big[\lim_{M\to\infty}(e^{-\beta H_0}e^{-\beta H_q})^M\Big]. \tag{6.5}$$

Finally, making use of the definition of the trace and some manipulations (see Appendix D.1), we get:

$$Z = \lim_{M\to\infty} C^{NM/2}\,\mathrm{Tr}[\exp(-\beta H_{eff})], \tag{6.6}$$

where

$$C = \frac{1}{2}\sinh\left(\frac{2\beta\Omega}{M}\right), \tag{6.7}$$

and

$$H_{eff} = -\sum_{i<j}\sum_{k=1}^{M}\frac{J_{ij}}{M}\sigma_i(k)\sigma_j(k) - \sum_{i}\sum_{k=1}^{M}\frac{h_i}{M}\sigma_i(k) - \frac{1}{2\beta}\sum_{i}\sum_{k=1}^{M}\sigma_i(k)\sigma_i(k+1)\ln\left[\coth\left(\frac{\beta\Omega}{M}\right)\right]. \tag{6.8}$$

The Hamiltonian H_{eff} is a classical one since $\sigma_i(k) = \pm 1$ are the eigenvalues of the z Pauli matrix σ_i^z. Note that the Hamiltonian (6.8) has an extra dimension represented by the index k. The dimension represented k is called Trotter direction, and note that in such direction the system just have connections in the nearest neighbors by the interaction $J' = \frac{1}{2\beta}\ln\left[\coth\left(\frac{\beta\Omega}{M}\right)\right]$. Then for each single qubit σ_i^z in the original Hamiltonian (6.1), corresponds a chain of M classical spins denoted by σ_i^k in the effective Hamiltonian (6.8)

6.2 Replica Quantum Boltzmann Machine

With the classical Hamiltonian (6.8) we are able to apply the replica formalism. First, we replicate the partition function (6.6) and calculate the configurational average:

$$[Z^n]_a = \int\prod_{i<j}P(J_{ij})dJ_{ij}\int\prod_{i}P(h_i)dh_i\,\mathrm{Tr}$$
$$\exp\left[\beta\sum_{i<j}\sum_{k=1}^{M}\sum_{\alpha}\frac{J_{ij}}{M}\sigma_i^\alpha(k)\sigma_j^\alpha(k) + \beta\sum_{i}\sum_{k=1}^{M}\sum_{\alpha}\frac{h_i}{M}\sigma_i^\alpha(k) + \beta G\sum_{i}\sum_{k=1}^{M}\sum_{\alpha}\sigma_i^\alpha(k)\sigma_i^\alpha(k+1)\right]. \tag{6.9}$$

where $G = \frac{1}{2\beta}\ln\left[\coth\left(\frac{\beta\Omega}{M}\right)\right]$ and

$$P(J_{ij}) = \sqrt{\frac{N}{2\pi J^2}}\exp\left[-\frac{N}{2J^2}\left(J_{ij} - \frac{J_0}{N}\right)^2\right]; \quad P(h_i) = \sqrt{\frac{1}{2\pi h^2}}\exp\left[-\frac{1}{2h^2}(h_i - h_0)^2\right], \tag{6.10}$$

with mean and variance given by equations (4.3) and (4.4), as in the classical *BM*. The process from here is equal to the classical cases. We solved the Gaussian integrals in Eq.(6.9) and some manipulations and *H-S transformations* later (see Appendix D.2 to

detailed calculations), we get:

$$[Z^n]_a = 1 - Nn\left[\frac{\beta^2 J^2}{4Mn}\sum_{\Delta K}\sum_{\alpha} r_\alpha^2(\Delta k) + \frac{\beta^2 J^2}{2Mn}\sum_{\Delta k}\sum_{\alpha<\gamma} q_{\alpha\gamma}^2(\Delta k) + \frac{\beta J_0}{2Mn}\sum_{\alpha,k} m_\alpha^2(k) - \frac{1}{n}\ln \mathrm{Tr}\, e^{-L}\right]. \tag{6.11}$$

where r, q, and m are variables introduced for mathematical purposes and we will show that these are the order parameters of the system, and

$$\begin{aligned} L = &-\sum_{\alpha<\gamma}\sum_{\Delta k}\left(\frac{\beta^2 J^2}{M^2} q_{\alpha\gamma}(\Delta k) + \frac{\beta^2 h^2}{M^2}\right)\sum_k \sigma^\alpha(k)\sigma^\gamma(k+\Delta k) \\ &- \beta G\sum_\alpha\sum_k \sigma^\alpha(k)\sigma^\alpha(k+1) - \sum_\alpha\sum_k\left(\frac{\beta J_0}{M} m_\alpha(k) + \frac{\beta h_0}{M}\right)\sigma^\alpha(k) \\ &- \frac{\beta^2}{2M^2}\sum_\alpha\sum_{\Delta k}\left(J^2 r_\alpha(\Delta k) + h^2\right)\sigma^\alpha(k)\sigma^\alpha(k+\Delta k), \end{aligned} \tag{6.12}$$

with the Eq.(6.11) at hand, we can write the free energy as:

$$\begin{aligned} -\beta f &= \lim_{n\to 0}\frac{[Z^n]_a - 1}{nN} = \\ &\lim_{n\to 0}\left(-\frac{\beta^2 J^2}{4Mn}\sum_{\Delta K}\sum_{\alpha} r_\alpha^2(\Delta k) - \frac{\beta^2 J^2}{2Mn}\sum_{\Delta k}\sum_{\alpha<\gamma} q_{\alpha\gamma}^2(\Delta k) - \frac{\beta J_0}{2Mn}\sum_{\alpha,k} m_\alpha^2(k) + \frac{1}{n}\ln \mathrm{Tr}\, e^{-L}\right). \end{aligned} \tag{6.13}$$

6.2.1 Replica Symmetric Solution

Now, we look for solutions under the well known *Replica Symmetric* and the *Static* [62, 63, 64] approximations: We do not consider the dependence of the order parameters on the replica and the Trotter indices:

$$m_\alpha(k) = m, \tag{6.14}$$

$$q_{\alpha\gamma}(\Delta k) = q, \tag{6.15}$$

$$r_\alpha(\Delta k) = r. \tag{6.16}$$

The free energy now, is:

$$f = \frac{\beta J^2}{4} r^2 - \frac{\beta J^2}{4} q^2 + \frac{J_0}{2} m^2 - \frac{1}{\beta}\int Dz \ln \int Dw 2\cosh(\lambda), \tag{6.17}$$

where

$$\lambda = \beta\sqrt{\Omega^2 + \left(\sqrt{\tilde{h}(q)}z + \sqrt{A}w + J_0 m + h_0\right)^2}, \tag{6.18}$$

and

$$\tilde{h}(q) = qJ^2 + h^2, \qquad A = J^2(r-q). \tag{6.19}$$

From the stationary conditions of the free energy, we get the equations of state:

$$m = \int DzY^{-1} \int Dw \sinh(\lambda) U^{-1} g, \tag{6.20}$$

$$q = \int Dz \left[Y^{-1} \int Dw \sinh(\lambda) U^{-1} g \right]^2, \tag{6.21}$$

$$r = \int DzY^{-1} \int Dw \left[\cosh(\lambda) U^{-2} g^2 - \frac{1}{\beta} \sinh(\lambda) U^{-3} g^2 + \frac{1}{\beta} \sinh \lambda U^{-1} \right], \tag{6.22}$$

with:

$$g = \sqrt{\tilde{h}(q)} z + \sqrt{A} w + J_0 m + h_0; \qquad U = \sqrt{\Omega^2 + g^2}; \qquad Y = \int Dw \cosh(\lambda). \tag{6.23}$$

The physical meaning of m and q are the same as in the classical BM: m is the magnetization and q represents the spin glass order parameter. Besides, the new order parameter r is a measure of the quantum fluctuations [65]. As we show in Appendix D.3 $r = 1$ when there is no transverse field $\Omega = 0$, hence the value $1 - r$ indicates the scale of the quantum fluctuations.

6.2.2 Phase Diagram at T=0

Now, our aim is to see the properties of the system at equilibrium without dissipation ($T = 0$). First of all we see that the equations of state Eq.(6.20), Eq.(6.21) and Eq.(6.22) can be reduced when $T = 0 (\beta \to \infty)$, in this limit the order parameter r is reduced to:

$$\begin{aligned} r &= \int DzY^{-1} \int Dw \cosh(\lambda) U^{-2} g^2 \\ &\geq \int DzY^{-1} \int Dw \sinh(\lambda) U^{-2} g^2 \geq \int Dz \left[Y^{-1} \int Dw \sinh(\lambda) U^{-2} g^2 \right]^2. \end{aligned} \tag{6.24}$$

The first equality in the above equation is due to the two last terms in Eq.(6.22) vanish when $\beta \to \infty$. On the other hand, as is well known the $\cosh \lambda$ function is always grater than or equal to the $\sinh \lambda$ function, this is reason for the first inequality in Eq.(6.24) and they becomes equal exactly in the limit $\beta \to \infty$ because in such limit $\sinh \lambda = \cosh \lambda$. Lastly, we know that the term g/U is always ≤ 1(it is 1 when $\Omega = 0$) and as Y is greater than or equal to $\int Dw \sinh \lambda$, thus, the second term in Eq.(6.24) is less than or equal to 1, consequently the last inequality is valid, and it becomes an equality, again, when $\beta \to \infty$. We remark the last term in the above equation is merely q, hence, in the limit $T = 0$ $r = q$. Finally, as $r = q$ then $A = 0$ so λ, g and U do not depend on w, therefore the equations of state becomes:

$$m = \int DzU^{-1} g, \tag{6.25}$$

$$q = \int Dz \left[U^{-1} g \right]^2, \tag{6.26}$$

where g and U are given by Eq.(6.23), but without the w term.

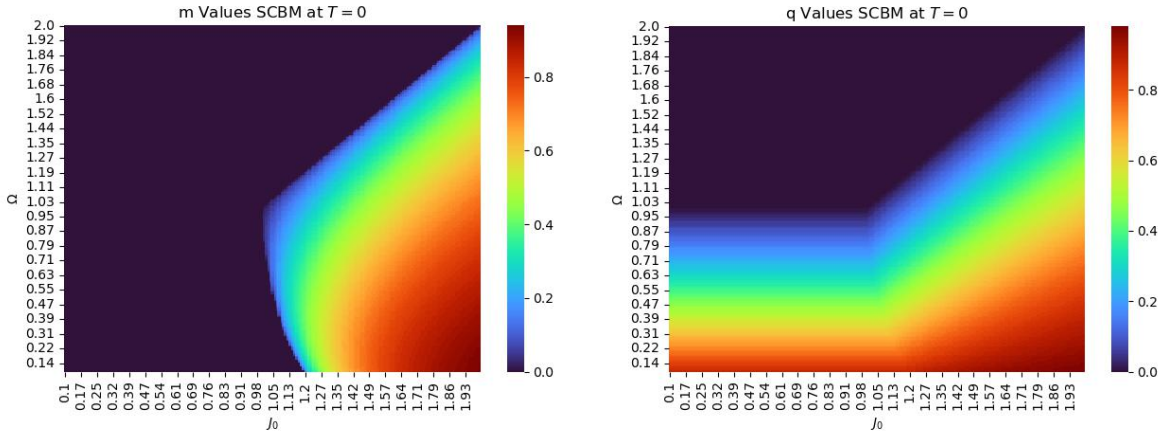

(a) m Phase diagram of the SCBM (b) q Phase diagram of the SCBM

Figure 17 – Phase Diagram of the Semi Classical Boltzmann Machine at $T = 0$ with bias: $h_0 = 0$ and $h = 0$. (a) Phase Diagram of the order parameter m and (b) Phase Diagram of the order parameter q.

To calculate the phase diagram, the equations of state (6.25) and (6.26) have been numerically solved. The result is drawn in fig. 17. Three phases are characterized by the two order parameters: the *Quantum Paramagnetic(QP)* phase with $m = q = 0$, the *Ferromagnetic(F* phase with $m \neq 0$ and $q \neq 0$ and finally, the *Spin Glass (SG)* Phase with $m = 0$ but $q \neq 0$. We note that the boundaries are the same as in the Classical case, but changing T by Ω [1] with the difference that the *Spin Glass* phase has no *Replica Symmetric Breaking*(see section 6.2.3).

In addition, we found that the mean bias h_0 and the variance bias h have the same effects as in the classical model: h_0 magnetize the network fig. 18, while the variance bias h reduces the QP and F phases leaving just the SG phase alive 19.

6.2.3 AT line at T=0

Now, we want to see the reliability of the *Replica Symmetric* solution, for this purpose we follow the same procedure to the classical *BM*. Here we will assume that the *replicon* eigenvalue is still the important one. Thus, we analyse the Hessian matrix of the function:

$$G = \frac{\beta^2 J^2}{2} \sum_{\alpha<\gamma} q_{\alpha\gamma}^2 - \ln \operatorname{Tr} e^{-L}. \tag{6.27}$$

We have set $q_{\alpha\gamma} = r_\alpha$ in anticipation of $q = r$ at $T = 0$. Thus, we only retain the relevant parts and L is given by Eq.(6.13) with just the terms involving q_α. In the limit

[1] We relax the notation for the axis names in the graphs for this chapter that actually are Ω/J and J_0/J, but we use $J = 1$ thus we relax the notation for the graphs

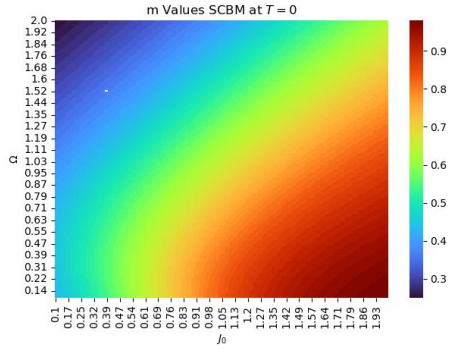

(a) m Phase Diagram, $h_0 = 0.5$

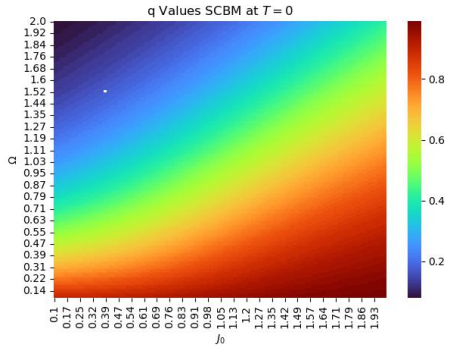

(b) q Phase Diagram, $h_0 = 0.5$

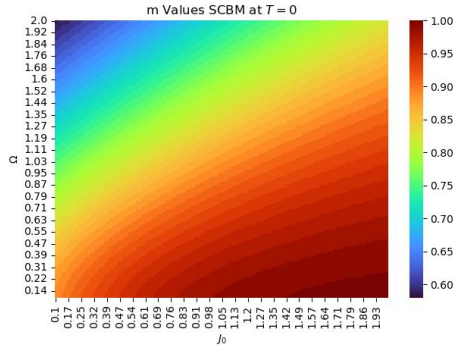

(c) m Phase Diagram, $h_0 = 1.5$

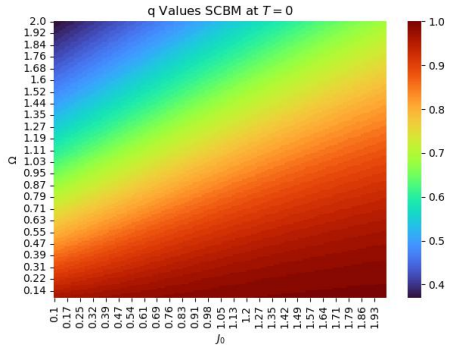

(d) q Phase Diagram, $h_0 = 1.5$

Figure 18 – Phase Diagram for the Semi Classical Boltzmann Machine with variant mean bias $h_0 = 0.5, 1.5$ and variance bias $h = 0$ (a) Phase diagram for the order parameter m corresponding to mean bias $h_0 = 0.5$. (b) Phase diagram for the order parameter q corresponding to mean bias $h_0 = 0.5$. (c) Phase diagram for the order parameter m corresponding to mean bias $h_0 = 1.5$. (c) Phase diagram for the order parameter q corresponding to mean bias $h_0 = 1.5$.

$\beta \to \infty$ the *log* term is quite small compared with β^2, thus:

$$G \approx \frac{\beta^2 J^2}{2} \sum_{\alpha<\gamma} q_{\alpha\gamma}^2. \tag{6.28}$$

Thus, the *replicon* eigenvalue gives:

$$\lambda_r = \beta^2 J^2, \tag{6.29}$$

which is always positive. Therefore, we do not have Replica Symmetric Breaking at any point in the solution.

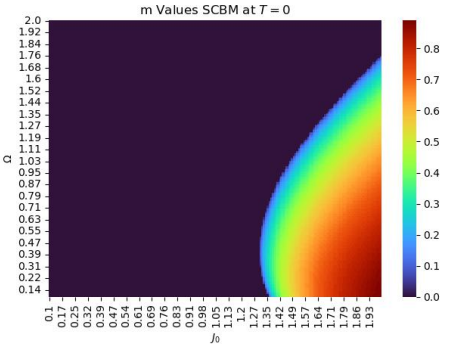

(a) m Phase Diagram, $h = 0.5$

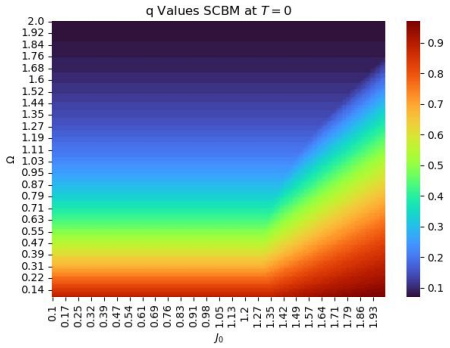

(b) q Phase Diagram, $h = 0.5$

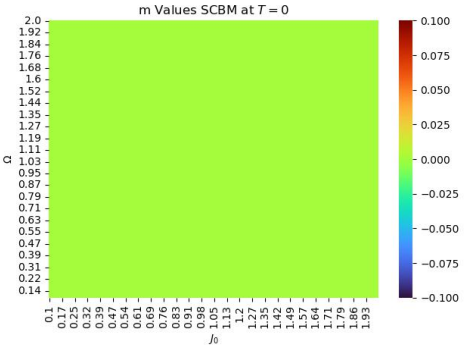

(c) m Phase Diagram, $h = 1.5$

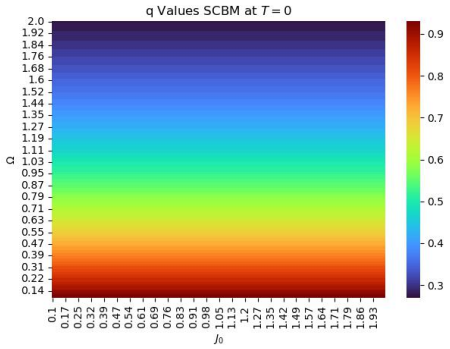

(d) q Phase Diagram, $h = 1.5$

Figure 19 – Phase Diagram for the Semi Classical Boltzmann Machine with mean bias $h_0 = 0$ and variant variance bias $h = 0.5, 1.5$ (a) Phase diagram for the order parameter m corresponding to variance bias $h = 0.5$. (b) Phase diagram for the order parameter q corresponding to variance bias $h = 0.5$. (c) Phase diagram for the order parameter m corresponding to variance bias $h = 1.5$. (c) Phase diagram for the order parameter q corresponding to variance bias $h = 1.5$.

7 Conclusions, Summary and Next Steps

By using the replica formalism, we obtained the mean-field state equations for classical and quantum Boltzmann machines, and with these, we plotted the phase diagrams for the different order parameters. We observed how temperature, synapses, and biases affected the systems in the case of classical models. Finally, in the case of the quantum model, we obtained the phase diagrams for different biases at $T = 0$.

To explain the replica method and how it relates to the mean-field (or semiclassical) approximation, we first solved a more general system we simply called the *BM*. Using replicas, we obtained two order parameters: m and q. The first is related to the net magnetization of the system, which gives us the level of ordering of the network, allowing us to distinguish between two regions: an ordered region corresponding to the F phase where the net magnetization is different from zero, and a disordered region, where the P and SG phases are found, characterized by having zero magnetization. This transition is important to us because it encompasses the *Learning* phase, where the network can explore and generalize configurations of real-world data. In this transition region, the system is flexible enough to adapt to new data configurations (disordered phase) while maintaining enough structure to avoid overfitting (ordered phase). The second order parameter q is the SG order parameter, measuring the correlation between spins of different replicas, but in the *Replica Symmetric Approximation*, this order parameter is related to the square of the magnetization in each neuron. Its name comes from the fact that with this order parameter we can distinguish the SG phase, which differs from the P phase by having $q \neq 0$, while in the P phase $q = 0$. Thus, we can see the difference between the P and SG phases: while both phases are characterized by having $m = 0$, this null magnetization arises from different circumstances. In the P phase, the net magnetization is zero because the individual magnetization in each neuron is also zero ($m_i = 0$), thus $q = 0$. On the other hand, in the SG phase, the individual magnetization can be different from zero ($m_i \neq 0$), but they can take both positive and negative values, resulting in a net magnetization of zero, and since the individual magnetizations are different from zero, we obtain $q \neq 0$.

After obtaining the state equations in the mean-field approximation, we first solved for $h_0 = h = 0$ analytically, finding the boundaries between the different phases (Fig. 3). This phase diagram matches the diagram for the SK model [9, 66]. The SK model for spin glasses is similar to the BM except that it does not consider external fields (neither random nor uniform for all spins), hence the phase diagrams match. To be more certain of the results, we also solved these equations numerically (for other scenarios, only this method will be used), and the results are shown in Fig. 4. In this figure, we can find the diagrams for the two order parameters and clearly distinguish the boundaries between

the different phases, and the agreement with the analytical solution is evident. Since the *Replica Symmetric Solution* is merely an ansatz and we found negative entropy at low temperatures, which does not make sense, we tested the viability of these symmetric solutions by checking the positivity of the eigenvalues of the Hessian matrix, specifically testing if the eigenvalue called the *Replicon* is positive. We found the famous *AT line* [56], showing that the P phase and most of the F phase are symmetric in the replica space, while the SG phase and a small part of the F phase exhibit spontaneous RSB, as seen in Fig. 9

With more confidence, we proceeded to the main part of the project and studied the effects of random biases on the system's properties. Assuming the biases follow a Gaussian distribution, we separately analyzed the effects of both the mean and the variance of this distribution. To see the effects of the mean bias, we considered a variance $h = 0$. With a variance of zero, we are examining the case where we have a uniform bias for all neurons equal to h_0, meaning we are analyzing a system with a constant bias. Figures 5 and 6 show that this field h_0 magnetizes the network, leading to the disappearance of the disordered region with $m = 0$ (dark blue region in both figures). Thus, the disappearance of the disordered phases (P and SG) also leads to a reduction in the regions exhibiting RSB, as shown in Fig. 10.

We also considered scenarios with different variances in the bias ($h = 0.5, 1.5$, and $h_0 = 0$), results shown in Figures 7 and 8. In this case, we did not observe a reduction in the regions with $m = 0$; instead, this region increased as the variance increased. However, there was an increase in the regions where q is different from zero, characteristic of the SG and F phases. In Fig. 7, we see that the F phase ($m \neq 0$ and $q \neq 0$) still survives, albeit reduced in size, while the P phase is nearly disappeared. When we further increased the variance to $h = 1.5$, we only observed a region with $m = 0$ and $q \neq 0$, characteristic of the SG phase. Despite the growth of phases exhibiting RSB (SG, F), in Fig. 11, we see that the region with RSB decreases. We attribute this behavior to explicit symmetry breaking in the replica space: when the bias variance h is non-zero, each neuron feels a different field, tending to orient each neuron in its direction. Combined with a zero mean bias ($h_0 = 0$), we get a privileged direction in each neuron, but calculating the mean results in a net zero magnetization.

After studying the more general form of the *Boltzmann Machine*, we moved on to analyze its bipartite model, called the RBM, where we consider two types of neurons: *visible* and *hidden*, with no connections between neurons within the same layer. In this model, we focused solely on examining the effects of biases on the network's properties. Like in the BM, we used the replica method to find the network's order parameters, identifying four of them: m, q for visible neurons, and $\bar{m}$, $\bar{q}$ for hidden neurons. Physically, these order parameters carry the same meaning as in the BM.

When calculating the phase diagram for the system without biases in Fig. 12, we found that it behaves similarly to its more general counterpart, showing that both visible and hidden neurons simultaneously exist in the same phases. When we introduced biases into the system, we observed that they directly affected neurons in the other layer. Specifically, applying a bias to the visible neurons directly influenced the phase diagrams of the hidden neurons, as we can observe in Figures 13, 14 and 15. This might seem counter intuitive, as one would expect biases to affect the neurons to which they are applied directly. However, this is expected when analyzing the state equations (5.23) and (5.24), where it becomes evident that the phase diagrams of one layer depend on the parameters and states of neurons in the other layer. Furthermore, the phase diagrams obtained show the same effects of biases on neuron properties, with the difference being that biases directly affect the opposite layer, impacting the layer where they are applied to a lesser extent. Therefore, the reasoning follows similarly to that of the *BM*.

As a final part, we studied the equilibrium properties of the QBM in the *semi classical* approximation, which we term the *SCBM*. We do not call it *QBM* because in this approximation, quantum correlations are not considered, and therefore some quantum effects related to these are absent. However, effects like superposition and tunneling are considered in this approximation. To use the replica method, we first transform the quantum Hamiltonian of the system into an effective classical Hamiltonian. This classical Hamiltonian has an additional dimension (*Trotter* direction) connecting the nearest neighbors of the neurons, and this synapse is constant, depending on the strength of the transverse field for all connections, which does not affect the disorder degree of the system.

When solving for the symmetric and static approximations, we obtained three order parameters. Two of them, commonly found in spin glasses (m and q), and another parameter(r) related to the degree of quantum fluctuations present in the system: $\Lambda = 1-r$. When there are no quantum fluctuations ($\Omega = 0$, $r = 1$), then $\Lambda = 0$, indicating no quantum fluctuations, suggesting the absence of quantum effects in the system, leading us to the classical limit.

Finally, we obtained phase diagrams for the *SCBM* at $T = 0$ under different scenarios with and without bias. Here, we highlight the similarity in phase diagrams with their classical counterparts (in fact, they are identical), suggesting that for this limit, quantum fluctuations have nearly the same effects as thermal fluctuations on the macroscopic properties of the system. We say *nearly* because despite the macroscopic properties of the system being identical, with Ω playing a role analogous to T, there is a small (but significant) difference. Upon analyzing stability, we found that symmetric solutions in the static approximation are stable across all points in the phase diagram, showing a restoration of replica symmetry, attributed to quantum tunneling effects between

"trapped" states separated by infinitely high barriers in the free energy landscape [67]. In the thermodynamic limit, these barriers narrow considerably as the system size increases, allowing for finite area tunneling possibilities [68].

In general terms, we conclude that the results presented in this thesis meet the initially set objectives and we believe they establish a solid foundation for future research. Although we hope to resolve some matters, we acknowledge the time constraints inherent in our work. Therefore, we encourage other researchers to go deeper into these topics, which we will list below:

- Since the results obtained were theoretical, it becomes useful to compare them either with other types of approaches, such as theoretical methods like cavity methods, or with numerical simulations using Monte Carlo methods, for example.
- Also, aiming to compare, especially critical points and studying types of phase transitions, it would be interesting to study the response functions as magnetic susceptibility, in order to see which type of phase transition is present.
- We focused on studying the properties of systems assuming symmetry in the replica space; however, in certain situations, these solutions are not viable due to Replica Symmetry Breaking as the SG Phase without bias in the classical case for example. It is thus necessary to consider an approach that takes into account this symmetry breaking to more accurately determine the phase boundaries.
- We just study the statically case before the training for the neural networks, it would be interesting also the study of its dynamical properties and see how is the change of the magnetization and the spin glass order parameter during the training.
- For the Quantum Boltzmann Machine, although we obtained a general form of the equations of state, we only solved them for $T = 0$ (where they reduce to a simpler form). Currently, we are solving them for finite temperatures and observing the behavior of the network in the $\Omega - T$ space, where we believe the competition between thermal and quantum fluctuations will lead to a phase different from those discussed here.
- With the goal of including quantum correlations in the macroscopic behavior of the system, especially near critical points, we will begin to study different simulation methods for open quantum systems and observe changes in phase diagrams, both for the $T = 0$ limit and for the entire $\Omega - T$ space.
- Finally, we intend to study the significance of these results and those obtained subsequently in this dissertation, in biological or artificial systems (in the context of physical machines capable of learning, rather than as machine learning algorithms).

Bibliography

[1] Ian Goodfellow, Yoshua Bengio, and Aaron Courville. *Deep Learning*. MIT Press, 2016. http://www.deeplearningbook.org. Cited on page 21.

[2] Zewen Li, Fan Liu, Wenjie Yang, Shouheng Peng, and Jun Zhou. A survey of convolutional neural networks: Analysis, applications, and prospects. *IEEE Transactions on Neural Networks and Learning Systems*, 33(12):6999–7019, 2022. Cited on page 21.

[3] Yoav Goldberg. A primer on neural network models for natural language processing. *Journal of Artificial Intelligence Research*, 57:345–420, 2016. Cited on page 21.

[4] Shengze Cai, Zhiping Mao, Zhicheng Wang, Minglang Yin, and George Em Karniadakis. Physics-informed neural networks (pinns) for fluid mechanics: A review. *Acta Mechanica Sinica*, 37(12):1727–1738, 2021. Cited on page 21.

[5] Salvatore Cuomo, Vincenzo Schiano Di Cola, Fabio Giampaolo, Gianluigi Rozza, Maziar Raissi, and Francesco Piccialli. Scientific machine learning through physics–informed neural networks: Where we are and what's next. *Journal of Scientific Computing*, 92(3):88, 2022. Cited on page 21.

[6] Giuseppe Carleo and Matthias Troyer. Solving the quantum many-body problem with artificial neural networks. *Science*, 355(6325):602–606, 2017. Cited 2 times in the pages 21 and 22.

[7] R. McEliece, E. Posner, E. Rodemich, and S. Venkatesh. The capacity of the hopfield associative memory. *IEEE Transactions on Information Theory*, 33(4):461–482, 1987. Cited on page 21.

[8] J J Hopfield. Neural networks and physical systems with emergent collective computational abilities. *Proceedings of the National Academy of Sciences*, 79(8):2554–2558, 1982. Cited on page 21.

[9] David Sherrington and Scott Kirkpatrick. Solvable model of a spin-glass. *Phys. Rev. Lett.*, 35:1792–1796, Dec 1975. Cited 4 times in the pages 21, 23, 42, and 71.

[10] Alberto Fachechi, Elena Agliari, and Adriano Barra. Dreaming neural networks: Forgetting spurious memories and reinforcing pure ones. *Neural Networks*, 112, 04 2019. Cited on page 21.

[11] Daniel J. Amit, Hanoch Gutfreund, and H. Sompolinsky. Spin-glass models of neural networks. *Phys. Rev. A*, 32:1007–1018, Aug 1985. Cited on page 21.

[12] David H. Ackley, Geoffrey E. Hinton, and Terrence J. Sejnowski. A learning algorithm for boltzmann machines. *Cognitive Science*, 9(1):147–169, 1985. Cited on page 21.

[13] Giancarlo Fissore. *Generative modeling : statistical physics of Restricted Boltzmann Machines, learning with missing information and scalable training of Linear Flows*. Theses, Université Paris-Saclay, March 2022. Cited on page 22.

[14] Maria Schuld and Francesco Petruccione. *Machine Learning with Quantum Computers*. Quantum Science and Technology. Springer Cham, 2 edition, October 2021. 30 b/w illustrations, 74 illustrations in colour. Cited on page 22.

[15] Neil B. Lovett, Cécile Crosnier, Martí Perarnau-Llobet, and Barry C. Sanders. Differential evolution for many-particle adaptive quantum metrology. *Phys. Rev. Lett.*, 110:220501, May 2013. Cited on page 22.

[16] Esma Aïmeur, Gilles Brassard, and Sébastien Gambs. Quantum speed-up for unsupervised learning. *Machine Learning*, 90:261–287, 2013. Cited on page 22.

[17] Giuseppe Davide Paparo, Vedran Dunjko, Adi Makmal, Miguel Angel Martin-Delgado, and Hans J. Briegel. Quantum speedup for active learning agents. *Phys. Rev. X*, 4:031002, Jul 2014. Cited on page 22.

[18] Kerstin Beer, Denys Bondarenko, Terry Farrelly, Tobias J. Osborne, Robert Salzmann, Daniel Scheiermann, and Robert Wolf. Training deep quantum neural networks. *Nature Communications*, 11:808, 2020. Cited on page 22.

[19] Alex Monràs, Gael Sentís, and Peter Wittek. Inductive supervised quantum learning. *Phys. Rev. Lett.*, 118:190503, May 2017. Cited on page 22.

[20] Chen-Yu Liu, Chu-Hsuan Abraham Lin, and Kuan-Cheng Chen. Learning Quantum Phase Estimation by Variational Quantum Circuits. 11 2023. Cited on page 22.

[21] E. Torrontegui and J. J. García-Ripoll. Unitary quantum perceptron as efficient universal approximator(a). *Europhysics Letters*, 125(3):30004, mar 2019. Cited on page 22.

[22] Nathan Killoran, Thomas R. Bromley, Juan Miguel Arrazola, Maria Schuld, Nicolás Quesada, and Seth Lloyd. Continuous-variable quantum neural networks. *Phys. Rev. Res.*, 1:033063, Oct 2019. Cited on page 22.

[23] Mohammad H. Amin, Evgeny Andriyash, Jason Rolfe, Bohdan Kulchytskyy, and Roger Melko. Quantum boltzmann machine. *Phys. Rev. X*, 8:021050, May 2018. Cited 3 times in the pages 22, 34, and 35.

[24] Maria Schuld, Ilya Sinayskiy, and Francesco Petruccione. The quest for a quantum neural network. *Quantum Information Processing*, 13:2567 – 2586, 2014. Cited on page 22.

[25] Flaviano Morone, Francesco Caltagirone, Elizabeth Harrison, and Giorgio Parisi. Replica theory and spin glasses. 09 2014. Cited on page 23.

[26] M. Aguilera, M. Igarashi, and H. Shimazaki. Nonequilibrium thermodynamics of the asymmetric sherrington-kirkpatrick model. *Nature Communications*, 14:3685, 2023. Cited on page 23.

[27] Hidetoshi Nishimori. *Statistical Physics of Spin Glasses and Information Processing: An Introduction*. Oxford University Press, 07 2001. Cited 6 times in the pages 23, 41, 45, 94, 96, and 97.

[28] Do-Hyun Kim, Jinhan Park, and Byungnam Kahng. Enhanced storage capacity with errors in scale-free hopfield neural networks: An analytical study. *PLoS ONE*, 12, 2016. Cited on page 23.

[29] A. Barra, G. Genovese, and F. Guerra. The replica symmetric approximation of the analogical neural network. *Journal of Statistical Physics*, 140:784–796, 2010. Cited on page 23.

[30] E. Nogueira, F. D. Nobre, F. A. da Costa, and S. Coutinho. Tricritical behavior in the sherrington-kirkpatrick spin glass under a bimodal random field. *Phys. Rev. E*, 57:5079–5086, May 1998. Cited on page 23.

[31] João M. de Araújo, Fernando D. Nobre, and Francisco A. da Costa. Tricritical points in the sherrington-kirkpatrick model in the presence of discrete random fields. *Phys. Rev. E*, 61:2232–2240, Mar 2000. Cited on page 23.

[32] R. F. Soares, F. D. Nobre, and J. R. L. de Almeida. Effects of a gaussian random field in the sherrington-kirkpatrick spin glass. *Phys. Rev. B*, 50:6151–6156, Sep 1994. Cited on page 23.

[33] Ioannis A. Hadjiagapiou. The sherrington–kirkpatrick spin glass model in the presence of a random field with a joint gaussian probability density function for the exchange interactions and random fields. *Physica A: Statistical Mechanics and its Applications*, 397:1–16, 2014. Cited on page 23.

[34] Sei Suzuki, Jun-ichi Inoue, and Bikas K. Chakrabarti. *Quantum Ising Phases and Transitions in Transverse Ising Models*, volume 859. 2013. Cited on page 23.

[35] Arnab Das and Bikas Chakrabarti. Quantum annealing and related optimization methods. *Quantum Annealing and Related Optimization Methods, Edited by A. Das*

and B.K. Chakrabarti. 2005 XIV, 378 p. 124 illus. Also available online. ISBN 3-540-27987-3. Berlin: Springer, 2005., 01 2005. Cited on page 24.

[36] E. T. Jaynes. Information theory and statistical mechanics. *Phys. Rev.*, 106:620–630, May 1957. Cited on page 27.

[37] A. N. Kolmogorov. *Foundations of the theory of probability;*. Chelsea Pub. Co., New York, 1950. Cited on page 29.

[38] Lars Onsager. Reciprocal relations in irreversible processes. i. *Phys. Rev.*, 37:405–426, Feb 1931. Cited on page 29.

[39] T. Tomé. *Dinâmica Estocástica e Irreversibilidade Vol. 35*. EDUSP, 2001. Cited on page 29.

[40] Marylou Gabrié, Eric W. Tramel, and Florent Krzakala. Training restricted boltzmann machines via the thouless-anderson-palmer free energy. In *Proceedings of the 28th International Conference on Neural Information Processing Systems - Volume 1*, NIPS'15, page 640–648, Cambridge, MA, USA, 2015. MIT Press. Cited on page 33.

[41] H J Kappen. Learning quantum models from quantum or classical data. *Journal of Physics A: Mathematical and Theoretical*, 53(21):214001, may 2020. Cited on page 33.

[42] Nihal Yapage and Hiroshi Nagaoka. An information geometrical approach to the mean-field approximation for quantum ising spin models. *Journal of Physics A: Mathematical and Theoretical*, 41(6):065005, jan 2008. Cited on page 34.

[43] Michael A. Nielsen and Isaac L. Chuang. *Quantum Computation and Quantum Information: 10th Anniversary Edition*. Cambridge University Press, 2010. Cited on page 35.

[44] Fabrizio Minganti and Alberto Biella. Open quantum systems – a brief introduction, 2024. Cited on page 36.

[45] Mária Kieferová and Nathan Wiebe. Tomography and generative training with quantum boltzmann machines. *Phys. Rev. A*, 96:062327, Dec 2017. Cited on page 36.

[46] Nathan Wiebe and Leonard Wossnig. Generative training of quantum Boltzmann machines with hidden units. 5 2019. Cited on page 36.

[47] Xavier Glorot and Yoshua Bengio. Understanding the difficulty of training deep feedforward neural networks. In Yee Whye Teh and Mike Titterington, editors, *Proceedings of the Thirteenth International Conference on Artificial Intelligence and*

Statistics, volume 9 of *Proceedings of Machine Learning Research*, pages 249–256, Chia Laguna Resort, Sardinia, Italy, 13–15 May 2010. PMLR. Cited on page 39.

[48] Nitish Srivastava, Geoffrey Hinton, Alex Krizhevsky, Ilya Sutskever, and Ruslan Salakhutdinov. Dropout: A simple way to prevent neural networks from overfitting. *Journal of Machine Learning Research*, 15(56):1929–1958, 2014. Cited on page 39.

[49] Yann LeCun, Yoshua Bengio, and Geoffrey Hinton. Deep learning. *nature*, 521(7553):436, 2015. Cited on page 39.

[50] M Mezard, G Parisi, and M Virasoro. *Spin Glass Theory and Beyond*. WORLD SCIENTIFIC, 1986. Cited on page 40.

[51] Alfredo Braunstein and Guilhem Semerjian. *The Cavity Method: From Exact Solutions to Algorithms*, chapter 19, pages 375–387. Cited 2 times in the pages 40 and 42.

[52] Ryuhei Mori. New understanding of the bethe approximation and the replica method. *ArXiv*, abs/1303.2168, 2013. Cited 2 times in the pages 40 and 42.

[53] Serge Galam. *Spontaneous Symmetry Breaking and the Transition to Disorder in Physics*, pages 157–168. Springer Berlin Heidelberg, Berlin, Heidelberg, 2004. Cited on page 44.

[54] Nigel Goldenfeld. *Lectures On Phase Transitions And The Renormalization Group*. CRC Press, 1st edition, 1992. Cited on page 44.

[55] Aron J. Beekman, Louk Rademaker, and Jasper van Wezel. An Introduction to Spontaneous Symmetry Breaking. *SciPost Phys. Lect. Notes*, 11:1, 2019. Cited on page 44.

[56] J R L de Almeida and D J Thouless. Stability of the sherrington-kirkpatrick solution of a spin glass model. *Journal of Physics A: Mathematical and General*, 11(5):983, may 1978. Cited 6 times in the pages 45, 49, 72, 94, 96, and 97.

[57] Gavin S. Hartnett, Edward Parker, and Edward Geist. Replica symmetry breaking in bipartite spin glasses and neural networks. *Phys. Rev. E*, 98:022116, Aug 2018. Cited 2 times in the pages 47 and 56.

[58] Kerson Huang. *Introduction to Statistical Physics*. Chapman and Hall/CRC, 2nd edition, 2009. Cited on page 50.

[59] Aurélien Decelle and Cyril Furtlehner. Restricted boltzmann machine: Recent advances and mean-field theory*. *Chinese Physics B*, 30(4):040202, apr 2021. Cited on page 53.

[60] Masuo Suzuki. Relationship among exactly soluble models of critical phenomena. i: 2d ising model, dimer problem and the generalized xy-model. *Progress of Theoretical Physics*, 46(5):1337–1359, 1971. Cited on page 63.

[61] Naomichi Hatano and Masuo Suzuki. Finding exponential product formulas of higher orders. *Lecture Notes in Physics*, 679:37–68, 2005. Cited on page 63.

[62] A J Bray and M A Moore. Replica theory of quantum spin glasses. *Journal of Physics C: Solid State Physics*, 13(24):L655, aug 1980. Cited on page 65.

[63] Tomoyuki Obuchi, Hidetoshi Nishimori, and David Sherrington. Phase diagram of the p-spin-interacting spin glass with ferromagnetic bias and a transverse field in the infinite- p limit. *Journal of the Physical Society of Japan*, 76(5):054002, 2007. Cited on page 65.

[64] Do-Hyun Kim and Jong-Jean Kim. Infinite-range ising spin glass with a transverse field under the static approximation. *Phys. Rev. B*, 66:054432, Aug 2002. Cited on page 65.

[65] Hidetoshi Nishimori and Yoshihiko Nonomura. Quantum Effects in Neural Networks. *Journal of the Physical Society of Japan*, 65(12):3780, December 1996. Cited on page 66.

[66] Vitor Sessak. *Inverse problems in spin models*. Theses, Université Pierre et Marie Curie - Paris VI, September 2010. Cited on page 71.

[67] Mukherjee Sudip. Role of quantum fluctuation in inducing ergodicity in the spin glass phase and its effect in quantum annealing. *Phil. Trans. R. Soc.*, 38, Jan 2023. Cited on page 74.

[68] P. Ray, B. K. Chakrabarti, and Arunava Chakrabarti. Sherrington-kirkpatrick model in a transverse field: Absence of replica symmetry breaking due to quantum fluctuations. *Phys. Rev. B*, 39:11828–11832, Jun 1989. Cited on page 74.

[69] Aurelien Decelle, Gabriel Fissore, and Cyril Furtlehner. Thermodynamics of restricted boltzmann machines and related learning dynamics. *Journal of Statistical Physics*, 172(6):1576–1608, 2018. Cited on page 100.

APPENDIX A – Replica Trick

To prove the relationship Eq.(4.9) we consider the function:

$$f(n) = \frac{Z^n - 1}{n}. \tag{A.1}$$

We can expand Z^n in a Taylor series around $n = 0$:

$$Z^n = e^{n \ln(Z)} = 1 + n \ln(Z) + \frac{(n \ln(Z))^2}{2!} + \frac{(n \ln(Z))^3}{3!} + \dots \ . \tag{A.2}$$

Substituting the Taylor series expansion into the function $f(n)$, we get:

$$f(n) = \frac{(1 + n \ln(Z) + \frac{(n \ln(Z))^2}{2!} + \frac{(n \ln(Z))^3}{3!} + \dots) - 1}{n}. \tag{A.3}$$

Simplifying the numerator:

$$f(n) = \frac{n \ln(Z) + \frac{(n \ln(Z))^2}{2!} + \frac{(n \ln(Z))^3}{3!} + \dots}{n}. \tag{A.4}$$

Now, divide each term in the numerator by n:

$$f(n) = \ln(Z) + \frac{n(\ln(Z))^2}{2!} + \frac{n^2(\ln(Z))^3}{3!} + \dots \ . \tag{A.5}$$

Then, we take the limit $n \to 0$, then, all terms containing n in the numerator tend to zero. Therefore:

$$\lim_{n \to 0} f(n) = \lim_{n \to 0} \left(\ln(Z) + \frac{n(\ln(Z))^2}{2!} + \frac{n^2(\ln(Z))^3}{3!} + \dots . \right) = \ln(Z). \tag{A.6}$$

Finally, taking the configurational average on both sides, we have demonstrated that:

$$[\ln(Z)]_a = \lim_{n \to 0} \frac{[Z^n]_a - 1}{n}, \tag{A.7}$$

Which using Eq.(A.2) can be recast as

$$[\ln(Z)]_a = \lim_{n \to 0} \frac{\ln[Z^n]_a}{n}, \tag{A.8}$$

APPENDIX B – Replica Boltzmann Machine

B.1 Replica Calculations

We start from the Hamiltonian:

$$H = -\sum_{i<j} J_{ij}\sigma_i\sigma_j - \sum_i h_i\sigma_i, \tag{B.1}$$

with the Synapses J_{ij} and the bias h_i following Gaussian distributions:

$$P(J_{ij}) = \sqrt{\frac{N}{2\pi J^2}}\exp\left[-\frac{N}{2J^2}\left(J_{ij}-\frac{J_0}{N}\right)^2\right]; \quad P(h_i) = \sqrt{\frac{1}{2\pi h^2}}\exp\left[-\frac{1}{2h^2}(h_i-h_0)^2\right], \tag{B.2}$$

with mean and variance

$$[J_{ij}]_a = \frac{J_0}{N}, \qquad [(\Delta J_{ij})^2]_a = \frac{J^2}{N}, \tag{B.3}$$

$$[h_i]_a = h_0, \qquad [(\Delta h_i)^2]_a = h^2, \tag{B.4}$$

where,

$$[\cdot]_a = \int \prod_{i<j} P(J_{ij})dJ_{ij} \int \prod_i P(h_i)dh_i, \tag{B.5}$$

being the configurational average.

Using the replica trick, we need to calculate the free energy per neuron:

$$f = -\frac{1}{\beta}\lim_{N\to\infty}\lim_{n\to 0}\frac{[Z^n]_a - 1}{Nn}. \tag{B.6}$$

With this at hand the first step is to calculate the replicated partition function:

$$[Z^n]_a = \int \prod_{i<j} P(J_{ij})dJ_{ij} \int \prod_i P(h_i)dh_i \,\mathrm{Tr}\exp\left[\beta\sum_{\alpha=1}^{n}\sum_{i<j} J_{ij}\sigma_i^\alpha\sigma_j^\alpha + \beta\sum_{\alpha=1}^{n}\sum_i h_i\sigma_i^\alpha\right]. \tag{B.7}$$

By using equations (B.2) we can write:

$$[Z^n]_a = \sqrt{\frac{N}{2\pi J^2}}\sqrt{\frac{1}{2\pi h^2}}\int\prod_{i<j}\exp\left[-\frac{N}{2J^2}\left(J_{ij}-\frac{J_0}{N}\right)^2\right]dJ_{ij}\int\prod_i\exp\left[-\frac{1}{2h^2}(h_i-h_0)^2\right]dh_i$$
$$\mathrm{Tr}\exp\left[\beta\sum_{\alpha=1}^{n}\sum_{i<j}J_{ij}\sigma_i^\alpha\sigma_j^\alpha+\beta\sum_{\alpha=1}^{n}\sum_i h_i\sigma_i^\alpha\right]. \quad \text{(B.8)}$$

We note that above we have two Gaussian integrals we are able to using the Gaussian integral formula(or if consider from right to left the so called *Hubbard-Stratonovich* (H-S) transformation):

$$\int dx\exp\big[-Ax^2+Bx\big]=\sqrt{\frac{\pi}{A}}\exp\left(\frac{B^2}{4A}\right), \quad \text{(B.9)}$$

we can get

$$[Z^n]_a = \mathrm{Tr}\prod_{i<j}\exp\left[\frac{J^2\beta^2}{2N}(\sum_\alpha\sigma_i^\alpha\sigma_j^\alpha)^2\right]\exp\left[\frac{J_0\beta}{N}\sum_\alpha\sigma_i^\alpha\sigma_j^\alpha\right]$$
$$\prod_i\exp\left[\frac{h^2\beta^2}{2}(\sum_\alpha\sigma_i^\alpha)^2\right]\exp\left[\beta h_0\sum_\alpha\sigma_i^\alpha\right]. \quad \text{(B.10)}$$

We need to rewrite some terms in the above equation

$$\sum_{i<j}\sum_\alpha\sum_\gamma\sigma_i^\alpha\sigma_j^\alpha\sigma_i^\gamma\sigma_j^\gamma=\frac{1}{2}nN^2+\frac{1}{2}\sum_{(\alpha,\gamma)}(\sum_i\sigma_i^\alpha\sigma_i^\gamma)^2, \quad \text{(B.11)}$$

$$\sum_{i<j}\sum_\alpha\sigma_i^\alpha\sigma_j^\alpha=\frac{1}{2}\sum_\alpha(\sigma_i^\alpha)^2, \quad \text{(B.12)}$$

and

$$\sum_i\sum_\alpha\sum_\gamma\sigma_i^\alpha\sigma_i^\gamma=Nn^2+\sum_i\sum_{(\alpha,\gamma)}\sigma_i^\alpha\sigma_i^\gamma. \quad \text{(B.13)}$$

Using the above we can write Eq. (B.10), as:

$$[Z^n]_a = \exp\left[\frac{\beta^2J^2}{4}nN\right]\exp\left[\frac{\beta^2h^2}{2}Nn^2\right]\mathrm{Tr}\exp\left[\frac{J^2\beta^2}{4N}\sum_{(\alpha,\gamma)}(\sum_i\sigma_i^\alpha\sigma_i^\gamma)^2\right]\exp\left[\frac{J_0\beta}{2N}\sum_\alpha(\sum_i\sigma_i^\alpha)^2\right]$$
$$\exp\left[\frac{h^2\beta^2}{2}\sum_i\sum_{(\alpha,\gamma)}\sigma_i^\alpha\sigma_i^\gamma\right]\exp\left[\beta h_0\sum_i\sum_\alpha\sigma_i^\alpha\right]. \quad \text{(B.14)}$$

The quadratic terms will be linearized by using the Eq.(B.9)

$$\exp\left[\frac{\beta^2 J^2}{2N}\sum_{\alpha<\gamma}(\sum_i \sigma_i^\alpha\sigma_i^\gamma)^2\right] \longrightarrow \qquad A=\frac{\beta^2J^2N}{2}, \qquad B=\beta^2J^2\sum_i\sigma_i^\alpha\sigma_i^\gamma, \tag{B.15}$$

and

$$\exp\left[\frac{\beta J_0}{2N}\sum_{\alpha}(\sum_i \sigma_i^\alpha)^2\right] \longrightarrow \qquad A=\frac{\beta J_0N}{2}, \qquad B=\beta J_0\sum_i\sigma_i^\alpha. \tag{B.16}$$

Then, we can write:

$$\prod_{\alpha<\gamma}\exp\left[\frac{J^2\beta^2}{2N}(\sum_i\sigma_i^\alpha\sigma_i^\gamma)^2\right]=\prod_{\alpha<\gamma}\int dq_{\alpha\gamma}\sqrt{\frac{\beta^2J^2N}{2\pi}}\exp\left[-\frac{\beta^2J^2N}{2}q_{\alpha\gamma}^2+\beta^2J^2\sum_i\sigma_i^\alpha\sigma_i^\gamma q_{\alpha\gamma}\right], \tag{B.17}$$

and

$$\prod_{\alpha}\exp\left[\frac{\beta J_0}{2N}(\sum_i\sigma_i^2)^2\right]=\prod_{\alpha}\int dm_\alpha\sqrt{\frac{\beta J_0N}{2\pi}}\exp\left[-\frac{\beta J_0N}{2}m_\alpha^2+\beta J_0\sum_i\sigma_i^\alpha m_\alpha\right]. \tag{B.18}$$

With this results, we have encountered the Equation (4.13):

$$\begin{aligned}[Z^n]_a = f(N,n)\int\prod_{\alpha<\gamma}dq_{\alpha\gamma}\int\prod_\alpha dm_\alpha\exp\left[-\frac{\beta^2J^2}{2}N\sum_{\alpha<\gamma}q_{\alpha\gamma}^2-\frac{\beta J_0}{2}N\sum_\alpha m_\alpha^2\right]\\ \operatorname{Tr}\exp\left[\beta^2\sum_{\alpha<\gamma}(J^2q_{\alpha\gamma}+h^2)\sum_i\sigma_i^\alpha\sigma_i^\gamma+\beta\sum_\alpha(J_0m_\alpha+h_0)\sum_i\sigma_i^\alpha\right],\end{aligned} \tag{B.19}$$

where we have set:

$$f(N,n)=\exp\left[\frac{\beta^2}{2}Nn(J^2+nh^2)\right]. \tag{B.20}$$

In the Equation (B.19), the constant terms were not considered because they are involved in a productory which depends on n, and we will take the limit $n\to 0$ they simply becomes in 1.

Now, we concentrate our efforts in the trace term. We note that such term can be written as:

$$\sum_{\{\sigma_i^\alpha\}}\prod_i\exp\left[\beta^2\sum_{\alpha<\gamma}(J^2q_{\alpha\gamma}+h^2)\sigma_i^\alpha\sigma_i^\gamma+\beta\sum_\alpha(J_0m_\alpha+h_0)\sigma_i^\alpha\right], \tag{B.21}$$

where we have used $\mathrm{Tr} = \sum_{\{\sigma_i^\alpha\}} = \prod_\alpha \prod_i \sum_{\sigma_i^\alpha}$. Note that, We wrote explicitly the trace and factorize the i dependence in the exponential. Then, factorizing the products, we are able to write:

$$\prod_i \prod_\alpha \sum_{\sigma_i^\alpha} \exp\left[\beta^2 \sum_{\alpha<\gamma} (J^2 q_{\alpha\gamma} + h^2)\sigma_i^\alpha \sigma_i^\gamma + \beta \sum_\alpha (J_0 m_\alpha + h_0)\sigma_i^\alpha\right]. \tag{B.22}$$

You should have noticed that we used α in both the summation and the neuron's superscripts. But it is simple to explain: the Product runs over the replicas, starting from α and ending in the last replica n, i.e., $\prod_{\alpha=\alpha}^{n} O_\alpha = O_\alpha O_\gamma \dots O_n$.

Now, we note that the product in i is equal for all $\alpha' s$, then, we can release the dependence in i:

$$\left[\prod_\alpha \sum_{\sigma^\alpha} \exp\left(\beta^2 \sum_{\alpha<\gamma} (J^2 q_{\alpha\gamma} + h^2)\sigma^\alpha \sigma^\gamma + \beta \sum_\alpha (J_0 m_\alpha + h_0)\sigma^\alpha\right)\right]^N, \tag{B.23}$$

from now, we will set the trace as: $\mathrm{Tr} = \prod_\alpha \sum_{\sigma^\alpha}$(this is the same Tr_α in section 4), where $\sigma^\alpha = \pm 1$ is an Ising variable. Finally, we get that the trace term can be written as:

$$\exp\left[N \ln \mathrm{Tr} \exp\left(\beta^2 \sum_{\alpha<\gamma} (J^2 q_{\alpha\gamma} + h^2)\sigma^\alpha \sigma^\gamma + \beta \sum_\alpha (J_0 m_\alpha + h_0)\sigma^\alpha\right)\right]. \tag{B.24}$$

and, the partition function becomes:

$$[Z^n]_a = f(N,n) \int \prod_{\alpha<\gamma} dq_{\alpha\gamma} \int \prod_\alpha dm_\alpha \exp\left[-\frac{\beta^2 J^2}{2} N \sum_{\alpha<\gamma} q_{\alpha\gamma}^2 - \frac{\beta J_0}{2} N \sum_\alpha m_\alpha^2\right] \exp\Big[N \ln \mathrm{Tr}\, e^L\Big], \tag{B.25}$$

where,

$$L = \beta^2 \sum_{\alpha<\gamma} (J^2 q_{\alpha\gamma} + h^2)\sigma^\alpha \sigma^\gamma + \beta \sum_\alpha (J_0 m_\alpha + h_0)\sigma^\alpha. \tag{B.26}$$

B.1.1 Steepest Descent Method

In Equation (B.25), we have an integral of the form

$$I \equiv \int dx \int dy \exp[-NG(x,y)]. \tag{B.27}$$

The basic idea behind the method to solve this type of integrals is that the negative exponential function is so rapidly decreasing as $N \to \infty$, that we only need to look at the contribution from where $G(x, y)$ is at its minimum(or the argument in the exponential is at its maximum). Lets say $G(x, y)$ is at its minimum at x_0 and y_0. Then we could approximate $G(x, y)$ the first terms of its Taylor expansion,

$$G(x,y) \approx G(x_0,y_0) + \frac{1}{2}\left[(x-x_0)^2 G_{xx}(x_0,y_0) + 2(x-x_0)(y-y_0)G_{xy}(x_0,y_0) + (y-y_0)^2 G_{yy}(x_0,y_0)\right]. \tag{B.28}$$

Then, the integral can be written as

$$I = e^{-NG(x_0,y_0)} \int dx \int dy \exp\Big[-\frac{N}{2}\left((x-x_0)^2 G_{xx}(x_0,y_0) + 2(x-x_0)(y-y_0)G_{xy}(x_0,y_0) + (y-y_0)^2 G_{yy}(x_0,y_0)\right)\Big]. \tag{B.29}$$

We write the above equation in vector notation

$$I = e^{-NG(x_0,y_0)} \int dx \int dy e^{-\frac{N}{2}(\vec{x}-\vec{x_0})^T HG(\vec{x}-\vec{x_0})} \tag{B.30}$$

where the vector $\vec{x} = (x, y)$ is the vector containing the variables, and HG is the *Hessian Matrix*:

$$HG = \begin{bmatrix} G_{xx} & G_{xy} \\ G_{yx} & G_{yy} \end{bmatrix}, \tag{B.31}$$

that contains the second derivatives of the function G.

Finally, the integral (B.30) is just a 2 dimensional Gaussian integral giving

$$I \approx e^{-NG(x_0,y_0)}. \tag{B.32}$$

Before continue, note that to evaluate the integral we need to use the limit $N \to \infty$ and in order to do this an inversion of the order of the limits is necessary. To do this the limits of integration in the free energy(Eq. (4.10)) must be changed.

For the point (x_0, y_0) be a minimum the Hessian Matrix HG must be positive definite, i.e., HG must has positive eigenvalues, this fact is important when we check the stability of the replica solutions.

Then the partition function in the thermodynamic limit gives

$$[Z^n]_a = f(N,n)\exp\left[-\frac{\beta^2 J^2}{2}N\sum_{\alpha<\gamma}q_{\alpha\gamma}^2 - \frac{\beta J_0}{2}N\sum_{\alpha}m_\alpha^2 + N\ln\Big(Tr_\alpha e^L\Big)\right]. \tag{B.33}$$

where, we set the extreme points as $x_0 = q_{\alpha\gamma}$, $y_0 = m_\alpha$, and

$$G(q_{\alpha\gamma}, m_\alpha) = \frac{\beta^2 J^2}{2}\sum_{\alpha<\gamma}q_{\alpha\gamma}^2 + \frac{\beta J_0}{2}\sum_{\alpha}m_\alpha^2 - \ln\Big(Tr_\alpha e^L\Big). \tag{B.34}$$

Expanding the right side of Eq. (B.33), we get

$$[Z^n]_a \approx 1 + Nn\left[\frac{\beta^2}{2}(J^2+nh^2) - \frac{\beta^2 J^2}{2n}\sum_{\alpha<\gamma}q_{\alpha\gamma}^2 - \frac{\beta J_0}{2n}\sum_{\alpha}m_\alpha^2] + \frac{1}{n}\ln\Big(Tr_\alpha e^L\Big).\right] \tag{B.35}$$

Finally, the average free energy per neuron (B.6), results:

$$-\beta f = \lim_{n\to 0}\left(\frac{\beta^2}{2}(J^2/2+nh^2) - \frac{\beta^2 J^2}{2n}\sum_{\alpha<\gamma}q_{\alpha\gamma}^2 - \frac{\beta J_0}{2n}\sum_{\alpha}m_\alpha^2 + \frac{1}{n}\operatorname{Tr}_\alpha e^L\right). \tag{B.36}$$

B.2 Replica Symmetric Solution

In this section we will evaluate the *Replica Symmetric(RS)* solution:

$$q_{\alpha\gamma} = q \qquad \forall\ \alpha\neq\gamma, \qquad\qquad q_{\alpha\gamma} = 0 \qquad \forall\ \alpha=\gamma, \tag{B.37}$$

$$m_\alpha = m \qquad \forall\ \alpha. \tag{B.38}$$

In this ansatz, the free energy of Eq. (B.36). becomes:

$$-\beta f = \frac{\beta^2 J^2}{4} - \lim_{n\to 0}\left(\frac{\beta^2 J^2}{2n}\frac{n(n-1)}{2}q^2 + \frac{\beta J_0}{2n}nm^2 - \frac{1}{n}\ln\operatorname{Tr} e^L\right). \tag{B.39}$$

We replaced the ansatz and did the summations. Evaluating the two first limits, we get

$$-\beta f = \frac{\beta^2 J^2}{2} + \frac{\beta^2 J^2}{4}q^2 - \frac{\beta J_0}{2}m^2 + \lim_{n\to 0}\frac{1}{n}\ln\operatorname{Tr} e^L. \tag{B.40}$$

Now, we will evaluate the last limit, first is straightforward to prove that:

$$\sum_{\alpha<\gamma}\sigma^\alpha\sigma^\gamma = \frac{1}{2}\left[\left(\sum_\alpha\sigma^\alpha\right)^2 - n\right]. \tag{B.41}$$

Therefore, we can write

$$e^L = \exp\left[\frac{\beta^2}{2}(J^2q + h^2)\left(\sum_\alpha \sigma^\alpha\right)^2 - \frac{n\beta^2}{2}(J^2q + h^2) + \beta(J_0m + h_0)\sum_\alpha \sigma^\alpha\right]. \tag{B.42}$$

The quadratic term can be linearized by a *H-S* transformation, with

$$A = \frac{\beta^2}{2}(J^2q + h^2); \qquad B = \beta^2(J^2q + h^2)\sum_\alpha \sigma^\alpha. \tag{B.43}$$

Then, Eq.(B.42) becomes

$$e^L = C\int dz \exp\left[-\frac{\beta^2}{2}(J^2q + h^2)z^2 + \beta^2(J^2q + h^2)z\sum_\alpha \sigma^\alpha\right] \exp\left[-\frac{\beta^2}{2}(J^2q + h^2)n + \beta(J_0m + h_0)\sum_\alpha \sigma^\alpha\right], \tag{B.44}$$

where $C = \sqrt{\frac{\beta^2(J^2q+h^2)}{2\pi}}$.

Now, we can obtain

$$\ln \mathrm{Tr}\, e^L = \ln C \exp\left[\frac{-\beta^2}{2}(J^2q + h^2)n\right]\int dz \exp\left[\frac{-\beta^2}{2}(J^2q + h^2)z^2\right] \mathrm{Tr}\exp\left[\left(\beta^2(J^2q + h^2)z + \beta(J_0m + h_0)\right)\sum_\alpha \sigma^\alpha\right]. \tag{B.45}$$

Following a similar procedure obtaining Eq.(B.23), we get

$$\mathrm{Tr}\exp\left[A\sum_\alpha \sigma^\alpha\right] = [2\cosh(A)]^n, \tag{B.46}$$

with $A = \beta^2(J^2q + h^2)z + \beta(J_0m + h_0)$.

Then, Eq.(B.48) can be written as:

$$\ln \mathrm{Tr}\, e^L = \ln C \exp\left[\frac{-\beta^2}{2}(J^2q + h^2)n\right]\int dz \exp\left[\frac{-\beta^2}{2}(J^2q + h^2)z^2 + n\ln[2\cosh(A)]\right]. \tag{B.47}$$

The integral in the equation above is easily rewritten by performing a substitution:

$$z = \beta(J^2q + h^2)^{1/2}z \longrightarrow \qquad dz = \beta(J^2q + h^2)^{1/2}dz = C\sqrt{2\pi}dz,$$

obtaining,

$$\mathrm{Tr}\, e^L = \ln\left[\exp\left(\frac{-\beta^2}{2}(J^2q + h^2)n\right)\int Dz \exp\Big[n\ln\Big(2\cosh\Big(\beta\tilde{H}(z)\Big)\Big)\Big]\right], \tag{B.48}$$

with $Dz = \frac{1}{\sqrt{2\pi}}e^{-z^2/2}$ and $\tilde{H}(z) = \sqrt{J^2q + h^2}z + J_0m + h_0$. Then,

$$\lim_{n\to 0}\frac{1}{n}\,\mathrm{Tr}_\alpha\, e^L = \int Dz \ln[2\cosh\Big(\beta\tilde{H}(z)\Big)] - \frac{\beta^2}{2}(J^2q + h^2). \tag{B.49}$$

Finally, the free energy (B.40) becomes:

$$-\beta f = \frac{\beta^2J^2}{4}(1-q)^2 - \frac{\beta J_0}{2}m^2 + \int Dz \ln[2\cosh\Big(\beta\tilde{H}(z)\Big)] - \frac{\beta^2}{2}h^2. \tag{B.50}$$

To end this section, we will calculate the order parameters using the condition of extreme of the free energy:

$$\beta\frac{\partial f}{\partial q} = -\frac{\beta^2J^2}{2}(1-q) + \int Dz \tanh\Big(\beta\tilde{H}(z)\Big)\frac{z\beta}{2}(J^2q + h^2)^{-1/2}J^2 = 0. \tag{B.51}$$

The integral in the equation above can be rewritten using integration by parts, with

$$u = \tanh\Big(\beta\tilde{H}(z)\Big) \qquad \textit{and} \qquad dv = e^{-z^2/2}zdz,$$

getting:

$$-\frac{\beta^2}{2}(1-q) + \frac{\beta^2}{2}\int Dz\,\mathrm{sech}^2(\beta\tilde{H}(z)) = 0. \tag{B.52}$$

Reordering, we get:

$$q = 1 - \int Dz\,\mathrm{sech}^2(\beta\tilde{H}(z)), \tag{B.53}$$

and finally

$$q = \int Dz \tanh^2(\beta \tilde{H}(z)). \tag{B.54}$$

Analogously, we obtain

$$m = \int Dz \tanh\Big(\beta \tilde{H}(z)\Big). \tag{B.55}$$

B.3 Analytical Boundaries of the Phase Diagram Without Bias

In this section we will find the analytical boundaries of the phase diagram for the system without bias.

B.3.1 Paramagnetic-Spin Glass Boundary

If the distribution of J_{ij} is centered in zero($J_0 = 0$), we get $\tilde{H}(z) = J\sqrt{q}z$ so the function $\tanh\Big(\beta \tilde{H}(z)\Big)$ is odd, then, from Eq.(B.55) $m = 0$(there is no F phase). Therefore, the free energy is

$$-\beta f = \frac{\beta^2 J^2}{4}(1-q)^2 + \int Dz \ln[2\cosh\Big(\beta \tilde{H}(z)\Big)], \tag{B.56}$$

and, the SG order parameter

$$q = \int Dz \tanh^2(\beta J\sqrt{q}z). \tag{B.57}$$

We rewrite the free energy as:

$$-\beta f = \frac{\beta^2 J^2}{4} - \frac{\beta^2 J^2}{2}q + \frac{\beta^2 J^2}{4}q^2 + \ln(2) + \int Dz \ln[\cosh\Big(\beta \tilde{H}(z)\Big)]. \tag{B.58}$$

Now, we expand the integrand in the last term in the above equation:

$$\ln[\cosh(x)] \approx \frac{x^2}{2} - \frac{x^4}{12} + \dots \ .$$

We obtain integrals of the form

$$I = \int_{-\infty}^{\infty} dz \frac{1}{\sqrt{2\pi}} e^{-z^2/2} z^{2n} = 2\int_{0}^{\infty} \frac{dz}{\sqrt{2\pi}} e^{-z^2/2} z^{2n}. \tag{B.59}$$

where, $n \in \mathbb{Z}^+$. In order to evaluate the integrals, we will use the *Gamma* function:

$$\Gamma(\xi + 1) = \int_0^{\infty} t^{\xi} e^{-t}. \tag{B.60}$$

Now, we write the integral (B.59) in the form of the gamma function making the substitution $t = z^2/2$, getting:

$$I = \frac{1}{\sqrt{\pi}} \int_0^\infty dt e^{-t} t^{n-1/2} 2^n = \frac{1}{\sqrt{\pi}} \Gamma\left(n + \frac{1}{2}\right) 2^n. \tag{B.61}$$

But, we know that

$$\Gamma\left(n + \frac{1}{2}\right) = \frac{(2n)!}{4^2 n!} \sqrt{\pi}. \tag{B.62}$$

Then

$$I = \frac{(2n)!}{2^n n!}. \tag{B.63}$$

Finally, the free energy is written as:

$$\beta f = -\ln(2) - \frac{\beta^2 J^2}{4} - \frac{\beta^2 J^2}{4}(1 - \beta^2 J^2) q^2. \tag{B.64}$$

According to the *Landau Theory* of phase transitions, the critical point is determined by the vanishing coefficient of the second order term q^2. Therefore, the critical point is given by:

$$\frac{K_B T_c}{J} = 1. \tag{B.65}$$

This is the *P-SG* Boundary. From here, we will set $K_B = 1$ without losing generality

B.3.2 Paramagnetic-Ferromagnetic Boundary

A Ferromagnetic solution may exists if $J_0 \neq 0$. Then, in order to obtain this boundary, we begin expanding to first order the integrand in Eq.(B.55):

$$m \approx \int \frac{dz}{\sqrt{2\pi}} e^{-z^2/2} (\beta J \sqrt{q} z) + \beta m J_0. \tag{B.66}$$

The integral in equation above is easily solved by making a substitution: $u = z^2/2$ that results in $I = 0$. Then, we obtain:

$$m \approx \beta m J_0. \tag{B.67}$$

Finally, the boundary for the $P - F$ phases is:

$$T_c = J_0. \tag{B.68}$$

B.3.3 Spin Glass-Ferromagnetic Boundary

At the end, the boundary between the SG and F phases is given only by numerically solving equations (B.54) and (B.55). It is difficult, because the order parameter q is nonzero in both phases, we first solved numerically Eq.(B.57) for $m = 0$, we calculated various q for different β, then we expand the equation for m obtaining:

$$T = J_0 \int \frac{1}{\sqrt{2\pi}} \operatorname{sech}^2(\beta J\sqrt{q}z)dz. \tag{B.69}$$

With the values of q calculated numerically, we solved numerically the above equation in order to obtain the boundary between the two phases.

B.4 Negative Entropy and AT Line

B.4.1 Negative Entropy of the Symmetric Solution

In this section, we will see a physical problem of the symmetric solution at low temperatures. From Eq.(B.54) we note that $q \to 1$ as $T \to 0(\beta \to \infty)$, as we see before we are in a regime when $m = 0$, i.e., we are placed in the SG phase. Now, as $q \to 1$, we assume:

$$q = 1 - aT \qquad\qquad (a > 0), \tag{B.70}$$

Then, using Eq.(B.53), we have, for $\beta \to \infty$

$$\begin{aligned} q = 1 - \int Dz \operatorname{sech}^2(\beta\tilde{H}(z)) = 1 - \frac{1}{\beta J}\int Dz \frac{d}{dz}\tanh(\beta JZ), \\ = 1 - \int Dz 2\delta(z) = 1 - \frac{2}{\sqrt{2\pi}\beta J} = 1 - \sqrt{\frac{2}{\pi}}\frac{T}{J}. \end{aligned} \tag{B.71}$$

This results confirm the assumption $q = 1 - aT$ with $a = \sqrt{\frac{2}{\pi}}\frac{1}{J}$.

The free energy at $T \to 0$, and using Eq.(B.70), is

$$-\beta f = \frac{1}{2\pi} + \int \ln[2\cosh(\beta J\sqrt{q}z)]. \tag{B.72}$$

The integral in the equation above gives:

$$I = 2\int_0^\infty Dz \ln[e^{-\beta J\sqrt{q}z} + e^{\beta J\sqrt{q}z}]. \tag{B.73}$$

In the limit $\beta \to \infty$,

$$I \approx 2\int_0^\infty Dz \ln[e^{\beta J\sqrt{q}z}] = 2\beta J\sqrt{q}\int_0^\infty \frac{1}{\sqrt{2\pi}}e^{-z^2/2}zdz = \sqrt{\frac{2}{\pi}}\beta J\sqrt{q}. \tag{B.74}$$

We expand to first order $\sqrt{q}$ around 1:

$$\sqrt{q} \approx \frac{q}{2} + \frac{1}{2} + \dots .$$

Thus, using our assumption $q = 1 - aT$, the free energy (B.72), becomes

$$f = \frac{T}{2\pi} - \sqrt{\frac{2}{\pi}}J. \tag{B.75}$$

Since, $f = \langle E(\sigma)\rangle - \frac{S}{\beta}$, we conclude that the entropy

$$S = -\frac{1}{2\pi}. \tag{B.76}$$

B.4.2 AT Line

In the previous section we prove that the solutions at low temperatures have negative entropy. We now test the appropriateness of the *RS* assumption. As we see in previous sections for the *RS* solution be reliable, the *Hessian* matrix must be definite positive, that is, it has positive eigenvalues. *Almeida and Thouless*[56] showed that the problematic eigenvalue is the one related to the *SG* order parameter $q_{\alpha\gamma}$, that is, that the replica symmetric problem is placed in such order parameter and the magnetization m_α does not depend on the replica's index being *RS*. For this section we will follow closely [27].

First we consider the Hessian Matrix Eq.(B.31):

$$HG = \begin{bmatrix} G_{xx} & G_{xy} \\ G_{yx} & G_{yy} \end{bmatrix}, \tag{B.77}$$

with,

$$G = \frac{\beta^2 J^2}{2}\sum_{\alpha<\gamma} q_{\alpha\gamma}^2 + \frac{\beta J_0}{2}\sum_\alpha m_\alpha^2 - \ln[\mathrm{Tr}\, e^L], \tag{B.78}$$

and,

$$L = \beta^2 \sum_{\alpha<\gamma}(J^2 q_{\alpha\gamma} + h^2)\sigma^\alpha\sigma^\gamma + \beta\sum_\alpha (J_0 m_\alpha + h_0)\sigma^\alpha. \tag{B.79}$$

Now the second derivatives in the *Hessian* are given by:

$$G_{xx} = \frac{\partial^2 G}{\partial m_\mu m_\alpha} = \beta J_0 \delta_{\mu\alpha} - \beta^2 J_0^2 \left(\langle \sigma^\alpha \sigma^\mu \rangle - \langle \sigma^\alpha \rangle \langle \sigma^\mu \rangle \right), \tag{B.80}$$

the crossed terms,

$$G_{xy} = \frac{\partial^2 G}{\partial q_{\alpha\gamma} m_\mu} = -\beta^2 J^2 J_0 \left(\langle \sigma^\alpha \sigma^\gamma \sigma^\mu \rangle - \langle \sigma^\alpha \sigma^\gamma \rangle \langle \sigma^\mu \rangle \right), \tag{B.81}$$

and, the terms related with q

$$G_{yy} = \frac{\partial^2 G}{\partial q_{\alpha\gamma} q_{\mu\lambda}} = \beta^2 J^2 \delta_{\alpha\gamma,\mu\lambda} - \beta^4 J^4 \left(\langle \sigma^\alpha \sigma^\gamma \sigma^\mu \sigma^\lambda \rangle \right) - \beta^4 J^4 \left(\langle \sigma^\alpha \sigma^\gamma \rangle \langle \sigma^\mu \sigma^\gamma \rangle \right). \tag{B.82}$$

Since we are computing the Hessian in the RS point, it is easy to see that it contains seven kinds of elements. The ones related only to the m parameter are:

$$A = \beta J_0 - \beta^2 J_0 (1 - m^2) \qquad for \qquad (\alpha = \mu), \tag{B.83}$$

and,

$$B = -\beta^2 J_0^2 (q - m^2) \qquad for \qquad (\alpha \neq \mu). \tag{B.84}$$

We have those related to the q order parameter

$$P = \beta^2 J^2 - \beta^4 J^4 (1 - q^2) \qquad for \qquad (\alpha = \mu), (\gamma = \lambda), \tag{B.85}$$

$$Q = -\beta^4 J^4 (q - q^2) \qquad for \qquad (\alpha = \mu), (\gamma \neq \lambda), \tag{B.86}$$

and,

$$R = -\beta^4 J^4 (r - q^2) \qquad for \qquad (\alpha \neq \mu), (\gamma = \lambda). \tag{B.87}$$

Finally, we have the crossed terms,

$$C = \beta^3 J^2 J_0 (m - mq) \qquad for \qquad (\alpha = \mu), \tag{B.88}$$

and,

$$D = \beta^3 J^2 J_0 (t - mq) \qquad for \qquad (\alpha = \mu). \tag{B.89}$$

with, $r = \int Dz \tanh^4[\beta\tilde{H}(z)]$ and $t = \int Dz \tanh^3[\beta\tilde{H}(z)]$.

In the P phase $m = q = r = t = 0$, so the only non zero terms are the diagonal elements $A = \beta J^0 - \beta^2 J_0^2$ and $P = \beta^2 J^2 - \beta^4 J^4$. Thus, the *Hessian* has two eigenvalues A and P, and in order to it be positive-definite they must be positive, $A > 0$ and $P > 0$, which gives the conditions:

$$T > J_0 \qquad and \qquad T > J, \tag{B.90}$$

which, are always satisfied in the P phase.

For the other two phases, we need to calculate the eigenvalues of the *Hessian*, with the eigenvalue equation:

$$HG\vec{V} = \lambda\vec{V}, \tag{B.91}$$

where,

$$\vec{V} = \begin{bmatrix} \{m_\alpha\} \\ \{q_{\alpha\gamma}\} \end{bmatrix},$$

with, $\{m_\alpha\} = (m_1\ m_2\ \ldots\ m_n)^T$ and $\{q_{\alpha\gamma}\} = (q_{12}\ q_{13}\ \ldots\ q_{n-1n})^T$, with dimensions n and $\frac{n(n-1)}{2}$, respectively.

We can find three classes of eigenvectors[27, 56]. The first $\vec{V}_1$, which is symmetric under the change of all indices, i.e., $m_\alpha = a\ \forall\alpha$ and $q_{\alpha\gamma} = b\forall\alpha,\gamma$. Then, for example, for three replicas the *Hessian* matrix becomes:

$$HG = \begin{bmatrix} A & B & B & C & C & D \\ B & A & B & C & D & C \\ B & B & A & D & C & C \\ C & C & D & P & Q & Q \\ C & D & C & Q & P & Q \\ D & C & C & Q & Q & P \end{bmatrix}, \tag{B.92}$$

with, $\vec{V}_1 = (a\ a\ a\ b\ b\ b)^T$. It is straightforward to show that this eigenvalue in the limit $n \to 0$, gives:

$$\lambda_1 = \frac{1}{2}\Big\{(A+(n-1)B+P-2(n-2)Q+\frac{1}{2}(n-2)(n-3)R) \pm\sqrt{\Big(A+(n-1)B-P-2(n-2)Q-\frac{1}{2}(n-2)(n-3)R\Big)^2+2(n-1)(2C+(n-1)D)^2}\Big\}. \tag{B.93}$$

The second eigenvector $\vec{V}_2$, which is symmetric under the interchange of all but one of the indices, i.e., $m_\alpha = a$(For a specific replica θ), $m_\alpha = b$(otherwise) and $q_{\alpha\gamma} = c$(when α or γ are equal to θ), $q_{\alpha\gamma}$(otherwise). We can assume $\theta = 1$ without loss of generality. It can be proven that this eigenvalue at the limit $n \to 0$ is equal to λ_1[27].

Finally, the third eigenvector $\vec{V}_3$, which is symmetric under the interchange of all but two of the indices, that is, $m_\alpha = a$(For two specific replicas θ and ν), $m_\alpha = b$(otherwise) and $q_{\alpha\gamma} = c$(when α or γ are equal to θ), $q_{\alpha\gamma} = d$(when α or γ are equal to ν), $q_{\alpha\gamma} = e$(otherwise). Using the orthogonality with the other two eigenvectors, it is easy to show that λ_3, gives

$$\lambda_3 = P - 2Q + R. \tag{B.94}$$

As *Almeida and Thouless* showed[56], this is the problematic eigenvalue, i.e, the other two are always positive and just λ_3 can take negative values. This eigenvalue is known as *Replicon*(This is the reason in the principal text we use the subscript r), and using Equations (B.85), (B.86) and (B.87), it gives

$$\lambda_3 = \beta^2 J^2[1-\beta^2 J^2(1-q^2)+2\beta^4 J^4 q(1-q^2)-\beta^4 J^4(r-q^2)]. \tag{B.95}$$

APPENDIX C – Replica Restricted Boltzmann Machine

C.1 Replica Calculations

In this appendix, we will detail the calculations for the *RBM*.

First, we consider the energy function of the model:

$$H(\sigma, s) = -\sum_{i}^{N_v}\sum_{a}^{N_h} J_{ia}\sigma_i s_a - \sum_{i}^{N_v}\sigma_i h_i - \sum_{a}^{N_h} s_a c_a. \tag{C.1}$$

As we know, the synapses and the bias follow the Gaussian distributions:

$$P(J_{ia}) = \sqrt{\frac{L}{2\pi J^2}}\exp\left[-\frac{L}{2J^2}\left(J_{ia} - \frac{J_0}{L}\right)^2\right]; \tag{C.2}$$

$$P(h_i) = \sqrt{\frac{1}{2\pi h^2}}\exp\left[-\frac{1}{2h^2}(h_i - h_0)^2\right]; \tag{C.3}$$

$$P(c_a) = \sqrt{\frac{1}{2\pi c^2}}\exp\left[-\frac{1}{2c^2}(c_a - c_0)^2\right], \tag{C.4}$$

with mean and variance given by equations (5.5),(5.6) and (5.7).

The following step is write the replicated partition function:

$$[Z^n]_a = \int\prod_{i,a} P(J_{ia})dJ_{ia}\int\prod_{i} P(h_i)dh_i\int\prod_{a} P(c_a)dc_a$$
$$\mathrm{Tr}\exp\left[\beta\sum_{\alpha}\sum_{i,a} J_{ia}\sigma_i^\alpha s_a^\alpha + \beta\sum_{\alpha}\sum_{i} h_i\sigma_i^\alpha + \beta\sum_{\alpha}\sum_{a} c_a s_a^\alpha\right]. \tag{C.5}$$

We note in the above equation that we can separate the exponential terms and invert the order of integrals and the trace, then we can evaluate the integrals separately, such integrals as you should note are simply Gaussian integrals that can be solved using Eq.(B.9), resulting in:

$$[Z^n]_a = \mathrm{Tr}\prod_{i,a}\exp\left[\frac{\beta^2 J^2}{2L}\left(\sum_\alpha \sigma_i^\alpha s_a^\alpha\right)^2 + \frac{\beta J_0}{L}\sum_\alpha \sigma_i^\alpha s_a^\alpha\right] \prod_i \exp\left[\frac{\beta^2 h^2}{2}\left(\sum_\alpha \sigma_i^\alpha\right)^2 + \beta h_0 \sum_\alpha \sigma_i^\alpha\right] \prod_a \exp\left[\frac{\beta^2 c^2}{2}\left(\sum_\alpha s_a^\alpha\right)^2 + \beta c_0 \sum_\alpha s_a^\alpha\right]. \quad \text{(C.6)}$$

Now, we use the following *H-S* transformations[69]:

$$\exp\left[\frac{\beta^2 J^2}{2L}\left(\sum_{i,a}\sum_{(\alpha,\gamma)} \sigma_i^\alpha \sigma_i^\gamma s_a^\alpha s_a^\gamma\right)\right] = \int\int \prod_{(\alpha,\gamma)} \frac{dq_{\alpha\gamma} d\bar{q}_{\alpha\gamma}}{2\pi} \exp\left[-\frac{\beta^2 J^2 L}{2} \underbrace{\sum_{(\alpha,\gamma)}\left(q_{\alpha\gamma}\bar{q}_{\alpha\gamma} - \frac{q_{\alpha\gamma}}{N_v}\sum_i \sigma_i^\alpha \sigma_i^\gamma - \frac{\bar{q}_{\alpha\gamma}}{N_h}\sum_a s_a^\alpha s_a^\gamma\right)}_{A_{q\bar{q}}}\right], \quad \text{(C.7)}$$

and,

$$\exp\left[\frac{\beta J_0}{L}\left(\sum_{i,a}\sum_\alpha \sigma_i^\alpha s_a^\alpha\right)\right] = \int\int \prod_\alpha \frac{dm_\alpha d\bar{m}_\alpha}{2\pi} \exp\left[-\frac{\beta J_0 L}{4} \underbrace{\sum_\alpha\left(m_\alpha \bar{m}_\alpha - \frac{m_\alpha}{N_v}\sum_i \sigma_i^\alpha - \frac{\bar{m}_\alpha}{N_h}\sum_a s_a^\alpha\right)}_{B_{m\bar{m}}}\right]. \quad \text{(C.8)}$$

With the above results, we can write Eq.(C.6) as

$$[Z^n]_a = \mathrm{Tr}\int\int \prod_{(\alpha,\gamma)} \frac{dq_{\alpha\gamma} d\bar{q}_{\alpha\gamma}}{2\pi} \exp\left[-\frac{\beta^2 J^2 L}{2} A_{q\bar{q}}\right] \int\int \prod_\alpha \frac{dm_\alpha d\bar{m}_\alpha}{2\pi} \exp\left[-\frac{\beta J_0 L}{4} B_{m\bar{m}}\right] \prod_{(\alpha,\gamma)} \exp\left[\frac{\beta^2 h^2}{2}\sum_i \sigma_i^\alpha \sigma_i^\gamma + \frac{\beta^2 c^2}{2}\sum_a s_a^\alpha s_a^\gamma\right] \prod_\alpha \exp\left[\beta h_0 \sum_i \sigma_i^\alpha + \beta c_0 \sum_a s_a^\alpha\right]. \quad \text{(C.9)}$$

Reordering, we get

$$[Z^n]_a = \int\int \prod_{(\alpha,\gamma)} dq_{\alpha\gamma} d\bar{q}_{\alpha\gamma} \int\int \prod_{\alpha} dm_\alpha d\bar{m}_\alpha \exp\left[-\frac{\beta^2 J^2}{2} L \sum_{(\alpha,\gamma)} q_{\alpha\gamma}\bar{q}_{\alpha\gamma} - \frac{\beta J_0}{4} L \sum_{\alpha} m_\alpha \bar{m}_\alpha\right]$$
$$\mathrm{Tr}_v \exp\left[\sum_{(\alpha,\gamma)} G_{\alpha\gamma} \sum_i \sigma_i^\alpha \sigma_i^\gamma + \sum_\alpha P_\alpha \sum_i \sigma_i^\alpha\right] \mathrm{Tr}_h \exp\left[\sum_{(\alpha,\gamma)} \bar{G}_{\alpha\gamma} \sum_a s_a^\alpha s_a^\gamma + \sum_\alpha \bar{P}_\alpha \sum_a s_a^\alpha\right], \tag{C.10}$$

where Tr_v and Tr_h are the traces over the visible and hidden neurons, respectively and with:

$$G_{\alpha\gamma} = \frac{\beta^2 J^2 q_{\alpha\gamma}}{2}\frac{L}{N_v} + \frac{\beta^2 h^2}{2}, \qquad P_\alpha = \beta J_0 m_\alpha \frac{L}{4N_v} + \beta h_0, \tag{C.11}$$
$$\bar{G}_{\alpha\gamma} = \frac{\beta^2 J^2 \bar{q}_{\alpha\gamma}}{2}\frac{L}{N_h} + \frac{\beta^2 c^2}{2}, \qquad \bar{P}_\alpha = \beta J_0 \bar{m}_\alpha \frac{L}{4N_h} + \beta c_0. \tag{C.12}$$

We ignored the constant terms because they are irrelevant in the following arguments. Now, the traces terms in Eq.(C.10), can be worked similarly as in the *BM*, giving:

$$\mathrm{Tr}_v \exp\left[\sum_{(\alpha,\gamma)} G_{\alpha\gamma} \sum_i \sigma_i^\alpha \sigma_i^\gamma + \sum_\alpha P_\alpha \sum_i \sigma_i^\alpha\right] = \sum_{\{\sigma^\alpha\}} \sum_{\{\sigma^\gamma\}} \cdots \sum_{\{\sigma^n\}} \prod_i \exp\left[\sum_{(\alpha,\gamma)} G_{\alpha\gamma}\sigma_i^\alpha\sigma_i^\gamma + \sum_\alpha P_\alpha \sigma_i^\alpha\right]$$
$$= \left[\sum_{\{\sigma^\alpha\}} \exp\left[\sum_{(\alpha,\gamma)} G_{\alpha\gamma}\sigma^\alpha\sigma^\gamma + \sum_\alpha P_\alpha\sigma^\alpha\right]\right]^{N_v} = \exp\left[N_v \ln \mathrm{Tr}_v \exp\left[\sum_{(\alpha,\gamma)} G_{\alpha\gamma}\sigma^\alpha\sigma^\gamma + \sum_\alpha P_\alpha\sigma^\alpha\right]\right],$$

analogously,

$$\mathrm{Tr}_h \exp\left[\sum_{(\alpha,\gamma)} \bar{G}_{\alpha\gamma} \sum_a s_a^\alpha s_a^\gamma + \sum_\alpha \bar{P}_\alpha \sum_a s_a^\alpha\right] = \exp\left[N_h \ln \mathrm{Tr}_h \exp\left[\sum_{(\alpha,\gamma)} \bar{G}_{\alpha\gamma} s^\alpha s^\gamma + \sum_\alpha \bar{P}_\alpha s^\alpha\right]\right].$$

With this results, Eq.(C.10) becomes

$$[Z^n]_a = \int\int \prod_{(\alpha,\gamma)} dq_{\alpha\gamma} d\bar{q}_{\alpha\gamma} \int\int \prod_{\alpha} dm_\alpha d\bar{m}_\alpha \exp\left\{-L\left(\frac{\beta^2 J^2}{2}\sum_{(\alpha,\gamma)} q_{\alpha\gamma}\bar{q}_{\alpha\gamma} + \frac{\beta J_0}{4}\sum_\alpha m_\alpha \bar{m}_\alpha\right.\right.$$
$$\left.\left. -\kappa \ln \mathrm{Tr}_v \exp\left[\sum_{(\alpha,\gamma)} G_{\alpha\gamma}\sigma^\alpha\sigma^\gamma + \sum_\alpha P_\alpha\sigma^\alpha\right] - \frac{1}{\kappa}\ln \mathrm{Tr}_h \exp\left[\sum_{(\alpha,\gamma)} \bar{G}_{\alpha\gamma} s^\alpha s^\gamma + \sum_\alpha \bar{P}_\alpha s^\alpha\right]\right)\right\}, \tag{C.13}$$

with, $\kappa = \sqrt{\frac{N_v}{N_h}}$.

We get a integral similar to the *BM*, which can be evaluated similarly using the steepest descent method, obtaining:

$$[Z^n]_a \approx \exp\left\{-L\left(\frac{\beta^2 J^2}{2}\sum_{(\alpha,\gamma)} q_{\alpha\gamma}\bar{q}_{\alpha\gamma} + \frac{\beta J_0}{4}\sum_{\alpha} m_\alpha \bar{m}_\alpha \right.\right.$$
$$\left.\left. -\kappa \ln \mathrm{Tr}_v \exp\left[\sum_{(\alpha,\gamma)} G_{\alpha\gamma}\sigma^\alpha\sigma^\gamma + \sum_\alpha P_\alpha \sigma^\alpha\right] - \frac{1}{\kappa}\ln \mathrm{Tr}_h \exp\left[\sum_{(\alpha,\gamma)} \bar{G}_{\alpha\gamma} s^\alpha s^\gamma + \sum_\alpha \bar{P}_\alpha s^\alpha\right]\right)\right\}. \tag{C.14}$$

Therefore, using Eq.(A.8), the free energy becomes

$$-\beta f = \lim_{n\to 0}\frac{1}{nL}\ln[e^{-L\tilde{f}(q_{\alpha\gamma},\bar{q}_{\alpha\gamma},m_\alpha,\bar{m}_\alpha)}] = -\lim_{n\to 0}\frac{1}{n}\tilde{f}(q_{\alpha\gamma},\bar{q}_{\alpha\gamma},m_\alpha,\bar{m}_\alpha), \tag{C.15}$$

with,

$$\tilde{f}(q_{\alpha\gamma},\bar{q}_{\alpha\gamma},m_\alpha,\bar{m}_\alpha) = \frac{\beta^2 J^2}{2}\sum_{(\alpha,\gamma)} q_{\alpha\gamma}\bar{q}_{\alpha\gamma} + \frac{\beta J_0}{4}\sum_\alpha m_\alpha \bar{m}_\alpha$$
$$-\kappa \ln \mathrm{Tr}_v \exp\left[\sum_{(\alpha,\gamma)} G_{\alpha\gamma}\sigma^\alpha\sigma^\gamma + \sum_\alpha P_\alpha\sigma^\alpha\right] - \frac{1}{\kappa}\ln \mathrm{Tr}_h \exp\left[\sum_{(\alpha,\gamma)} \bar{G}_{\alpha\gamma}s^\alpha s^\gamma + \sum_\alpha \bar{P}_\alpha s^\alpha\right]. \tag{C.16}$$

The order parameters are obtained with the condition of extreme in the free energy:

$$\frac{\partial \tilde{f}}{\partial q_{\alpha\gamma}} = \frac{\beta^2 J^2}{2}\bar{q}_{\alpha\gamma} - \frac{\beta^2 J^2}{2N_v} L\kappa \frac{\mathrm{Tr}_v\, \sigma^\alpha\sigma^\gamma \exp\left[\sum_{(\alpha,\gamma)} G_{\alpha\gamma}\sigma^\alpha\sigma^\gamma + \sum_\alpha P_\alpha\sigma^\alpha\right]}{\mathrm{Tr}_v \exp\left[\sum_{(\alpha,\gamma)} G_{\alpha\gamma}\sigma^\alpha\sigma^\gamma + \sum_\alpha P_\alpha\sigma^\alpha\right]} = 0.$$

thus, the Spin Glass order parameter for the hidden neurons is

$$\bar{q}_{\alpha\gamma} = \langle \sigma^\alpha\sigma^\gamma\rangle_v. \tag{C.17}$$

Analogously, we get the other order parameters and putting all together

$$q_{\alpha\gamma} = <\sigma^\alpha\sigma^\gamma>_h, \qquad m_\alpha = <\sigma^\alpha>_h, \tag{C.18}$$
$$\bar{q}_{\alpha\gamma} = <s^\alpha s^\gamma>_v, \qquad \bar{m}_\alpha = <s^\alpha>_v\ . \tag{C.19}$$

C.2 Replica Symmetric Solution

Now, in order to evaluate the limit $n \to 0$ we specify the dependence of the order parameters on the replicas. Such dependence's consists in that the order parameters are *Replica Symmetric(RS)*:

$$q_{\alpha\gamma} = q \qquad \forall\ \alpha \neq \gamma, \qquad\qquad \bar{q}_{\alpha\gamma} = \bar{q} \qquad \forall\ \alpha \neq \gamma, \tag{C.20}$$

$$m_\alpha = m \qquad \forall\ \alpha, \qquad\qquad \bar{m}_\alpha = \bar{m} \qquad \forall\ \alpha. \tag{C.21}$$

Using this assumption, we get.

$$\begin{aligned} -\beta f = -\lim_{n\to 0}\frac{1}{n}\left(\frac{\beta^2 J^2}{2}q\bar{q}n(n-1) + \frac{\beta J_0}{4}m\bar{m}n - \kappa\Psi_v - \frac{1}{\kappa}\Psi_h\right) \\ = \frac{\beta^2 J^2}{2}q\bar{q} - \frac{\beta J_0}{4}m\bar{m} + \lim_{n\to 0}\frac{1}{n}(\kappa\Psi_v + \frac{1}{\kappa}\Psi_h), \end{aligned} \tag{C.22}$$

with,

$$\Psi_v = \ln \mathrm{Tr}_v \exp\left(G\sum_{(\alpha,\gamma)}\sigma^\alpha\sigma^\gamma + P\sum_\alpha \sigma^\alpha\right) \qquad\qquad v \longleftrightarrow h. \tag{C.23}$$

Now, we need to take the limit in the two last terms:

$$\mathcal{O} = \lim_{n\to 0}\frac{\kappa}{n}\Psi_v \qquad\qquad v \longleftrightarrow h. \tag{C.24}$$

First, we can write:

$$\sum_{\alpha,\gamma}\sigma^\alpha\sigma^\gamma = \left(\sum_\alpha \sigma^\alpha\right)^2 = n + \sum_{(\alpha,\gamma)}\sigma^\alpha\sigma^\gamma. \tag{C.25}$$

Therefore, Eq.(C.24) becomes

$$\mathcal{O} = \lim_{n\to 0}\frac{\kappa}{n}\ln \mathrm{Tr}_v \exp\left[G\left(\sum_\alpha \sigma^\alpha\right)^2 - Gn + \sum_\alpha P_\alpha\sigma^\alpha\right] \qquad\qquad v \longleftrightarrow h. \tag{C.26}$$

Using Eq.(B.9) with $A = G/4$ and $B = G\sum_\alpha \sigma^\alpha$, we obtain

$$\mathcal{O} = \lim_{n\to 0}\frac{\kappa}{n}\ln\left[\sqrt{\frac{4\pi}{G}}e^{-Gn}\int dz e^{-Gz^2/4}\,\mathrm{Tr}_v \exp\left[(Gz+P)\sum_\alpha \sigma^\alpha\right]\right]. \tag{C.27}$$

Now, we rewrite the trace term:

$$\mathrm{Tr}_v \exp\left[(Gz+P)\sum_\alpha \sigma^\alpha\right] = \sum_{\{\sigma^\alpha\}} \cdots \sum_{\{\sigma^n\}} \prod_\alpha \exp[(Gz+P)\sigma^\alpha] = \cdots = [2\cosh(Gz+P)]^n. \tag{C.28}$$

Replacing $z^2 = Gz^2/2$, we obtain

$$\mathcal{O} = \lim_{n\to 0} \frac{\kappa}{n} \ln \int Dz \exp\Big[n \ln 2\cosh\Big(\sqrt{2G}z + P\Big) - Gn\Big]. \tag{C.29}$$

As the argument of the exponential tends to zero we can expand around zero this term:

$$\mathcal{O} \approx \lim_{n\to 0} \frac{\kappa}{n} \ln \left[1 + n\int Dz \ln 2\cosh\Big(\sqrt{2G}z + P\Big) - Gn\right]. \tag{C.30}$$

Using $\ln(1+x) \approx x - \frac{x^2}{2} + \ldots$, we get

$$\mathcal{O} \approx \kappa \int Dz \ln 2\cosh\Big(\sqrt{2G}z + P\Big) - \kappa G. \qquad\qquad v \longleftrightarrow h. \tag{C.31}$$

Then, the free energy becomes

$$-\beta f = \frac{\beta^2 J^2}{2} q\bar{q} - \frac{\beta J_0}{4} m\bar{m} + \kappa \int Dz \ln 2\cosh\Big(\sqrt{2G}z + P\Big) + \frac{1}{\kappa}\int Dz \ln 2\cosh\Big(\sqrt{2\bar{G}}z + \bar{P}\Big) - \kappa G - \frac{1}{\kappa}\bar{G}, \tag{C.32}$$

where,

$$G = \frac{\beta^2 J^2 q}{2}\frac{L}{N_v} + \frac{\beta^2 h^2}{2}, \qquad P = \beta J_0 m \frac{L}{4N_v} + \beta h_0, \tag{C.33}$$

$$\bar{G} = \frac{\beta^2 J^2 \bar{q}}{2}\frac{L}{N_h} + \frac{\beta^2 c^2}{2}, \qquad \bar{P} = \beta J_0 \bar{m} \frac{L}{4N_h} + \beta c_0. \tag{C.34}$$

Finally, the order parameters can be found by the condition $\frac{\partial f}{\partial q} = \frac{\partial f}{\partial \bar{q}} = \frac{\partial f}{\partial m} = \frac{\partial f}{\partial \bar{m}} = 0$:

$$q = \int Dz \tanh^2(\sqrt{2\bar{G}}z + \bar{P}), \qquad m = \int Dz \tanh\Big(\sqrt{2\bar{G}}z + \bar{P}\Big), \tag{C.35}$$

$$\bar{q} = \int Dz \tanh^2(\sqrt{2G}z + P), \qquad \bar{m} = \int Dz \tanh\Big(\sqrt{2G}z + P\Big), \tag{C.36}$$

C.3 Supplementary Figures

In this section we put some supplementary figures for the section 5.2

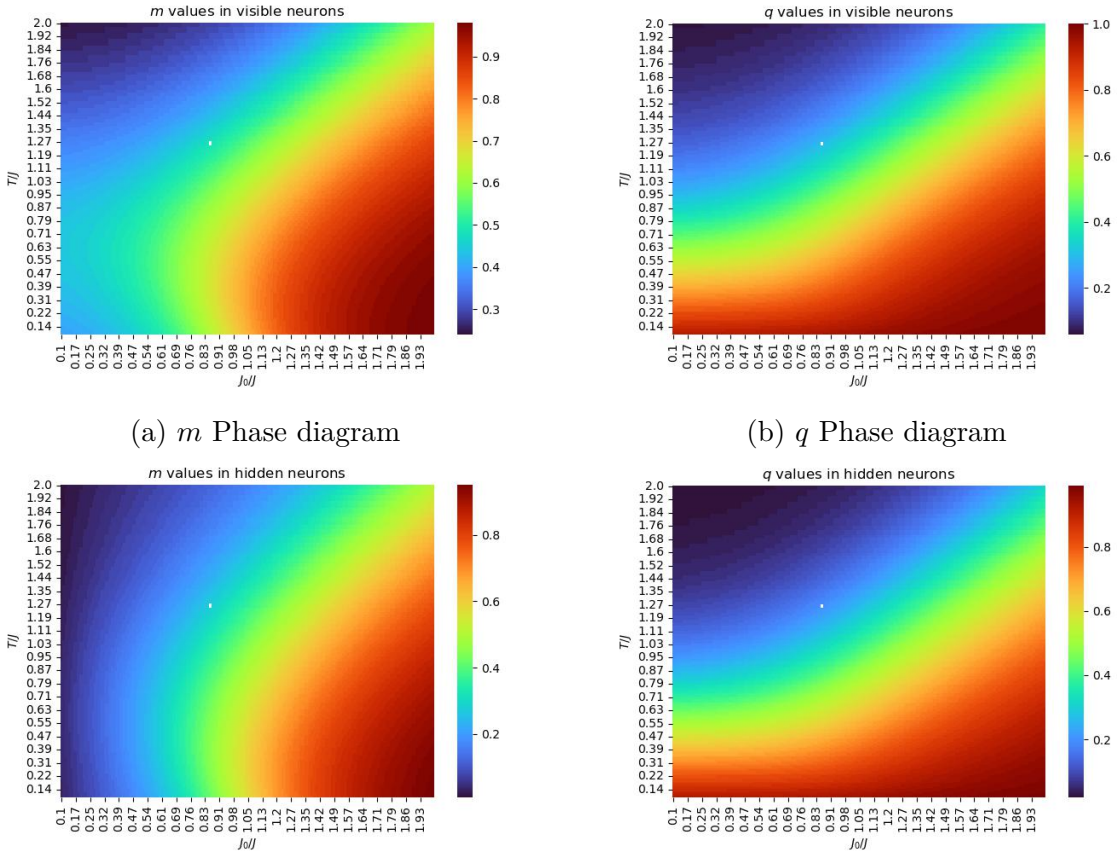

(a) m Phase diagram

(b) q Phase diagram

(c) $\bar{m}$ Phase diagram

(d) $\bar{q}$ Phase diagram

Figure 20 – Phase diagram for the Restricted Boltzmann Machine with mean and variance bias: $h_0 = 0$, $h = 0$, $c_0 = 0.5$ and $c = 0$. (a). Phase diagram for the order parameter m corresponding to the visible neurons. (b). Phase diagram for the order parameter q corresponding to the visible neurons. (c). Phase diagram for the order parameter $\bar{m}$ corresponding to the hidden neurons. (d). Phase diagram for the order parameter $\bar{q}$ corresponding to the hidden neurons.

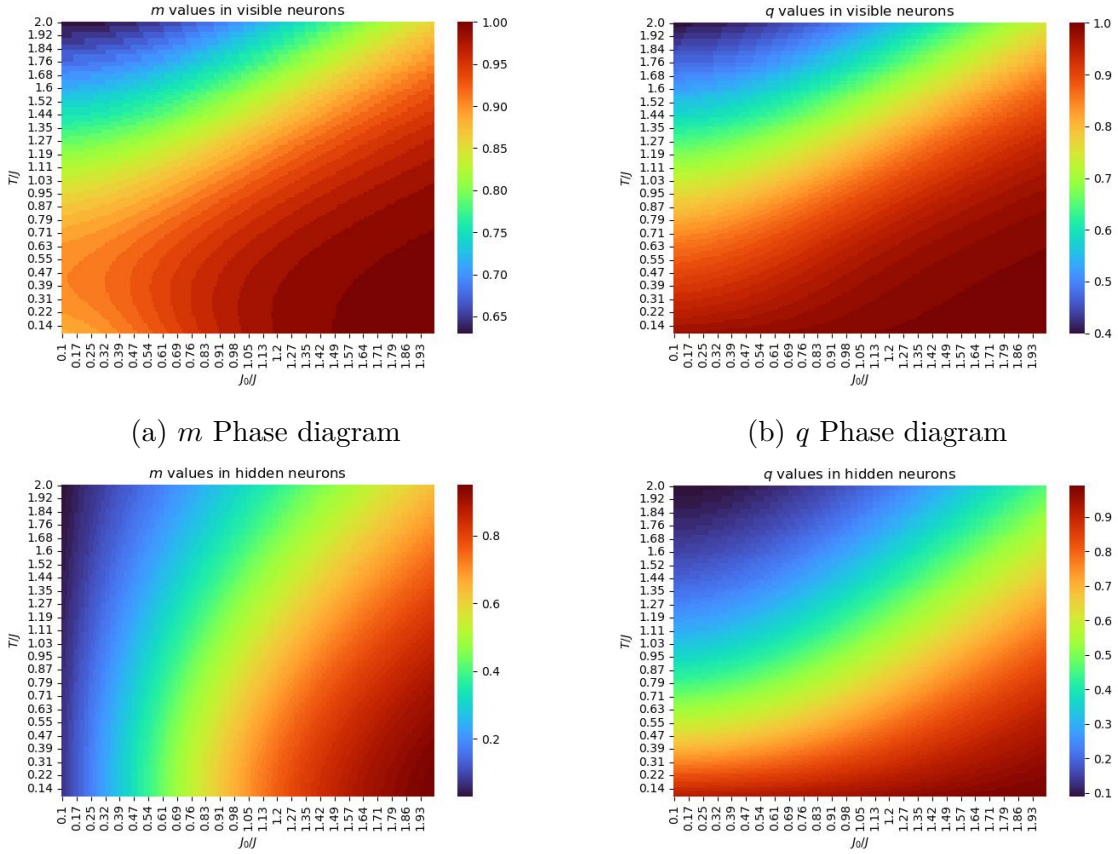

(a) m Phase diagram

(b) q Phase diagram

(c) $\bar{m}$ Phase diagram

(d) $\bar{q}$ Phase diagram

Figure 21 – Phase diagram for the Restricted Boltzmann Machine with mean and variance bias: $h_0 = 0$, $h = 0$, $c_0 = 1.5$ and $c = 0$. (a). Phase diagram for the order parameter m corresponding to the visible neurons. (b). Phase diagram for the order parameter q corresponding to the visible neurons. (c). Phase diagram for the order parameter $\bar{m}$ corresponding to the hidden neurons. (d). Phase diagram for the order parameter $\bar{q}$ corresponding to the hidden neurons.

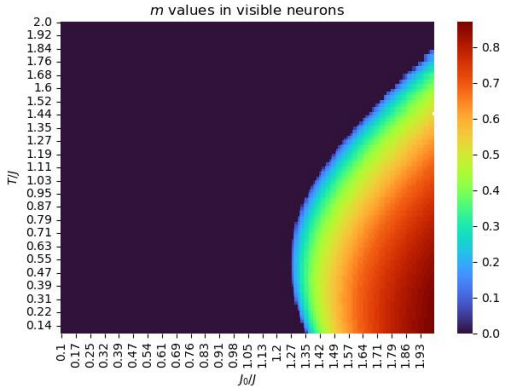

(a) m Phase diagram

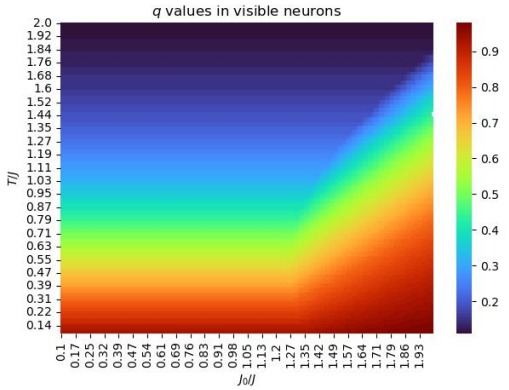

(b) q Phase diagram

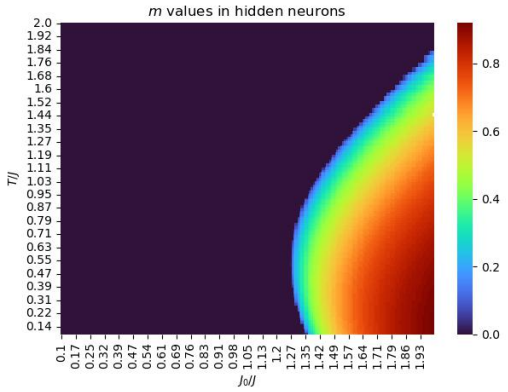

(c) $\bar{m}$ Phase diagram

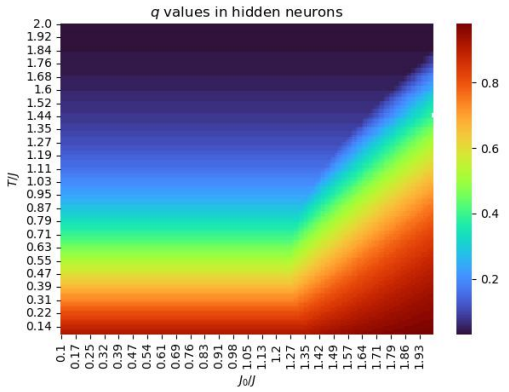

(d) $\bar{q}$ Phase diagram

Figure 22 – Phase diagram for the Restricted Boltzmann Machine with mean and variance bias: $h_0 = 0$, $h = 0$, $c_0 = 0$ and $c = 0.5$. (a). Phase diagram for the order parameter m corresponding to the visible neurons. (b). Phase diagram for the order parameter q corresponding to the visible neurons. (c). Phase diagram for the order parameter $\bar{m}$ corresponding to the hidden neurons. (d). Phase diagram for the order parameter $\bar{q}$ corresponding to the hidden neurons.

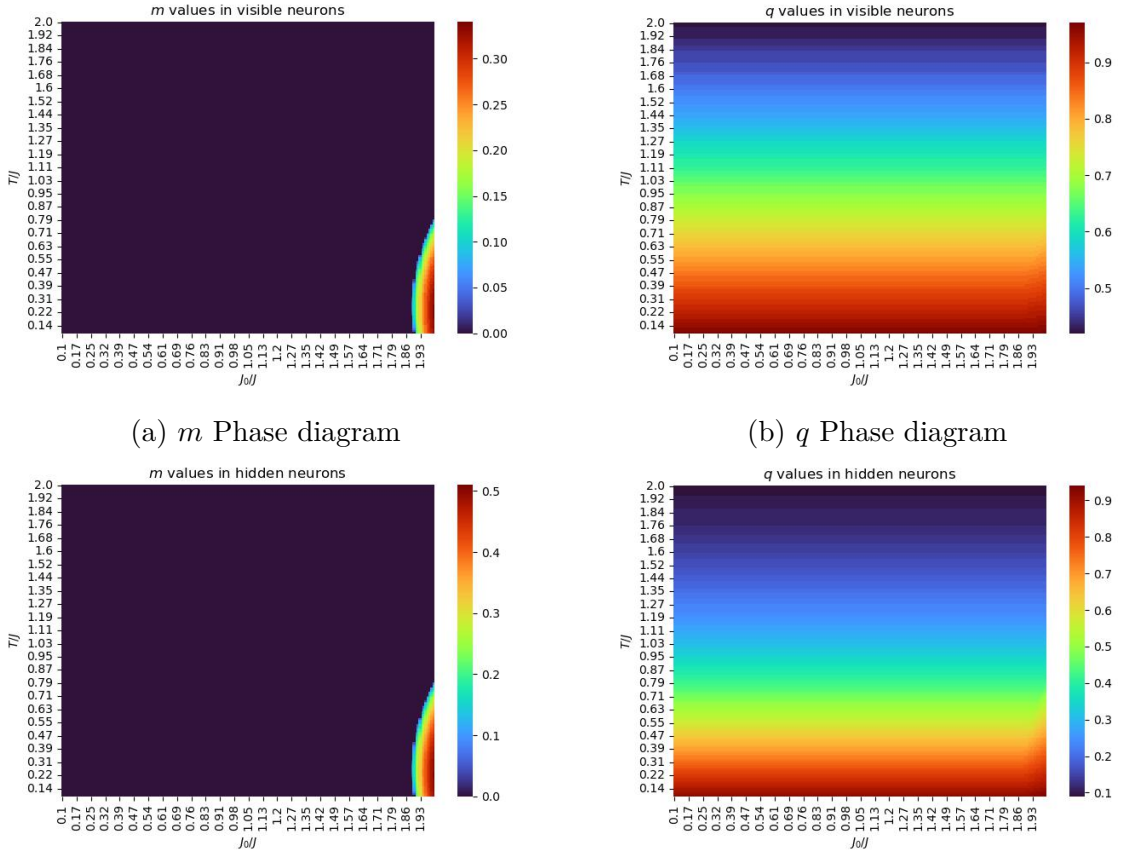

(a) m Phase diagram

(b) q Phase diagram

(c) $\bar{m}$ Phase diagram

(d) $\bar{q}$ Phase diagram

Figure 23 – Phase diagram for the Restricted Boltzmann Machine with mean and variance bias: $h_0 = 0$, $h = 0$, $c_0 = 0$ and $c = 1.5$. (a). Phase diagram for the order parameter m corresponding to the visible neurons. (b). Phase diagram for the order parameter q corresponding to the visible neurons. (c). Phase diagram for the order parameter $\bar{m}$ corresponding to the hidden neurons. (d). Phase diagram for the order parameter $\bar{q}$ corresponding to the hidden neurons.

APPENDIX D – Replica Quantum Boltzmann Machine(Semi classical Boltzmann Machine)

D.1 Suzuki-Trotter Formalism to the Quantum Boltzmann Machine

The idea behind the Suzuki-Trotter formalism is to transform a d-dimensional quantum Hamiltonian into a $(d+1)$-dimensional effective classical Hamiltonian. let us start considering the quantum Hamiltonian of our system(Eq.(6.1))

$$H(\sigma) = -\sum_{i<j} J_{ij}\sigma_i^z\sigma_j^z - \sum_i h_i\sigma_i^z - \Omega\sum_i \sigma_i^x. \tag{D.1}$$

At equilibrium, it follows the Boltzmann distribution given by the following density matrix:

$$\rho = \frac{e^{-\beta H(\sigma)}}{Z}, \tag{D.2}$$

where, $Z = \operatorname{Tr} e^{-\beta H(\sigma)}$ is the partition function

Then, we separate the above Hamiltonian into two parts: a diagonal and a non Diagonal Hamiltonian:

$$H(\sigma) = H_0 + H_q, \tag{D.3}$$

with:

$$H_0 = -\sum_{i<j} J_{ij}\sigma_i^z\sigma_j^z - \sum_i h_i\sigma_i^z, \qquad H_q = -\Omega\sum_i \sigma_i^x. \tag{D.4}$$

Then, the partition function reads:

$$Z = \operatorname{Tr} e^{-\beta(H_0+H_q)}. \tag{D.5}$$

Now, consider the Trotter formula:

$$e^{A+B} = \lim_{M\to\infty} (e^{A/M} e^{B/M})^M. \tag{D.6}$$

This formula holds even when $[A, B] \neq 0$. Applying the formula above, the partition function (D.5). reads:

$$Z = \mathrm{Tr}\Big[\lim_{M\to\infty} (e^{-\beta H_0} e^{-\beta H_q})^M\Big]. \tag{D.7}$$

Using the definition of trace, we can write:

$$Z = \lim_{M\to\infty} \sum_{\{\sigma\}} \langle\sigma| \left(e^{-\beta H_0} e^{-\beta H_q}\right)^M |\sigma\rangle \,. \tag{D.8}$$

where, $|\sigma\rangle = |\sigma_1, \ldots, \sigma_N\rangle$ is a spin configuration of the whole system, the sum over σ is a sum over all possible configurations. Thus Eq.(D.8) can be written as:

$$Z = \lim_{M\to\infty} \sum_{\{\sigma\}} \langle\sigma| \left(e^{-\beta H_0} e^{-\beta H_q}\right) \ldots \left(e^{-\beta H_0} e^{-\beta H_q}\right) |\sigma\rangle \,. \tag{D.9}$$

Now, we introduce M identity operators:

$$\mathcal{I} = \sum_{\{\sigma_k\}} |\sigma_k\rangle \langle\sigma_k| \,, \tag{D.10}$$

with, $k = 1, 2, \ldots, M$. We insert this operators in between the M products in Eq.(D.9), obtaining:

$$Z = \lim_{M\to\infty} \mathrm{Tr} \prod_{k=1}^{M} \left\langle \sigma_1^k, \ldots, \sigma_N^k \right| e^{-\beta H_0} e^{-\beta H_q} \left| \sigma_1^{k+1}, \ldots, \sigma_N^{k+1} \right\rangle, \tag{D.11}$$

where, $\sigma_i^k = \pm 1$ are the eigenvalues of σ_i^z and a with the boundary condition $\left|\sigma^{M+1}\right\rangle = |\sigma^1\rangle$.

Now we need to work out the matrix elements appearing (D.11). To do this we first will use the following identity:

$$e^{a\sigma^x} = \cosh(a) + \sigma^x \sinh(a). \tag{D.12}$$

With this we can write:

$$\langle\uparrow| e^{a\sigma^x} |\uparrow\rangle = \langle\downarrow| e^{a\sigma^x} |\downarrow\rangle = \cosh a = \left[\frac{1}{2} \sinh(2a) \coth(a)\right]^{1/2}, \tag{D.13}$$

and,

$$\langle\uparrow| e^{a\sigma^x} |\downarrow\rangle = \langle\downarrow| e^{a\sigma^x} |\uparrow\rangle = \sinh a = \left[\frac{1}{2}\frac{\sinh(2a)}{\coth(a)}\right]^{1/2}. \tag{D.14}$$

We have used the fact $\sigma^x |\uparrow\rangle = |\downarrow\rangle$ and $\sigma^x |\downarrow\rangle = |\uparrow\rangle$, if we represent the eigenstates of σ^z as $|\uparrow\rangle = (1\ 0)^T$ and $|\downarrow\rangle = (0\ 1)^T$. Using this, we get

$$\prod_k \left\langle \sigma_1^k, \ldots, \sigma_N^k \right| e^{\frac{\beta\Omega}{M}\sum_i \sigma_i^x} \left| \sigma_1^{k+1}, \ldots, \sigma_N^{k+1} \right\rangle = \left[\frac{1}{2}\sinh\left(2\frac{\beta\Omega}{M}\right)\right]^{MN/2} \exp\left[\frac{1}{2}\sum_i\sum_k \sigma_i^k\sigma_i^{k+1} \ln\coth\left(\frac{\beta\Omega}{M}\right)\right]. \tag{D.15}$$

Then, it is straightforward to prove that:

$$\prod_k \left\langle \sigma_1^k, \ldots, \sigma_N^k \right| e^{-\frac{\beta}{M}H_0} \left| \sigma_1^{k+1}, \ldots, \sigma_N^{k+1} \right\rangle = \exp\left[\frac{\beta}{M}\sum_{i<j}\sum_k J_{ij}\sigma_i^k\sigma_j^k + \frac{\beta}{M}\sum_i\sum_k h_i\sigma_i^k\right]. \tag{D.16}$$

Therefore, the partition function (D.11), becomes:

$$Z = \lim_{M\to\infty} C^{NM/2}\,\mathrm{Tr}\exp[-\beta H_{eff}], \tag{D.17}$$

where, $C = \frac{1}{2}\sinh\left(2\frac{\beta\Omega}{M}\right)$ and,

$$H_{eff} = -\sum_{i<j}\sum_{k=1}^{M}\frac{J_{ij}}{M}\sigma_i(k)\sigma_j(k) - \sum_i\sum_{k=1}^{M}\frac{h_i}{M}\sigma_i(k) - \frac{1}{2\beta}\sum_i\sum_{k=1}^{M}\sigma_i(k)\sigma_i(k+1)\ln\left[\coth\left(\frac{\beta\Omega}{M}\right)\right], \tag{D.18}$$

We have change the notation by $\sigma_i^k = \sigma_i(k)$.

D.2 Replica Quantum Boltzmann Machine

Now, with the effective classical Hamiltonian at hand, firs we will replicate it and use the configurational average:

$$[Z^n]_a = \int\prod_{i<j} P(J_{ij})dJ_{ij}\int\prod_i P(h_i)dh_i\,\mathrm{Tr}$$
$$\exp\left[\beta\sum_{i<j}\sum_{k=1}^{M}\sum_\alpha\frac{J_{ij}}{M}\sigma_i^\alpha(k)\sigma_j^\alpha(k) + \beta\sum_i\sum_{k=1}^{M}\sum_\alpha\frac{h_i}{M}\sigma_i^\alpha(k) + \beta G\sum_i\sum_{k=1}^{M}\sum_\alpha\sigma_i^\alpha(k)\sigma_i^\alpha(k+1)\right]. \tag{D.19}$$

where, $G = \frac{1}{2\beta} \ln \left[\coth\left(\frac{\beta\Omega}{M}\right) \right]$. As in the classical cases, the synapses and bias follow the Gaussian distributions:

$$P(J_{ij}) = \sqrt{\frac{N}{2\pi J^2}} \exp\left[-\frac{N}{2J^2} \left(J_{ij} - \frac{J_0}{N} \right)^2 \right]; \quad P(h_i) = \sqrt{\frac{1}{2\pi h^2}} \exp\left[-\frac{1}{2h^2} (h_i - h_0)^2 \right], \tag{D.20}$$

with mean and variance:

$$[J_{ij}]_a = \frac{J_0}{N}, \qquad [(\Delta J_{ij})^2]_a = \frac{J^2}{N}, \tag{D.21}$$

$$[h_i]_a = h_0, \qquad [(\Delta h_i)^2]_a = h^2, \tag{D.22}$$

where $[]_a$ is the configurational average. In Eq.(D.19), the integrals are Gaussian which can be solved easily, obtaining:

$$[Z^n]_a = \mathrm{Tr} \exp\left[\frac{\beta^2 J^2}{2M^2 N} \sum_{i<j} \sum_{k,k'} \sum_{\alpha,\gamma} \sigma_i^\alpha(k)\sigma_j^\alpha(k)\sigma_i^\gamma(k')\sigma_j^\gamma(k') + \frac{\beta J_0}{NM} \sum_{i<j} \sum_{k} \sum_{\alpha} \sigma_i^\alpha(k)\sigma_j^\alpha(k) \right]$$
$$\exp\left[\frac{\beta^2 h^2}{2M^2} \sum_{i} \sum_{k,k'} \sum_{\alpha,\gamma} \sigma_i^\alpha(k)\sigma_i^\gamma(k') + \frac{\beta h_0}{M} \sum_{i,k,\alpha} \sigma_i^\alpha(k) + \beta G \sum_{i,k,\alpha} \sigma_i^\alpha(k)\sigma_i^\alpha(k+1) \right]. \tag{D.23}$$

Now, we can write:

$$\sum_{i<j} \sum_{k.k'} \sum_{\alpha,\gamma} \sigma_i^\alpha(k)\sigma_j^\alpha(k)\sigma_i^\gamma(k')\sigma_j^\gamma(k') = \frac{1}{2} \sum_{k,k',\alpha} \left(\sum_i \sigma_i^\alpha(k)\sigma_i^\alpha(k') \right)^2 + \sum_{k,k'} \sum_{\alpha<\gamma} \left(\sum_i \sigma_i^\alpha(k)\sigma_i^\gamma(k') \right)^2, \tag{D.24}$$

$$\sum_{i<j} \sum_{k,\alpha} \sigma_i^\alpha(k)\sigma_j^\alpha(k) = \frac{1}{2} \sum_{k,\alpha} \left(\sum_i \sigma_i^\alpha(k) \right)^2. \tag{D.25}$$

and,

$$\sum_{i,k,k'} \sum_{\alpha,\gamma} \sigma_i^\alpha(k)\sigma_i^\gamma(k') = \sum_{i,k,k',\alpha} \sigma_i^\alpha(k)\sigma_i^\alpha(k') + 2 \sum_{i,k,k'} \sum_{\alpha<\gamma} \sigma_i^\alpha(k)\sigma_i^\gamma(k'). \tag{D.26}$$

With the above results, the replicated partition function becomes (D.23), becomes

$$[Z^n]_a = \mathrm{Tr}\exp\left[\frac{\beta^2 J^2}{4M^2N}\sum_{k,k',\alpha}\left(\sum_i \sigma_i^\alpha(k)\sigma_i^\alpha(k')\right)^2 + \frac{\beta^2 J^2}{2M^2N}\sum_{k,k'}\sum_{\alpha<\gamma}\left(\sum_i \sigma_i^\alpha(k)\sigma_i^\gamma(k')\right)^2\right]$$
$$\exp\left[\frac{\beta J_0}{2MN}\sum_{k,\alpha}\left(\sum_i \sigma_i^\alpha(k)\right)^2 + \frac{\beta h^2}{2M^2}\sum_{k,k',\alpha}\sum_i \sigma_i^\alpha(k)\sigma_i^\alpha(k')\right]$$
$$\exp\left[\frac{\beta^2 h^2}{M^2}\sum_{i,k,k'}\sum_{\alpha<\gamma}\sigma_i^\alpha(k)\sigma_i^\gamma(k') + \frac{\beta h_0}{M}\sum_{i,k,\alpha}\sigma_i^\alpha(k) + \beta G\sum_{i,k,\alpha}\sigma_i^\alpha(k)\sigma_i^\alpha(k+1)\right]. \quad \text{(D.27)}$$

Note in the above equation, we have three quadratic terms, they can be linearized by H-S transformations (B.9):

$$\prod_{\alpha,k,k'}\exp\left[\frac{\beta^2 J^2}{4M^2N}\left(\sum_i \sigma_i^\alpha(k)\sigma_i^\alpha(k')\right)^2\right] \longrightarrow \quad A = \frac{\beta^2 J^2 N}{4M^2}, \quad B = \frac{\beta^2 J^2}{2M^2}\sum_i \sigma_i^\alpha(k)\sigma_i^\alpha(k'), \quad \text{(D.28)}$$

$$\prod_{\alpha<\gamma}\prod_{k,k'}\exp\left[\frac{\beta^2 J^2}{2M^2N}\left(\sum_i \sigma_i^\alpha(k)\sigma_i^\gamma(k')\right)^2\right] \longrightarrow \quad A = \frac{\beta^2 J^2 N}{2M^2}, \quad B = \frac{\beta^2 J^2}{M^2}\sum_i \sigma_i^\alpha(k)\sigma_i^\gamma(k'), \quad \text{(D.29)}$$

and

$$\prod_{\alpha,k}\exp\left[\frac{\beta J_0}{2MN}\left(\sum_i \sigma_i^\alpha(k)\right)^2\right] \longrightarrow \qquad A = \frac{\beta J_0 N}{2M}, \qquad B = \frac{\beta J_0}{M}\sum_i \sigma_i^\alpha(k). \quad \text{(D.30)}$$

After linearize the quadratic terms in Eq.(D.27), we get:

$$[Z^n]_a = \prod_{\alpha,k,k'}\int dr_\alpha(k,k')\prod_{\alpha<\gamma,k,k'}\int dq_{\alpha\gamma}(k,k')\prod_{\alpha,k}\int dm_\alpha(k,k')$$
$$\exp\left[-\frac{\beta^2 J^2}{4M^2}N\sum_{k,k',\alpha} r_\alpha^2(k,k') - \frac{\beta^2 J^2}{2M^2}N\sum_{\alpha<\gamma}\sum_{k,k'} q_{\alpha\gamma}^2(k,k') - \frac{\beta J_0}{2M}N\sum_{k,\alpha} m_\alpha^2(k)\right]$$
$$\mathrm{Tr}\exp\left[\frac{\beta^2}{2M^2}\sum_{i,k,k',\alpha}(r_\alpha(k,k')J^2 + h^2)\sigma_i^\alpha(k)\sigma_i^\alpha(k') + \sum_{\alpha<\gamma,k,k'}(\frac{\beta^2 J^2}{M^2}q_{\alpha\gamma}(k,k') + \frac{\beta^2 h^2}{M^2})\sum_i \sigma_i^\alpha(k)\sigma_i^\gamma(k')\right]$$
$$\exp\left[\sum_{\alpha,k}(\frac{\beta J_0}{M}m_\alpha(k) + \frac{\beta h_0}{M})\sum_i \sigma_i^\alpha(k) + \beta G\sum_{i,k,\alpha}\sigma_i^\alpha(k)\sigma_i^\alpha(k+1)\right]. \quad \text{(D.31)}$$

We note that in the above equation, we have not correlations between the qubits. This is called the Semi classical approximation, the price for making this approximation is

correlations between qubits in the replica space and correlations in the Trotter direction. From here we will call the system *Replica Quantum Boltzmann Machine* or *Semi Classical Boltzmann Machine*. The trace terms can be worked out, note that all the terms after the trace have a summation over the i, this summation can be factorized and thus the partition function, can be written as

$$[Z^n]_a = \prod_{\alpha,k,k'} \int dr_\alpha(k,k') \prod_{\alpha<\gamma,k,k'} \int dq_{\alpha\gamma}(k,k') \prod_{\alpha,k} \int dm_\alpha(k,k')$$
$$\exp\left[-\frac{\beta^2 J^2}{4M^2} N \sum_{k,k',\alpha} r_\alpha^2(k,k') - \frac{\beta^2 J^2}{2M^2} N \sum_{\alpha<\gamma} \sum_{k,k'} q_{\alpha\gamma}^2(k,k') - \frac{\beta J_0}{2M} N \sum_{k,\alpha} m_\alpha^2(k) + N \ln \mathrm{Tr}\, e^{-L}\right], \tag{D.32}$$

with,

$$L = -\frac{\beta^2}{M^2} \sum_{\alpha<\gamma} \sum_{k,k'} \left(J^2 q_{\alpha\gamma}(k,k') + h^2\right) \sigma^\alpha(k)\sigma^\gamma(k') - \frac{\beta^2}{2M^2} \sum_{\alpha,k,k'} \left(J^2 r_\alpha(k,k') + h^2\right) \sigma^\alpha(k)\sigma^\alpha(k')$$
$$- \beta G \sum_{k,\alpha} \sigma^\alpha(k)\sigma^\alpha(k+1) - \frac{\beta}{M} \sum_{\alpha,k} \left(J_0 m_\alpha(k) + h_0\right). \tag{D.33}$$

If we write the integrand of Eq.(D.32) as e^{-Nf}, the Steepest descent Method yields the partition function:

$$[Z^n]_a = \exp\left[Nn\left(-\frac{\beta^2 J^2}{4nM^2} \sum_{k,k',\alpha} r_\alpha^2(k,k') - \frac{\beta^2 J^2}{2nM^2} \sum_{\alpha<\gamma} \sum_{k,k'} q_{\alpha\gamma}^2(k,k') - \frac{\beta J_0}{2nM} \sum_{k,\alpha} m_\alpha^2(k) + \frac{1}{n} \ln \mathrm{Tr}\, e^{-L}\right)\right]. \tag{D.34}$$

We expand the exponential around zero,

$$[Z^n]_a \approx 1 + Nn\left(-\frac{\beta^2 J^2}{4nM^2} \sum_{k,k',\alpha} r_\alpha^2(k,k') - \frac{\beta^2 J^2}{2nM^2} \sum_{\alpha<\gamma} \sum_{k,k'} q_{\alpha\gamma}^2(k,k') - \frac{\beta J_0}{2nM} \sum_{k,\alpha} m_\alpha^2(k) + \frac{1}{n} \ln \mathrm{Tr}\, e^{-L}\right). \tag{D.35}$$

Now, we assume Trotter invariance so $q_{\alpha\gamma}(k,k)$ and $r_\alpha(k,k)$ are only functions of $\Delta k \equiv k - k'$. Therefore, the partition function can be written as:

$$[Z^n]_a \approx 1 + Nn\left(-\frac{\beta^2 J^2}{4nM} \sum_{\Delta k,\alpha} r_\alpha^2(\Delta k) - \frac{\beta^2 J^2}{2nM} \sum_{\alpha<\gamma} \sum_{\Delta k} q_{\alpha\gamma}^2(\Delta k) - \frac{\beta J_0}{2nM} \sum_{k,\alpha} m_\alpha^2(k) + \frac{1}{n} \ln \mathrm{Tr}\, e^{-L}\right), \tag{D.36}$$

with

$$L = -\frac{\beta^2}{M^2}\sum_{\alpha<\gamma}\sum_{\Delta k}\left(J^2 q_{\alpha\gamma}(\Delta k)+h^2\right)\sum_k \sigma^\alpha(k)\sigma^\gamma(k+\Delta k) - \beta G\sum_\alpha\sum_k \sigma^\alpha(k)\sigma^\alpha(k+1) - \frac{\beta}{M}\sum_\alpha\sum_k\left(J_0 m_\alpha(k)+h_0\right)\sigma^\alpha(k) - \frac{\beta^2}{2M^2}\sum_\alpha\sum_{\Delta k}\left(J^2 r_\alpha(\Delta k)+h^2\right)\sigma^\alpha(k)\sigma^\alpha(k+\Delta k). \quad \text{(D.37)}$$

Therefore, using the above results, the free energy can be written as:

$$-\beta f = \lim_{n\to 0}\frac{[Z^n]_a - 1}{nN} = \lim_{n\to 0}\left(-\frac{\beta^2 J^2}{4Mn}\sum_{\Delta K}\sum_\alpha r_\alpha^2(\Delta k) - \frac{\beta^2 J^2}{2Mn}\sum_{\Delta k}\sum_{\alpha<\gamma} q_{\alpha\gamma}^2(\Delta k) - \frac{\beta J_0}{2Mn}\sum_{\alpha,k} m_\alpha^2(k) + \frac{1}{n}\ln \mathrm{Tr}\, e^{-L}\right). \quad \text{(D.38)}$$

Now, the condition of extreme of f necessary for solve the integral by the steepest descend method give the equations of state:

$$r_\alpha(\Delta k) = \langle \sigma^\alpha(0)\sigma^\alpha(\Delta k)\rangle, \quad \text{(D.39)}$$

$$m_\alpha(k) = \langle \sigma^\alpha(0)\rangle, \quad \text{(D.40)}$$

$$q_{\alpha\gamma}(\Delta k) = \langle \sigma^\alpha(0)\sigma^\gamma(\Delta k)\rangle, \quad \text{(D.41)}$$

where the averages are with respect to e^{-L}, with L given by Eq.(D.47) and we have used Trotter invariance.

D.2.1 Replica Symmetric and Static Approximations

The equations of state (D.39), (D.40) and (D.41) are very difficult to solve, we instead look for solutions under the *RS* and *Static* approximations:

$$m_\alpha(k) = m, \quad \text{(D.42)}$$

$$q_{\alpha\gamma}(\Delta k) = q, \quad \text{(D.43)}$$

$$r_\alpha(\Delta k) = r. \quad \text{(D.44)}$$

This yields

$$-\beta f = \lim_{n\to 0}\left(-\frac{\beta^2 J^2}{4}r^2 - \frac{\beta^2 J^2}{4}q^2(n-1) - \frac{\beta J_0}{2}m^2 + \frac{1}{n}\ln \mathrm{Tr}\, e^{-L}\right). \tag{D.45}$$

That can be written as:

$$-\beta f = -\frac{\beta^2 J^2}{4}r^2 + \frac{\beta^2 J^2}{4}q^2 - \frac{\beta J_0}{2}m^2 + \lim_{n\to 0}\frac{1}{n}\ln \mathrm{Tr}\, e^{-L}, \tag{D.46}$$

with,

$$\begin{aligned} L = &-\frac{\beta^2}{M^2}\left(J^2 q + h^2\right)\sum_{\alpha<\gamma}\sum_{\Delta k}\sum_{k}\sigma^{\alpha}(k)\sigma^{\gamma}(k+\Delta k) \\ &- \beta G\sum_{\alpha}\sum_{k}\sigma^{\alpha}(k)\sigma^{\alpha}(k+1) - \frac{\beta}{M}\left(J_0 m + h_0\right)\sum_{\alpha}\sum_{k}\sigma^{\alpha}(k) \\ &- \frac{\beta^2}{2M^2}\left(J^2 r + h^2\right)\sum_{\alpha}\sum_{\Delta k}\sigma^{\alpha}(k)\sigma^{\alpha}(k+\Delta k). \end{aligned} \tag{D.47}$$

We can combine the q with the r and G terms and the m term with the G term:

$$L = -\frac{\beta^2}{2M^2}\tilde{h}(q)\left(\sum_{\alpha,k}\sigma^{\alpha}(k)\right)^2 - \sum_{k,\alpha}\sigma^{\alpha}(k)\left(\frac{\beta}{M}\tilde{h}_0(m,G) - \frac{\beta^2}{2M^2}\tilde{r}(q,r)\right), \tag{D.48}$$

with,

$$\tilde{h}(q) = J^2 q + h^2,$$

$$\tilde{h}_0(m,G) = GM\sigma^{\alpha}(k+1) + J_0 m + h_0,$$

$$\tilde{r}(q,r) = J^2(q-r)\sum_{\Delta k}\sigma^{\alpha}(k+\Delta k).$$

We have used the relationship:

$$\left(\sum_{\alpha,k}\sigma^{\alpha}(k)\right)^2 = \sum_{\alpha,\gamma,k,k'}\sigma^{\alpha}(k)\sigma^{\gamma}(k') = \sum_{\alpha,k,k'}\sigma^{\alpha}(k)\sigma^{\alpha}(k') + \sum_{k,k'}\sum_{(\alpha,\Gamma)}\sigma^{\alpha}(k)\sigma^{\gamma}(k').$$

We decouple the quadratic term in Eq.(D.48) by a H-S transformation, therefore, we get

$$\ln \mathrm{Tr}\, e^{-L} = \ln \left[\frac{\beta}{M} \sqrt{\frac{\tilde{h}(q)}{2\pi}} \int dz \exp\left[-\frac{\beta^2}{2M^2} \tilde{h}(q) z^2 \right] \right.$$
$$\left. \mathrm{Tr} \exp\left[\frac{\beta^2}{M^2} z \tilde{h}(q) \sum_k \sigma(k) + \sum_k \sigma(k) \left(\frac{\beta}{M} \tilde{h}_0(m, G) - \frac{\beta^2}{2M^2} \tilde{r}(q, r) \right) \right] \right]. \quad \text{(D.49)}$$

The integral above can be rewritten taking $z^2 = \frac{\beta^2}{M^2} \tilde{h}(q) z^2$,

$$\ln \mathrm{Tr}\, e^{-L} = \ln \left[\int Dz \exp\left[n \ln \mathrm{Tr} \exp\left[\tilde{H}(z) \right] \right] \right], \quad \text{(D.50)}$$

with,

$$\tilde{H}(z) = \frac{\beta}{M} \sqrt{\tilde{h}(q)} z \sum_k \sigma(k) + \sum_k \sigma(k) \left(\frac{\beta}{M} \tilde{h}_0(m, G) - \frac{\beta^2}{2M^2} \tilde{r}(q, r) \right). \quad \text{(D.51)}$$

Expanding the integrand in right side of Eq.(D.50), we get:

$$\ln \mathrm{Tr}\, e^{-L} = n \int Dz \ln \exp\left[\tilde{H}(z) \right], \quad \text{(D.52)}$$

with, $Dz = \frac{1}{\sqrt{2\pi}} e^{-z^2/2} dz$. Then, the free energy becomes

$$-\beta f = -\frac{\beta^2 J^2}{4} r^2 + \frac{\beta^2 J^2}{4} q^2 - \frac{\beta J_0}{2} m^2 + \int Dz \ln \mathrm{Tr} \exp\left[\tilde{H}(z) \right]. \quad \text{(D.53)}$$

Now, we rewrite Eq.(D.51) as:

$$\tilde{H}(z) = \frac{\beta}{M} \sqrt{\tilde{h}(q)} z \sum_k \sigma(k) + \frac{\beta}{M} \sum_k \sigma(k) \tilde{h}_0(m, G) + \frac{\beta^2}{2M^2} A \left(\sum_k \sigma(k) \right)^2, \quad \text{(D.54)}$$

with, $A = J^2(r - q)$ and we have used $\left(\sum_k \sigma(k) \right)^2 = \sum_k \sum_{k'} \sigma(k)\sigma(k') = \sum_k \sum_{\Delta k} \sigma(k)\sigma(k + \Delta k)$.

The quadratic term can be linearized by a H-S transformation, obtaining:

$$f = \frac{\beta J^2}{4} r^2 - \frac{\beta J^2}{4} q^2 + \frac{J_0}{2} m^2 - \frac{1}{\beta} \int Dz \ln \int Dw \, \mathrm{Tr} \exp\left[\tilde{H}(z, w) \right], \quad \text{(D.55)}$$

where,

$$\tilde{H}(z, w) = \frac{\beta}{M} \sqrt{\tilde{h}(q)} z \sum_k \sigma(k) + \frac{\beta}{M} \sum_k \sigma(k) \tilde{h}_0(m, G) + \frac{\beta}{M} \sqrt{A} w \sum_k \sigma(k). \quad \text{(D.56)}$$

In the limit when $M \to \infty$ we can use the Trotter formula:

$$\tilde{Z} \equiv \lim_{M\to\infty} Tr \exp\Big[\tilde{H}(z,w)\Big] = \mathrm{Tr}\exp\Big[\beta(\sqrt{\tilde{h}(q)}z + \sqrt{A}w + J_0 m + h_0)\sigma^z + \beta\Omega\sigma^x\Big]. \quad \text{(D.57)}$$

Where, σ^z and σ^x are the Pauli matrices and evaluating the Trace, we get:

$$\tilde{Z} = 2\cosh[\lambda], \quad \text{(D.58)}$$

with,

$$\lambda = \beta\sqrt{\Omega^2 + \Big(\sqrt{\tilde{h}(q)}z + \sqrt{A}w + J_0 m + h_0\Big)^2}. \quad \text{(D.59)}$$

.

Therefore, the free energy becomes:

$$f = \frac{\beta J^2}{4}r^2 - \frac{\beta J^2}{4}q^2 + \frac{J_0}{2}m^2 - \frac{1}{\beta}\int Dz \ln \int Dw 2\cosh(\lambda), \quad \text{(D.60)}$$

D.3 Classical Limit

The classical limit is the limit when $\Omega = 0$, then at this limit corresponds to $\ln\coth[\frac{\beta\Omega}{M}] \to \infty$. Hence all spins in the Trotter direction k are fully correlated, thus from Eq.(D.39):

$$r_\alpha(\Delta K) = \langle \sigma^\alpha(k)\sigma^\alpha(\Delta k)\rangle = 1. \quad \text{(D.61)}$$

Then, the last term in Eq.(D.51) is constant, thus it cancels when computing the expectation values, and as the spins are equal $\sigma(k) = \sigma\ \forall\ k$, we get

$$\tilde{H}(z) = \beta\sqrt{J^2 q + h^2}2\sigma + \beta(J_0 m + h_0)\sigma, \quad \text{(D.62)}$$

where $\sigma = \pm 1$. Note that we recover the classical form of $\tilde{H}(z)$, reducing the semi classical model to the classical one